Systems Toxicology – Inflammation

TABLE OF CONTENTS

1. INTRODUCTION 8
2. CIGARETTE SMOKING-RELATED INFLAMMATION IN CVD, COPD, AND LUNG CANCER 9
   - 2.1 Cardiovascular Disease 9
   - 2.2 Chronic Obstructive Pulmonary Disease 10
   - 2.3 Lung Cancer 11
3. QUANTIFYING THE IMPACT OF CIGARETTE SMOKE ON CARDIOVASCULAR AND LUNG INFLAMMATION USING A NETWORK-BASED APPROACH 12
   - 3.1 Tools for the Assessment of Cardiovascular Inflammation in Experimental Models 12
     - 3.1.1 *In Vitro* Systems for the Study of Cigarette Smoke-Related Cardiovascular Inflammation 12
       - 3.1.1.1 Adhesion Assay 12
       - 3.1.1.2 Transendothelial Migration Assay 13
     - 3.1.2 *In Vivo* Systems for the Study of Cigarette Smoke-Related Cardiovascular Inflammation 13
   - 3.2 Tools for the Assessment of Pulmonary Inflammation in Experimental Models 14
     - 3.2.1 *In Vitro* Systems for the Study of Cigarette Smoke-Related Pulmonary Inflammation 14
     - 3.2.2 *In Vivo* Systems for the Study of Cigarette Smoke-Related Pulmonary Inflammation 16
     - 3.2.3 Systems Biology Tools 17
   - 3.3 Assessment of Inflammation *In Vitro* and *In Vivo* – Results 19
     - 3.3.1 Results from *In Vitro* Studies 21
       - 3.3.1.1 Adhesion Assay 21
       - 3.3.1.2 Transendothelial Migration Assay 28
       - 3.3.1.3 THS2.2 Aerosol Fraction Impact Assessment Study 30
       - 3.3.1.4 Oral Organotypic Study 35
       - 3.3.1.5 Nasal Organotypic Study 40

3.3.1.6 Bronchial Organotypic Study 47
3.3.2 Results from *In Vivo* Studies 53
3.3.2.1 Rat OECD Studies 53
3.3.2.1.1 Rat OECD THS2.2 Study 53
3.3.2.1.2 Rat OECD THS2.2 Menthol Study 64
3.3.2.2 *Apoe*$^{-/-}$ THS Study 75
3.3.2.3 A/J Study 84
4. CONCLUSIONS 89
5. REFERENCES 90

LIST OF FIGURES

Figure 1. The Inflammatory Process Network (IPN) 17
Figure 2. The Cardiovascular Inflammatory Process Network (CV-IPN) 18
Figure 3. Network perturbations in human coronary arterial endothelial cells treated with 3R4F cigarette smoke and THS2.2 aerosol aqueous extracts 22
Figure 4. Relative network perturbation amplitude (NPA) scores of specific Cardiovascular Inflammatory Process Network (CV-IPN) subnetworks in human coronary arterial endothelial cells treated with 3R4F cigarette smoke and THS2.2 aerosol aqueous extracts 23
Figure 5. Altered expression levels of genes encoding cellular adhesion molecules (CAMs) in human coronary artery endothelial cells treated with 3R4F cigarette smoke and THS2.2 aerosol aqueous extracts 24
Figure 6. Alterations in inflammatory protein markers released into MM6 cell culture supernatants following treatment with 3R4F cigarette smoke and THS2.2 aerosol aqueous extracts 25
Figure 7. Network perturbations in MM6 cells following treatment with 3R4F cigarette smoke and THS2.2 aerosol aqueous extracts 27
Figure 8. Altered cytokine levels in the supernatants of THP-1 cells treated with 3R4F cigarette smoke and THS2.2 aerosol aqueous extracts 29
Figure 9. Effect of 3R4F cigarette smoke and THS2.2 aerosol extract on THP-1 monocyte transendothelial migration 30
Figure 10. Network model-based analysis of the biological impact factor (BIF) in normal human bronchial epithelial cells following exposure to 3R4F cigarette smoke and THS2.2 aerosol fractions 32
Figure 11. Network perturbations in normal human bronchial epithelial cells following exposure to 3R4F smoke and THS2.2 aerosol fractions 34

Figure 12. Network model-based analysis of the biological impact factor (BIF) in EpiOral™ tissues following exposure to 3R4F cigarette smoke and THS2.2 aerosol compared with air controls 36
Figure 13. Network perturbations in EpiOral™ tissues following exposure to 3R4F cigarette smoke and THS2.2 aerosol compared with air controls..... 37
Figure 14. Relative network perturbation amplitude (NPA) scores of specific Inflammatory Process Network (IPN) subnetworks in EpiOral™ tissues following exposure to 3R4F cigarette smoke and THS2.2 aerosol..... 38
Figure 15. Altered expression levels of genes linked to inflammation in EpiOral™ tissues following exposure to 3R4F cigarette smoke and THS2.2 aerosol.... 39
Figure 16. Altered levels of inflammation protein markers in conditioned media of EpiOral™ tissues following exposure to 3R4F cigarette smoke and THS2.2 aerosol 40
Figure 17. Network model-based analysis of the biological impact factor (BIF) in nasal MucilAir™ tissues following exposure to 3R4F cigarette smoke and THS2.2 aerosol compared with air controls 42
Figure 18. Network perturbations in nasal MucilAir™ tissues following exposure to 3R4F cigarette smoke and THS2.2 aerosol compared with air controls..... 43
Figure 19. Relative network perturbation amplitude (NPA) scores of specific Inflammatory Process Network (IPN) subnetworks in nasal MucilAir™ tissues following exposure to 3R4F cigarette smoke and THS2.2 aerosol.... 44
Figure 20. Altered expression levels of genes linked to inflammation in nasal MucilAir™ tissues following exposure to 3R4F cigarette smoke and THS2.2 aerosol 45
Figure 21. Altered levels of inflammation protein markers in conditioned media of nasal MucilAir™ tissues following exposure to 3R4F cigarette smoke and THS2.2 aerosol 46
Figure 22. Network model-based analysis of the biological impact factor (BIF) in bronchial MucilAir™ tissues following exposure to 3R4F cigarette smoke and THS2.2 aerosol compared with air controls..... 47
Figure 23. Network perturbations in bronchial MucilAir™ tissues following exposure to 3R4F cigarette smoke and THS2.2 aerosol compared with air controls..... 49
Figure 24. Relative network perturbation amplitude (NPA) scores of specific Inflammatory Process Network (IPN) subnetworks in bronchial MucilAir™ tissues following exposure to 3R4F cigarette smoke and THS2.2 aerosol.... 50
Figure 25. Altered expression levels of genes linked to inflammation in bronchial MucilAir™ tissues following exposure to 3R4F cigarette smoke and THS2.2 aerosol 51

Figure 26. Altered levels of inflammation protein markers in conditioned media of bronchial MucilAir™ tissues following exposure to 3R4F cigarette smoke and THS2.2 aerosol 52
Figure 27. Network perturbations in rat nasal epithelial tissues following exposure to 3R4F cigarette smoke and THS2.2 aerosol compared with air controls 55
Figure 28. Relative network perturbation amplitude (NPA) scores of the Tissue Damage subnetwork in nasal respiratory epithelia of male rats exposed to 3R4F cigarette smoke and THS2.2 aerosol 56
Figure 29. Altered expression levels of genes linked to inflammation in nasal epithelial tissues of male rats following exposure to 3R4F cigarette smoke and THS2.2 aerosol 57
Figure 30. Network perturbations in rat lung tissues following exposure to 3R4F cigarette smoke and THS2.2 aerosol compared with air controls 59
Figure 31. Altered expression levels of genes linked to inflammation in lung tissues of male rats following exposure to 3R4F cigarette smoke and THS2.2 aerosol 60
Figure 32. Alterations in levels of soluble inflammation mediators in bronchoalveolar lavage fluid of male rats exposed to 3R4F cigarette smoke or THS2.2 aerosol 62
Figure 33. Alterations in levels of soluble inflammation mediators in bronchoalveolar lavage fluid of female rats exposed to 3R4F cigarette smoke or THS2.2 aerosol 63
Figure 34. Network perturbations in rat nasal epithelial tissues following exposure to reference cigarette smoke and THS2.2M aerosol compared with air controls 66
Figure 35. Relative network perturbation amplitude (NPA) scores of specific Inflammatory Process Network (IPN) subnetworks in nasal epithelial tissues of female rats exposed to reference cigarette smoke and THS2.2M aerosol . 68
Figure 36. Altered expression levels of genes linked to inflammation in rat nasal epithelial tissues following exposure to reference cigarette smoke and THS2.2M aerosol 69
Figure 37. Network perturbations in rat lung tissues following exposure to reference cigarette smoke and THS2.2M aerosol compared with air controls 71
Figure 38. Altered expression levels of genes linked to inflammation in rat lung tissues following exposure to reference cigarette smoke and THS2.2M aerosol 72
Figure 39. Alterations in levels of soluble inflammation mediators in bronchoalveolar lavage fluid of male rats exposed to 3R4F cigarette smoke or THS2.2M aerosol 73

Figure 40. Alterations in levels of soluble inflammation mediators in bronchoalveolar lavage fluid of female rats exposed to 3R4F cigarette smoke or THS2.2M aerosol 74
Figure 41. Network perturbations in *Apoe*$^{-/-}$ mouse nasal tissues following exposure to 3R4F cigarette smoke and THS2.2 aerosol compared with air controls..... 77
Figure 42. Network perturbations in *Apoe*$^{-/-}$ mouse lung tissues following exposure to 3R4F cigarette smoke and THS2.2 aerosol compared with air controls..... 79
Figure 43. Relative network perturbation amplitude (NPA) scores of specific Inflammatory Process Network (IPN) subnetworks in *Apoe*$^{-/-}$ mouse lung tissues following exposure to 3R4F cigarette smoke and THS2.2 aerosol.... 80
Figure 44. Altered expression levels of proteins in *Apoe*$^{-/-}$ mouse lung tissues following exposure to 3R4F cigarette smoke and THS2.2 aerosol 82
Figure 45. Alterations in levels of soluble inflammation mediators in bronchoalveolar lavage fluid of *Apoe*$^{-/-}$ mice exposed to 3R4F cigarette smoke or THS2.2 aerosol 83
Figure 46. Network perturbations in A/J mouse nasal tissues following exposure to 3R4F cigarette smoke and THS2.2 aerosol compared with air controls..... 86
Figure 47. Network perturbation amplification (NPA) scores in A/J mouse tracheal tissues following exposure to 3R4F cigarette smoke and THS2.2 aerosol compared with air controls..... 88

LIST OF TABLES

Table 1. Non-Clinical Studies with Measures of Inflammation 20

ABBREVIATIONS

AE	Aqueous extract
Apoe	Apolipoprotein E
BALF	Bronchoalveolar lavage fluid
BIF	Biological impact factor
CAM	Cell adhesion molecule
CCL	Chemokine (C-C motif) ligand
CD40-L	CD40 ligand
CFA	Cell Fate
CIM	Cell invasion/migration
COPD	Chronic obstructive pulmonary disease
CPR	Cell Proliferation
CS	Cigarette smoke
CSC	Cigarette smoke condensate
CSE	Cigarette smoke extract
CSF	Colony-stimulating factor
CST	Cell Stress
CTGF	Connective tissue growth factor
CVD	Cardiovascular disease
CV-IPN	Cardiovascular Inflammatory Process Network
CXCL	Chemokine (C-X-C motif) ligand
DEG	Differentially expressed gene
EGF	Epidermal growth factor
G-CSF	Granulocyte-colony stimulating factor
GM-CSF	Granulocyte macrophage-colony stimulating factor
HCAEC	Human coronary artery endothelial cell
HM	High menthol
ICAM-1	Intercellular adhesion molecule 1
IL	Interleukin
IP-10	Interferon gamma-induced protein 10
IPN	Inflammatory Process Network
ISO	International Organization for Standardization

LCN2	Lipocalin 2
LM	Low menthol
MM6	Mono Mac 6
MMP	Matrix metalloproteinase
MRC	Mentholated reference cigarette
mRNA	Messenger ribonucleic acid
NFκB	Nuclear factor kappa-light-chain-enhancer of activated B cells
NHBEC	Normal human bronchial epithelial cells
NPA	Network perturbation amplitude
OECD	Organisation for Economic Co-operation and Development
PAI-1	Plasminogen activator inhibitor
PMI	Philip Morris International
PTGS2	Prostaglandin-endoperoxide synthase 2
RBIF	Relative biological impact factor
REF	Reference
SRP	Systems response profile
TEM	Transendothelial migration
TGF	Transforming growth factor
THS	Tobacco heating system
TIMP-1	Tissue inhibitor of metalloproteinases 1
TNFα	Tumor necrosis factor alpha
TPM	Total particulate matter
TRA	Tissue Repair and Angiogenesis
VCAM-1	Vascular cell adhesion molecule 1
VEGF	Vascular endothelial growth factor

1. INTRODUCTION

The 2013 U.S. Surgeon General's Report "How Tobacco Smoke Causes Diseases" identifies inflammation and oxidative stress, among others, as key mechanisms underlying all major smoking-related diseases (Health & Services, 2010).

Cigarette smoking is causally linked to the development of cardiovascular disease (CVD) contributing to endothelial injury and dysfunction, a pro-atherogenic lipid profile, chronic inflammation and an abnormally increased tendency toward coagulation. Evidence gathered in *in vitro* and *in vivo* studies as well as population-based observational studies has led to the recognition of vascular inflammatory processes as central to all stages of atherogenesis, from local endothelial dysfunction to plaque development and rupture (Libby et al, 2002a; Ross, 1999b).

Chronic obstructive pulmonary disease (COPD) is a respiratory disease characterized by progressive airflow limitation and is associated with an abnormal inflammatory response of the lung to noxious particles and gases (Committee, 2013). The development of COPD in smokers has been linked to a number of sustained cellular stress responses including that of the endoplasmic reticulum, hypoxic stress and autophagic stress (Chen et al, 2008; Hengstermann & Müller, 2008; Hwang et al, 2010; Malhotra et al, 2009; Vasilios, 2008). Most, if not all, of these responses are the result of oxidative insults that arise from direct exposure to cigarette smoke (CS) and cause tissue injury through oxidative stress. Concomitantly, cigarette smoke-related oxidative stress also leads to the recruitment and activation of immune and inflammatory cells and the release of pro-inflammatory mediators which in turn produce a number of (endogenous) oxidative stressors capable of perpetuating an inflammatory response.

There is overwhelming evidence that cigarette smoking is the major cause of lung cancer in most human populations, and an increased risk of lung cancer in smokers has been demonstrated in a number of epidemiological studies (Doll & Peto, 1981; Doll et al, 2004; Harris et al, 2004; Wakai et al, 2006). Most, if not all, of the inflammatory processes identified in smokers with COPD can also be observed in smokers with lung cancer, suggesting a shared etiology, and it has been shown that COPD is a risk factor for the development of lung cancer in smokers (Federico et al, 2007). Further to inflammatory processes promoting a microenvironment favoring tumor formation, direct damage to DNA, proteins and lipids by reactive oxygen species (ROS) and reactive nitrogen species (RNS) is also known to contribute to the initiation of events that ultimately lead to lung cancer (Azad et al, 2008). In addition, the perpetual interplay between oxidative stress and chronic inflammation is known to contribute to tumor progression and metastasis (Condeelis & Pollard, 2006; Pollard, 2004).

The following section of this dossier is aimed at providing a brief overview of inflammatory responses in the cardiovascular and pulmonary systems and *in vitro* and *in vivo* models and the systems biological tools with which they can be assessed. It also describes results using these tools in the evaluation of cellular stress responses to cigarette smoke exposure relative to the exposure to Philip Morris International's (PMI) potential modified risk tobacco product, the tobacco heating system (THS)2.2.

2. CIGARETTE SMOKING-RELATED INFLAMMATION IN CVD, COPD, AND LUNG CANCER

Inflammation can be triggered by various insults, such as infection, tissue injury, and cellular stress. This first line defense mechanism rapidly triggers the release of pro-inflammatory substances, including cytokines, free radicals, hormones and other small molecules to combat the stressor by initiating inflammation-resolving processes such as the adaptive immune response (Berridge, 2012). However, a number of other cells also participate in the concerted effort to limit and repair tissue injury. For example, damage to endothelial cells can result in the activation of the complement system and the release of thrombin, which leads to subsequent initiation of the coagulation factor cascade, platelet aggregation and clot formation, thus contributing to injury repair and tissue remodeling (Berridge, 2012; Deng et al, 2009; Shen et al, 2004). Various transcription factors including nuclear factor kappa B (NFκB), activator protein 1 and early growth response 1 induce the expression of gene products integral to the inflammatory response thus controlling the production of inflammatory mediators while also indirectly contributing to the activation of the cells involved (Deng et al, 2009). While this acute inflammatory response can lead to pathological consequences, it is in itself not a disease but a means to maintain homeostasis, and how the response is eventually executed typically depends on the original trigger. If resolution of acute inflammation is not achieved, ongoing stress such as chronic exposure to cigarette smoke leads to the development of smoking-related diseases (Demirovic & Rattan, 2013; Glover-Cutter et al, 2013).

2.1 Cardiovascular Disease

CVD describes a group of diseases affecting the heart and blood vessels which can be broadly classified into coronary heart disease, cerebrovascular disease and peripheral vascular disease. Build-up of fatty deposits called atherosclerotic plaques on the inner walls of the blood vessels supplying the heart or brain is the common feature shared by these diseases, and the resulting vessel blockage with narrowing of the vascular lumen and induction of a hypercoagulable state leads to serious, and at times fatal, events such as myocardial infarction or stroke (Services, 2010). Cigarette smoking is one of the major risk factors for CVD, and evidence to date from *in vitro*, *in vivo* and population-based studies has led to the recognition of vascular inflammatory processes as central to all stages of atherogenesis, from local endothelial dysfunction to plaque development and rupture (Libby et al, 2002b; Ross, 1999a).

Healthy endothelium produces a range of factors that regulate vascular tone, cellular adhesion, thromboresistance, smooth muscle cell proliferation, and vessel wall inflammation in response to inflammatory and oxidative stimuli (Münzel et al, 2008). Endothelium is maintained in a quiescent state through the inhibitory signaling of nitric oxide, an important vasodilator (Deanfield et al, 2007). When the endothelium is injured, a host response is evoked that involves a switch from nitric oxide-mediated silencing of cellular processes to redox signaling, ultimately resulting in the activation of transcription factors such as NFκB and subsequent production of inflammatory mediators including interleukin (IL)-1, IL-8, and tumor necrosis factor alpha (TNFα) (Mudau et al, 2012; Yang et al, 2006). These in turn trigger the production of cellular adhesion molecules

such as P-selectin and integrins, among others, attracting platelets to the site of endothelial injury. The process of adhesion leads to platelet activation and the subsequent release of growth factors (e.g., platelet-derived growth factor, transforming growth factor beta, epidermal growth factor (EGF), and basic fibroblast growth factor), chemokines (e.g., chemokine (C-C motif) ligand 5 (CCL5), chemokine (C-X-C motif) ligands 4 and 5 (CXCL4, CXCL5)), cytokines (e.g., IL-1β), chemoattractants (e.g., macrophage inflammatory protein-1 alpha), and coagulation factors (e.g., factor V, factor IX, plasminogen, and plasminogen activator inhibitor (PAI-1)) that in turn promote the recruitment of monocytes to the site of inflammation, platelet aggregation, coagulation, cell survival and proliferation (Gawaz et al, 2005). Monocytes that have been attracted to the sites of endothelial damage attach to the endothelial surface, transmigrate to the subendothelial space and differentiate into macrophages which begin to secrete pro-inflammatory mediators supporting the establishment of chronic inflammation (Facchinetti et al, 2007; Libby, 2012). These macrophages also phagocytose oxidized lipids, which are elevated in smokers (Bloomer, 2007; Yamaguchi et al, 2005), and develop into lipid-laden foam cells, eventually forming the fatty streaks that are the first visible signs of atherosclerosis (Fearon et al, 2011). Attracted T cells release cytokines that attract vascular smooth muscle cells which start migrating into the vessel just beneath the endothelial cell layer where they proliferate and contribute to the growth of the developing plaque. In humans, the final stage of atheroma formation is reached after years of continuous exposure to environmental noxious stimuli such as cigarette smoke and a diet rich in saturated fats and poor in antioxidants (Celermajer, 1997). The natural disease progression results in plaque growth and vessel remodeling to maintain a functional lumen size. Although atherosclerotic plaques remain clinically silent for decades, they may evolve to become advanced lesions that are prone to calcification, cap thinning, hemorrhage and rupture. Platelets play a major role in the advanced stages of plaque development where neovascularization, thrombosis, plaque erosion and rupture constitute fatal complications.

2.2 Chronic Obstructive Pulmonary Disease

Pulmonary cells are also exceptionally susceptible to the harmful effects of environmental insults including cigarette smoke, and chronic exposure to cigarette smoke has been linked to the development and progression of a variety of lung diseases including COPD (Barnes, 2008; Tuder et al, 2006). Although the specific sequence of events leading to the development of these lung diseases is still under active investigation, recent studies suggest a central contribution by inflammatory responses to their pathogenesis (Chung & Adcock, 2008; Sopori, 2002; Tetley, 2005).

Upon injury (e.g., following infection, tissue injury, or exposure to noxious agents), the healthy lung can mount an effective acute inflammatory response aimed at eliminating the insult, limiting the extent of tissue damage and protecting the host (Levy & Serhan, 2014). Depending on the trigger of inflammation, inflammatory molecules are released, signaling to circulating leukocytes and attracting them to the site of injury. Well-known key players in this process are resident macrophages which execute an acute phase response to the inflammatory trigger and release pro-inflammatory cytokines such as IL-1β and TNFα. These, in turn, increase endothelial permeability and enhance endothelial cell production of additional IL-1β as well as IL-6 and IL-8 which cause rapid

recruitment of neutrophils to the site of injury (Sadik et al, 2011). There is evidence that mast cells can also contribute to leukocyte recruitment by producing histamine, leukotrienes and prostaglandins thus increasing vascular permeability and permitting rapid influx of neutrophils and other leukocytes such as monocytes. Through interaction with lung epithelial cells, neutrophils produce lipoxins, in particular lipoxin A4, which engage with their receptor(s) regulating neutrophil apoptosis and promoting phagocytosis of apoptotic neutrophils by monocyte-derived macrophages to clear the inflamed tissue (Barnig & Levy, 2015; Levy & Serhan, 2014; Serhan et al, 2007). At the same time, neutrophilic resolvins and protectins, potent anti-inflammatory lipid mediators, exert their effects by reducing neutrophil infiltration and enhancing macrophage phagocytic capabilities, thus limiting and resolving inflammation (Kohli & Levy, 2009; Levy & Serhan, 2014).

Exposure to cigarette smoke has been reported to induce or potentiate inflammation through a variety of mechanisms involving multiple cell types (Barnes et al, 2003; Stampfli & Anderson, 2009; Thorley & Tetley, 2007a). Airway epithelial cells, resident lung macrophages and dendritic cells are the initial cellular targets of cigarette smoke exposure, and, in response, these cells produce potent chemoattractants that recruit inflammatory cells from the systemic circulation, notably neutrophils, macrophages, and T cells, into the lung microenvironment (Barnes et al, 2003; Stampfli & Anderson, 2009; Yoshida & Tuder, 2007). Chronic exposure can lead to increased airway cell damage or death, which further exacerbates pulmonary inflammation through the release of damage-associated molecular pattern molecules (Chen & Nunez, 2010; Morbini et al, 2006; Reynolds et al, 2011). Additionally, recent research suggests that chronic cigarette smoke exposure can alter the pro- and anti-inflammatory activity of cells within the inflamed pulmonary environment (Curtis et al, 2007; Hodge et al, 2007; King et al, 1988; Mucida & Cheroutre, 2010; Woodruff et al, 2005). Although the exact mechanisms remain to be fully elucidated, cigarette smoke can modulate and enhance pulmonary inflammation through several distinct yet partially overlapping mechanisms involving several different cell types. Over time, the persistence of these mechanisms in the lung can lead to the goblet cell metaplasia/mucus hypersecretion, airway remodeling, and alveolar destruction phenotypes that are linked to COPD (Barnes, 2004; Murugan & Peck, 2009; Rogers, 2007).

2.3 Lung Cancer

Lung cancer in smokers exhibits most, if not all, of the inflammatory processes reported to underlie the pathogenesis of COPD, suggesting a shared etiology between the two diseases. Additionally, recent research suggests that cigarette smoking-related chronic lung inflammation can also alter the pro- and anti-inflammatory activity of cells within the inflamed pulmonary environment (Curtis et al, 2007; Hodge et al, 2007). Moreover, the chronic production of ROS by immune cells can lead to DNA damage which can, if not repaired adequately, give rise to mutations and interfere with natural safeguarding processes aimed at eliminating damaged cells. Over time, these mutations can accumulate, providing a survival advantage. The resulting initiated population can then further profit from the multitude of growth-promoting soluble mediators released during chronic inflammation and facilitate tumor growth.

3. QUANTIFYING THE IMPACT OF CIGARETTE SMOKE ON CARDIOVASCULAR AND LUNG INFLAMMATION USING A NETWORK-BASED APPROACH

3.1 Tools for the Assessment of Cardiovascular Inflammation in Experimental Models

3.1.1 *In Vitro* Systems for the Study of Cigarette Smoke-Related Cardiovascular Inflammation

Atherosclerosis is the principal form of CVD and is characterized by inflammatory processes that govern the development of atherosclerotic lesions and their progression up until plaque rupture. Because of its complex pathology, atherogenesis is difficult to recapitulate in *in vitro* models although some aspects, including activation of the vascular endothelium and leukocyte recruitment, adhesion and transmigration can be reasonably well modeled to provide useful insights into the biological effects of cigarette smoke and its constituents on the pathogenesis of CVD (as has been expertly reviewed by Fearon *et al.* (Fearon et al, 2013)). PMI has chosen two assays to model processes occurring at an early stage in the process of atherogenesis in smokers: (1) monocyte adhesion to endothelial cells (adhesion assay); and (2) transendothelial migration (TEM) assay.

3.1.1.1 Adhesion Assay

The vascular endothelium constitutes a physical barrier between the circulation and underlying tissue fulfilling a plethora of physiological functions that are critical to organismal homeostasis (Sima et al, 2009). When the endothelium is damaged (e.g., under conditions of chronic stress), endothelial dysfunction can ensue and ultimately lead to atherosclerosis (Rajendran et al, 2013). One characteristic of endothelial dysfunction is endothelial cell activation resulting in the expression of pro-inflammatory mediators (cytokines, chemokines) and cell adhesion molecules. These, in turn, function as chemoattractants to circulating leukocytes and platelets and tether them to the endothelium. Cigarette smoking has previously been shown to modify the adhesive properties of the endothelium, leading to higher rates of leukocyte–endothelial cell adhesion (Adams et al, 1997; Dovgan et al, 1994; Duplaa et al, 1993; Jongkind et al, 1995). This could also be confirmed *in vitro* using cigarette smoke extract (CSE) or cigarette smoke condensate (CSC) to directly treat endothelial cells, demonstrating that this effect is primarily mediated by CS-induced upregulation of cell adhesion molecules (CAM) such as intercellular cellular adhesion molecule 1 (ICAM-1) and vascular cell adhesion molecule 1 (VCAM-1) expression on the surface of endothelial cells (Chen et al, 2014; Giunzioni et al, 2014; Kalra et al, 1994; Rius et al, 2013; Shen et al, 1996). In addition, soluble inflammatory mediators such as TNFα are released from CSE-activated leukocytes and act as potential inducers of CAM expression on endothelial cells, thus resulting in increased leukocyte adhesion (Poussin et al, 2014; Poussin et al, 2015; Zhang et al, 2002).

3.1.1.2 Transendothelial Migration Assay

Transendothelial migration (TEM) follows leukocyte adhesion as the next critical step in atherogenesis and is thought to be mediated by CAM (Blake & Ridker, 2001). This process can be mimicked *in vitro* by traditional Boyden chamber assay or, alternatively, the Transwell® system under static or flow conditions, and relevant transmigration assays have been described in detail (Muller & Luscinskas, 2008). Due to its ease of use, the Transwell® system under static conditions is commonly employed, adding leukocytes to endothelial cells grown on top of a permeable membrane and supplying a suitable chemoattractant in the bottom reservoir of the cell culture dish. Leukocytes capable of migrating through the endothelial cell layer and membrane can then be recovered from the bottom chamber and counted to determine the transmigration rate. Using this approach with N-formylmethionyl-leucyl-phenylalanine as chemoattractant, TEM increased when monocytes and endothelial cells were directly treated with CSC or when endothelial cells were incubated with conditioned medium from CSC-treated monocytes, but not when monocytes were pre-treated with CSC (Giunzioni et al, 2014). A similar observation was made using both the traditional Boyden chamber assay and real-time impedance measurements: pre-treatment of monocytes with CSE decreased TEM toward CXCL12 (also known as stromal cell-derived factor 1), while pre-treatment of endothelial cells resulted in increased transmigration rates (van der Toorn et al, 2015b).

3.1.2 *In Vivo* Systems for the Study of Cigarette Smoke-Related Cardiovascular Inflammation

While providing significant new insights into mechanisms underlying atherogenesis in humans, *in vitro* models can never fully reproduce the interplay between the different cell types in an organism and the spectrum of biological processes occurring during the development of atherosclerosis. However, many gaps in our understanding of these processes can be filled by knowledge gained from animal models, and cardiovascular disease research has employed such models since the early 1900s (Leong et al, 2015). Although atherosclerosis can be observed in many species fed a high-fat diet including hamsters, guinea pigs, rabbits, dogs and pigs, the mouse remains the most frequently used animal model owing to its easy maintenance and low cost (Getz & Reardon, 2012). However, mice are rather resistant to diet-induced atherogenesis, and it is known that – unlike in humans – HDL cholesterol is the main lipoprotein in the mouse, and mice do not express cholesteryl ester transfer protein, a plasma protein facilitating exchange of esterified cholesterol and triglycerides from lipoproteins (Getz & Reardon, 2012). In addition, atherosclerotic lesions in the mouse also differ from human disease in other aspects; e.g., they preferentially form in the aortic root and typically do not develop a fibrous cap, so unstable plaques are uncharacteristic (Getz & Reardon, 2012). Most of these differences, however, could be addressed by the generation of genetically modified mice, of which the *Apoe* knockout ($Apoe^{-/-}$) model has become the most widely studied murine atherosclerosis model. Developed in the early 1990s, this model was shown to be hypercholesterolemic even on normal chow and to exhibit the full spectrum of lesions occurring during the development of atherosclerosis in humans (Nakashima et al, 1994; Plump et al, 1992; Zhang et al, 1992). Studies using the $Apoe^{-/-}$ mouse with additional genetic modifications (knockout of *Rag2* or P-selectin, or overexpression of *Crp*) confirmed that chronic inflammation plays a major role in the development of

atherosclerotic lesions in this animal (Daugherty et al, 1997; Dong et al, 2000; Paul et al, 2004). Experimental evidence suggests that CS exposure accelerates atherosclerosis in *Apoe*$^{-/-}$ mice, with increased intimal thickness, plaque size and plaque area in exposed relative to control animals (Catanzaro et al, 2007; Gairola et al, 2001; Gairola et al, 2010; Kunitomo et al, 2009; Schroeter et al, 2008; Tani et al, 2004; Von Holt et al, 2009). Global lipid profiling demonstrated substantial accumulation of cholesteryl esters, phospholipids, ceramides and sphingomyelins in the aortic wall and significantly elevated plasma cholesterol levels in cigarette smoke-exposed *Apoe*$^{-/-}$ mice when compared with air-exposed mice (Boué et al, 2012). Importantly, in *Apoe*$^{-/-}$ mice that were first exposed to cigarette smoke for 3 months before being switched to air exposure for another 3 months (mimicking smoking cessation), the aortic plaque area was smaller than that in mice exposed for 6 months, with aortic arches containing approximately 50% less total cholesterol and overall decreased lipid levels (by lipid class) in plaques and plasma (Lietz et al, 2013), indicating that this mouse model also recapitulates the cardiovascular benefits of smoking cessation that is seen in humans. Further, we and others also noted a distinct pulmonary inflammatory response to cigarette smoke in the *Apoe*$^{-/-}$ mouse, characterized by the influx of leukocytes into the lungs and elevated levels of pro-inflammatory mediators in bronchoalveolar lavage fluid (BALF), eventually culminating in alveolar destruction reminiscent of emphysema (Arunachalam et al, 2010; Boué et al, 2013). This suggests that the *Apoe*$^{-/-}$ mouse model may also prove useful in COPD research, in particular, when addressing questions regarding cigarette smoke-related comorbidities.

3.2 Tools for the Assessment of Pulmonary Inflammation in Experimental Models

Our current knowledge about the role of inflammation in cigarette smoking-related lung disease is built on decades of research on the molecular underpinnings of specific inflammatory processes including epithelial pro-inflammatory responses or macrophage activation following exposure of individual cell types to cigarette smoke (de Boer et al, 2000; Mio et al, 1997; Murugan & Peck, 2009; Parsanejad et al, 2008; Russell et al, 2002). There are, however, no defined *in vitro* models of COPD capable of recapitulating the complexity of the disease. More recently, the availability of systems-wide technologies (e.g., transcriptomics, proteomics, and metabolomics) have enabled pulmonary inflammation following cigarette smoke exposure *in vivo* or *in vitro* to be analyzed using complex global data sets encompassing thousands of differentially expressed molecular species. These investigations have made significant inroads into our understanding of the temporal and cell-type specific complexities of inflammation, especially when applied to human systems (Adair-Kirk et al, 2008; Heguy et al, 2006).

3.2.1 *In Vitro* Systems for the Study of Cigarette Smoke-Related Pulmonary Inflammation

There are many studies examining the effects of cigarette smoke in lung epithelial cells that are either genetically immortalized or cancerous, simply because of their legacy value and ease of maintenance. These studies have demonstrated that lung epithelial cells respond to acute cigarette smoke exposure by producing an increased amount of IL-6, IL-8, MCP-1, and the chemokine Regulated on activation, normal T cell expressed and

secreted (CCL5), albeit with varying success (Lee et al, 2015; Li et al, 2012; Puljic & Pahl, 2003; Richter et al, 2002; Starrett & Blake, 2011; Victoni et al, 2014). However, there is growing criticism as to the validity of employing continuous cell lines in disease modeling (Adamson et al, 2011), in particular since observed biological effects in response to various stimuli are now known to differ considerably from those seen in primary human airway cells (Ghio et al, 2013; Ioannidis et al, 2013; Koning et al, 2012; Lopez-Souza et al, 2004). Moreover, some of the early effects of CS exposure appear to be more adequately reflected in primary (rather than immortal) lung epithelial cells grown under submerged conditions *in vitro*, as evidenced by comparison with epithelial cells obtained by bronchial brushing of smokers (Dvorak et al, 2011; Martinez-Anton et al, 2013). Nevertheless, classical, submerged cultures of primary bronchial epithelial cells only permit limited conclusions, as several structural properties such as the polarization of cells are lost *in vitro* (Paquette et al, 2003). A suitable alternative that is finding increasing use for the testing of inhaled toxicants exists: Raising a confluent layer of primary large or small airway epithelial cells – grown on a porous membrane in the presence of essential growth factors, hormones and micronutrients – to the air–liquid interface induces terminal differentiation and ultimately leads to the formation of a pseudostratified airway epithelium that closely resembles that seen in the human airways (Gray et al, 1996; Jetten, 1989; Paquette et al, 2003). Well-differentiated cultures created in this fashion consist of ciliated and non-ciliated columnar epithelial, goblet, and basal cells. They exhibit tight junctions, display functional cilia and are capable of mucus production which accumulates at the apical surface, atop a thin layer of airway surface liquid (Adamson et al, 2011; Prytherch et al, 2011). The functional and morphological similarities of these cultures to human airway epithelium, for this reason also called organotypic cultures, make them prime candidates for the evaluation of cigarette smoke and its fractions *in vitro*. Ready-to-use bronchial organotypic cultures such as EpiAirway™ (AIR100; MatTek Corp., Ashland, MA, USA) and MucilAir™ (Epithelix SàRL, Geneva, Switzerland) are now commercially available and have been PMI's primary choice of *in vitro* system for the past few years. Using the EpiAirway™ system, cigarette smoke exposure caused changes in gene and microRNA expression resembling that seen in epithelial cells collected from large and small airways of current and former smokers and was characterized by a distinct dose- and time-dependent oxidative stress response resulting in NFκB inhibition (Kuehn et al, 2015; Mathis et al, 2015; Mathis et al, 2013). Additional tests with the full-thickness (fibroblast-containing) bronchial and nasal MucilAir™ cultures demonstrated significant increases in MCP-1 (CCL2), IL-8 (CXCL8), vascular endothelial growth factor (VEGF), granulocyte colony-stimulating factor (G-CSF), granulocyte macrophage colony-stimulating factor (GM-CSF), and interferon-γ-inducible protein 10 (IP-10; CXCL10) levels at 24 hours following repeated CS exposure (Talikka et al, 2014). Furthermore, a marked increase in soluble mediators of inflammation and tissue remodeling including MCP-1, soluble ICAM-1 (sICAM-1), IL-8, G-CSF, EGF, CXCL1, tissue inhibitor of metalloproteinase 1 (TIMP-1), and macrophage inflammatory protein-3 alpha (MIP-3α; CCL20) was seen in the basal medium of bronchial MucilAir™ cultures without fibroblasts at 48 hours following CS exposure (Iskandar et al, 2015). Together, these data suggest that organotypic cultures are a suitable *in vitro* system to model acute inflammatory responses to CS exposure.

3.2.2 *In Vivo* Systems for the Study of Cigarette Smoke-Related Pulmonary Inflammation

Many cellular and molecular mechanisms involved in the pathogenesis of COPD in humans are also observed in murine models of pulmonary emphysema (Brusselle et al, 2006), with several features shared between human early stage disease and mouse disease development which primarily recapitulates the emphysema component (Churg et al, 2011). Lesions in mice caused by chronic cigarette smoke exposure resemble centrilobular human emphysema both morphologically and physiologically (Churg et al, 2008). Small airway remodeling, an important cause of airflow obstruction in cigarette smokers with COPD (Hogg et al, 2004), is also observed in cigarette smoke-exposed mice (Churg et al, 2008). In addition, exposure activates the innate immune response cascade in mice, leading to protease/anti-protease imbalances in lung tissue and eventual alveolar wall degradation, suggesting that murine models can also replicate these features of human COPD (Yoshida & Tuder, 2007). Finally, as observed in humans, the small airways from smoke-exposed C57BL/6 mice exhibit persistent upregulation of type I pro-collagen and pro-fibrotic cytokine gene expression, which would be expected to contribute to airway remodeling (Churg et al, 2006). However, murine models of emphysema have several limitations. First, these models only display a subset of disease phenotypes and do not fully recapitulate airflow limitation from chronic small airway obstruction, which defines COPD (Hogg et al, 2004). Second, there are considerable differences in respiratory physiology and anatomy between mice and humans, making disease modeling difficult. In contrast to humans, mice are obligate nose breathers and filter tobacco smoke differently. Additionally, the submucosal glands in mice are limited to the trachea, and mice lack a cough reflex, which further delineates the pulmonary physiology between the two species (Groneberg & Chung, 2004). Importantly, pulmonary emphysema in humans is classified according to the distribution of the airspace enlargement within the acini in centriacinar emphysema, and in cigarette smokers with COPD, significant airspace enlargement occurs primarily across the three generations of respiratory bronchioles (Hogg et al, 2004). However, rodents lack clearly defined respiratory bronchioles and distinct lobular architecture, further obscuring anatomically equivalent comparisons of disease development (March et al, 2000). Third, key species differences also exist in the innate and adaptive immune responses, which play a critical role in the initiation and maintenance of disease. These include differences in the expression of defensins, toll-like receptors, and chemokine receptors, as well as a unique repertoire of active chemokines in each species. Differences in adaptive immunity include immunoglobulin subtypes, Th1/Th2 differentiation dynamics, and the roles and ratios of $CD4^+$ and $CD8^+$ T cell populations, together with co-stimulatory molecule expression and function (Mestas & Hughes, 2004). The theory of an autoimmune component to advanced COPD contributing to the self-perpetuating nature of the disease in humans could not be corroborated in mice (Taraseviciene-Stewart et al, 2005). Fourth, unlike in humans, CS exposure-induced emphysema in mice does not progress after smoking cessation, and mice never develop spontaneous exacerbations. Finally, mice do not develop the more severe COPD symptoms that are characteristic of the human Global Initiative for Chronic Obstructive Lung Disease stages III and IV. Despite these differences, the observed features of cigarette smoke-related lung disease suggest that mouse models can aid our understanding of key aspects, such as inflammation, underlying human COPD pathophysiology.

3.2.3 Systems Biology Tools

PMI have constructed a portfolio of network models describing biological processes involved in the toxicological effects of cigarette smoke exposure in the lungs of mice, rats and humans (Gebel et al, 2013; Schlage et al, 2011; Westra et al, 2011; Westra et al, 2013). The so-called Inflammatory Process Network (IPN) model describes the initial inflammatory pathways that are known to be influenced by cigarette smoke exposure in pulmonary cells (epithelial cells, macrophages, dendritic cells, and megakaryocytes) of normal unexposed lungs as well as in immune cells recruited from the circulation following exposure to cigarette smoke (neutrophils, T cells, natural killer cells, and mast cell progenitors) (Westra et al, 2013). Together, these processes address epithelial cell barrier defense, epithelial mucus secretion, and the recruitment and activation of the various immune cell types involved in inflammatory responses to an inhaled biologically active substance or toxicant (Figure 1).

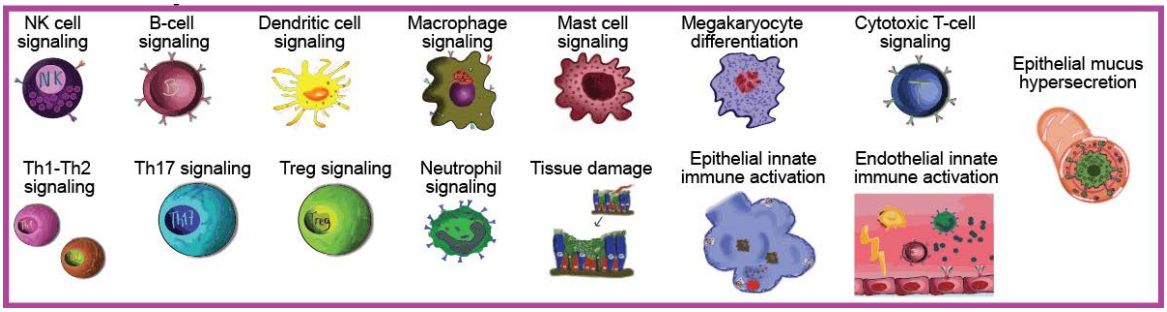


Figure 1. The Inflammatory Process Network (IPN)

This Inflammatory Process Network is designed to encapsulate the pulmonary inflammation-related signaling in response to cigarette smoke. Its constituent 15 sub-models represent the signaling that occurs in the main cell types involved in cigarette smoke-induced pulmonary inflammation, including epithelial cells and macrophages.

The IPN model has been built with a focus on human biology, and, in addition, two species-specific Knowledge Assembly Models (KAMs) representing rat and murine biology are available that contain orthologous causal assertions derived from rat or mouse sources (Westra et al, 2011). Following the calculation of the systems response profile (SRP) derived from the differential expression of genes in exposed relative to control groups, the impact of an exposure is measured on every node in the network models. By combining these individual node-related measures, a quantitative measure of the impact of the exposure on the network as a whole, the network perturbation amplitude (NPA), can be derived (Martin et al, 2012). PMI recently described two case-studies that exemplify the application of this approach in the context of cigarette smoke exposure-related perturbations of our xenobiotic metabolism network model in human bronchial biopsies (Iskandar et al, 2013), and the approach was shown to be sensitive to capturing inflammatory changes in the lung due to smoke exposure and reflected the recovery following the cessation period (Hoeng et al, 2014), highlighting the value of applying such an approach to product assessment studies.

More recently, the existing model portfolio was complemented by the construction of a network encompassing key vascular processes modulated by inflammatory stimuli that lead to the development of atherosclerosis (Cardiovascular Inflammatory Process Network or CV-IPN) (De León et al, 2014). Integrating current knowledge in the literature and large human and murine gene expression data sets, CV-IPN captures the signaling mechanisms related to the release of growth and chemotactic factors as well as the migration and proliferation of smooth muscle cells, excess lipid uptake by macrophages and the subsequent promotion of their differentiation into foam cells, platelet activation and plaque instability (Figure 2). Applying various gene expression data sets, both human and mouse biology of atherogenesis and advanced atherosclerosis were shown to be adequately represented and allowed for the computation of the NPA as previously outlined (Martin et al, 2012).

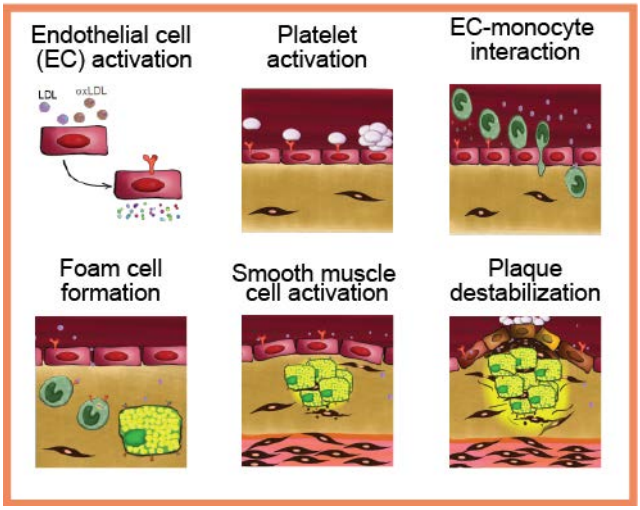


Figure 2. The Cardiovascular Inflammatory Process Network (CV-IPN)

The CV-IPN is a modular network model of vascular biology and inflammation. Each subnetwork represents a fundamental set of biological functions, and cellular and molecular players: Endothelial cell (EC) Activation, Platelet Activation, EC-Monocyte Interaction, Foam Cell Formation, and SMC Activation. The Plaque Destabilization subnetwork primarily captures those mechanisms resulting in plaque instability in advanced atherosclerotic disease.

3.3 Assessment of Inflammation *In Vitro* and *In Vivo* – Results

A number of non-clinical studies were performed in laboratory animals to identify potential hazards and to characterize mechanisms underlying tobacco-related diseases associated with the use of THS2.2 (Table 1). Among these studies, the 90-day inhalation rat studies, as described in Organisation for Economic Co-operation and Development (OECD) Guideline 413 (OECD), aimed to characterize the adverse effects caused by repeated daily inhalation exposure to aerosols generated from THS2.2 or THS2.2 Menthol (THS2.2M) for 90 days. An additional post-exposure period of 42 days was included in both studies to allow for the assessment of the reversibility or delayed occurrence of findings. Lung inflammation, histology of respiratory and non-respiratory organs, and various blood-based parameters were evaluated at the end of the 90-day inhalation and 42-day recovery periods. To obtain an understanding of the toxicity pathways (including inflammatory responses) involved in the response to the exposure, additional molecular endpoints including multi-analyte profiling in BALF and transcriptomics and proteomics analyses of lung and nasal epithelium after 90 days, or the 42-day recovery period were examined. Furthermore, to investigate hallmarks of COPD and CVD and general exposure effects over an 8-month period in *Apoe*$^{-/-}$ mice exposed to CS from 3R4F reference cigarettes or to the mainstream aerosol of THS2.2, and to assess the consequences of cessation or switching to THS2.2 after 2 months of CS exposure. Engaging a systems toxicology approach, exposure effects including inflammatory responses were investigated using conventional toxicology parameters, such as physiology and histopathology of respiratory and non-respiratory organs, combined with transcriptomics, lipidomics, and proteomics measurements.

These rodent studies were further complemented by a series of *in vitro* studies to assess the impact of exposure to 3R4F CS and THS2.2 aerosol on oral, nasal and bronchial organotypic tissues cultured at the air–liquid interface. Various endpoints including the assessment of cytotoxicity and activity of cytochrome P450 1A1/1B1, histological evaluation, and transcriptomics were assessed at different time points following an acute 28-minute exposure. In addition, *in vitro* studies were performed in human coronary artery endothelial cells (HCAECs) to study changes in their adhesive properties towards monocytes following treatment with aqueous extracts from 3R4F CS and THS2.2 aerosol. Alternatively, conditioned media from monocytes pre-incubated with these aqueous extracts were used to challenge endothelial cells. For both approaches, a functional adhesion assay was combined with transcriptomics and inflammatory protein marker data to investigate changes in this model system at the molecular level (Table 1).

Table 1. Non-Clinical Studies with Measures of Inflammation

Study	Type	Design	Reference
Adhesion assay	*In vitro*	Parallel-group (air (sham), RC[a], and THS2.2 aerosol extracts)	1604_CVD_Adhesion Assay_SR (Poussin et al, 2016)
Transendothelial migration assay	*In vitro*	Parallel-group (air (sham), RC[a], and THS2.2 aerosol extracts)	(van der Toorn et al, 2015a)
Fraction impact	*In vitro*	Parallel-group (air (sham), RC, and THS2.2 aerosol fractions)	167321_High_Content_Screening_SysTox_SR (Gonzalez-Suarez et al, 2016)
Organotypic buccal	*In vitro*	Parallel-group (air (sham), RC, and THS2.2 aerosols)	1743_Organotypic_Buccal_SR (Zanetti et al, 2016)
Organotypic nasal	*In vitro*	Parallel-group (air (sham), RC, and THS2.2 aerosols)	1722_Organotypic_Nasal_SR (Iskandar et al, 2016)
Organotypic bronchial	*In vitro*	Parallel-group (air (sham), RC, and THS2.2 aerosols)	1709_Organotypic_Bronch_SR
Rat OECD THS2.2	*In vivo*	TG413 (air (sham), RC, and THS2.2)	15006_150082_150083 THS_SR
Rat OECD THS2.2M	*In vivo*	TG413 (air (sham), RC, and THS2.2M aerosols)	15025_176500 THS_ SR
Apoe$^{-/-}$ THS2.2	*In vivo*	Parallel-group, switching (air (sham), RC, and THS2.2 aerosols, cessation, switching)	15015_CVD_SR (Lo Sasso et al, 2016a; Lo Sasso et al, 2016b; Phillips et al, 2016)
A/J lung cancer	*In vivo*	Parallel-group (air (sham), RC, and THS2.2 aerosols)	15020_AJ LC_QA-checked Interim Report

[a] 3R4F reference cigarette. Abbreviations: RC, reference cigarette; THS, tobacco heating system; M, menthol; OECD, Organisation for Economic Co-operation and Development; TG, Test Guideline.

The following part of this section provides an overview of the results from the assessment of parameters and endpoints related to inflammation in the cardiovascular and pulmonary systems in these pre-clinical studies.

3.3.1 Results from *In Vitro* Studies

3.3.1.1 Adhesion Assay

Using the previously established adhesion assay (Poussin et al, 2014; Poussin et al, 2015), the indirect and direct effects of aqueous extracts derived from 3R4F cigarette smoke (CSE) and THS2.2 aerosol (AE) on the adhesion of monocytes to endothelial cells were investigated. First, in the indirect approach, monocytic Mono Mac 6 (MM6) cells were exposed to CSE and AE for 2 hours, and the resulting supernatants were used to treat monolayers of serum-starved HCAECs for 4 hours prior to the addition of untreated DRAQ5™-labeled MM6 cells. Adhesion of the labeled MM6 cells was then evaluated on fixed cells using a high-content screening platform. Alternatively, HCAECs were treated with freshly prepared extracts (fresh direct approach) or with extracts that were aged for 2 hours at 37°C and stored at −20°C until use (direct approach).

Following exposure of endothelial cells to conditioned media from treated MM6 cells in the indirect approach, monocyte–endothelial cell adhesion was promoted at low concentrations of 3R4F CSE and THS2.2 AE. Compared with CSE, 10- and 20-times higher concentrations of THS AE were necessary for indirect and fresh direct treatments, respectively, to induce comparable adhesion rates of MM6 cells to HCAECs. In addition, the highest concentrations of both 3R4F CSE and THS2.2 AE using the fresh direct approach significantly decreased the number of HCAECs. The other conditions did not affect HCAEC numbers. In contrast, when HCAECs were exposed to a high concentration of previously frozen (direct approach) or freshly prepared CSE (fresh direct approach), MM6 cell–HCAEC adhesion was not observed (Poussin et al, 2016).

Transcriptomics profiling was performed on HCAEC samples following treatment with conditioned media, unconditioned media, or fresh aqueous aerosol/smoke extracts for 4 hours to investigate the underlying mechanisms of indirect, direct and fresh direct treatment effects, as previously described (Poussin et al, 2014; Poussin et al, 2015). The HCAEC SRPs showed a concentration-dependent increase in the number of differentially expressed genes (DEGs) in all 3R4F CSE treatments. At the same concentrations, far fewer genes were statistically significantly altered following treatment with THS2.2 AE than following CSE exposure. Even treatment with THS2.2 AE at concentrations 10- to 20-times higher than those of 3R4F CSE did not lead to as many statistically significantly DEGs as treatment with CSE, independent of the mode of exposure.

Threshold-free computational network analysis indicated maximum biological impact (relative biological impact factor (RBIF) = 100%; reference (REF)) following indirect treatment at the lowest dose of 3R4F CSE, affecting a broad spectrum of networks. A comparable pattern of networks was perturbed at the higher concentration of 3R4F CSE with similar underlying mechanisms, albeit with a lower amplitude. At the same concentrations, the overall magnitude of perturbation elicited by treatment with THS2.2 AE represented only 1% and 3% of the total perturbation of the reference, respectively, while it was 78% at the highest concentration with highly and similarly perturbed biology. The pattern and magnitude of network perturbations following direct and fresh direct treatment differed from those seen with the indirect treatment (Figure 3).

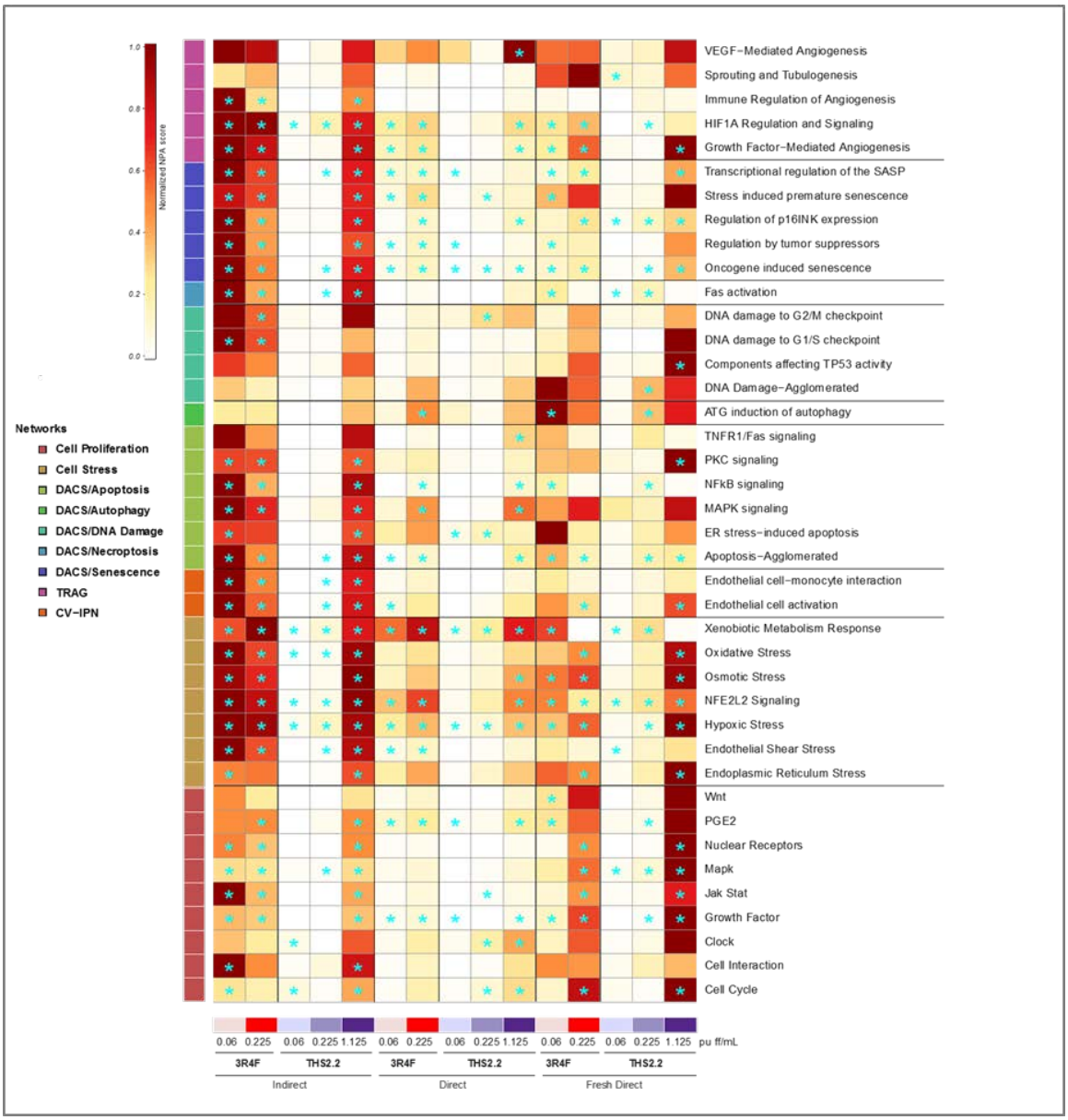


Figure 3. Network perturbations in human coronary arterial endothelial cells treated with 3R4F cigarette smoke and THS2.2 aerosol aqueous extracts

Heatmap of network perturbation amplitude (NPA) scores summarizing subnetworks that were significantly perturbed in at least one treatment. A network is considered perturbed if, in addition to the significance of the NPA score with respect to the experimental variation, the two companion statistics (O and K) derived to inform on the specificity of the NPA score with respect to the biology described in the network, are significant. Significantly perturbed networks are indicated by * (i.e. O and K statistic *p*-values <0.05 and significant with respect to the experimental variation). Abbreviations: DACS, DNA damage, autophagy, cell death, and senescence; TRAG, Tissue repair and angiogenesis; CV-IPN, Cardiovascular inflammatory process network.

Closer examination of CV-IPN perturbations revealed that the different treatment modes used in this study elicited differential effects on the HCAECs. Perturbations of the Endothelial Cell Activation and Endothelial Cell-Monocyte Interaction subnetworks were most pronounced in HCAECs with 3R4F CSE or THS2.2 AE at the high concentration. This suggests that mechanisms governing the expression of CAMs on endothelial cells and the subsequent adhesion of monocytes are predominantly driven by monocyte-derived soluble inflammatory mediators. Although increased endothelial cell activation was also observed in HCAEC treated with both extracts at high concentrations following the direct and fresh direct approaches, it was not accompanied by significant perturbations of the Endothelial Cell-Monocyte Interaction subnetwork (Figure 4).

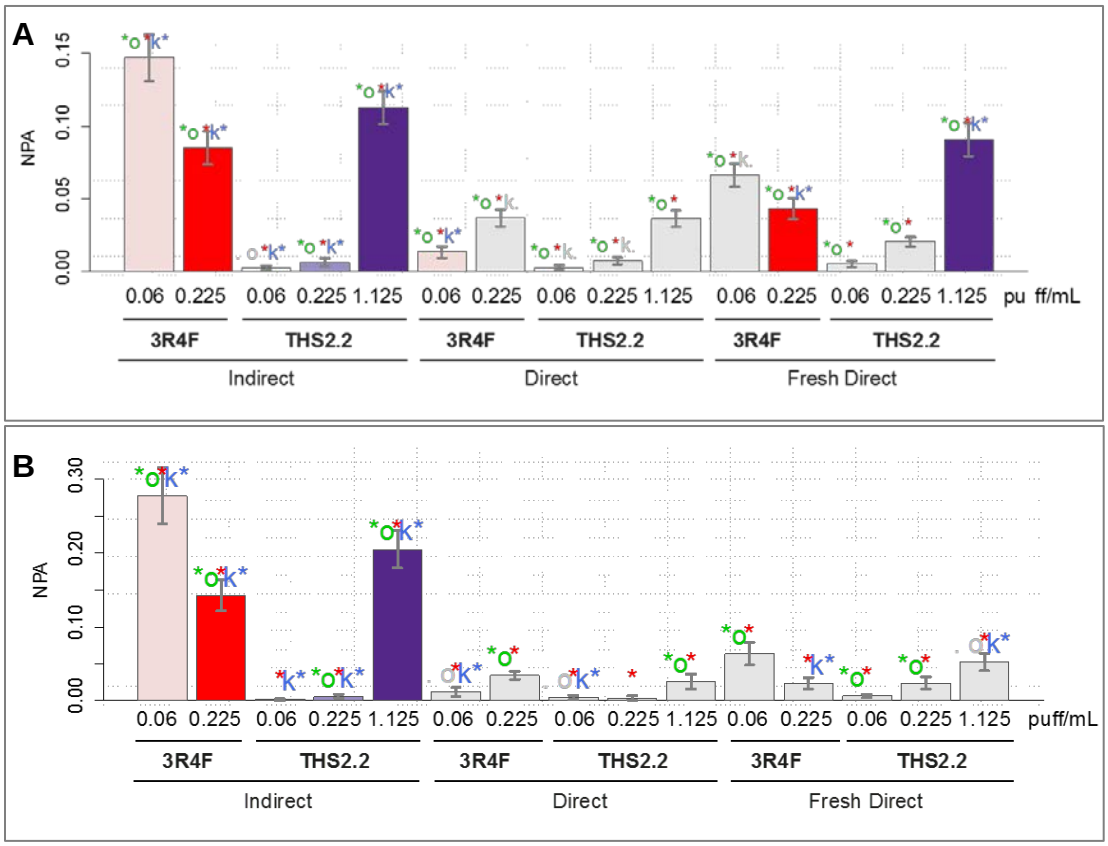


Figure 4. Relative network perturbation amplitude (NPA) scores of specific Cardiovascular Inflammatory Process Network (CV-IPN) subnetworks in human coronary arterial endothelial cells treated with 3R4F cigarette smoke and THS2.2 aerosol aqueous extracts

The relative NPA scores for the (A) Endothelial Cell Activation and (B) Endothelial Cell Monocyte Interaction subnetwork models are shown, with their confidence interval accounting for experimental variation. Percentages give the relative NPA score for the subnetworks compared with the reference (treatment comparison showing the highest perturbation). In addition, companion statistics derived to inform on the specificity of the NPA score with respect to the biology described in the respective subnetwork models are shown as *O and K*, respectively, if their *p*-values are below the significance level. Symbol legend:*, O and K statistic *p*-values <0.05; .O and K., *p*-values between 0.05 and 0.1.

Endothelial cell activation was further corroborated by examining the expression of various genes encoding CAMs including ICAM-1 and VCAM-1 which have previously been implicated in the promotion of monocyte adhesion to endothelial cells by CS (Scott & Palmer, 2003). Treatment of HCAECs with 3R4F CSE using the direct or fresh direct protocol did not lead to increased CAM gene expression. In contrast, indirectly treated HCAECs exhibited upregulation of several CAMs. In addition, there was little difference in CAM expression patterns between the two extracts, in particular, at the high THS2.2 AE concentration (Figure 5).

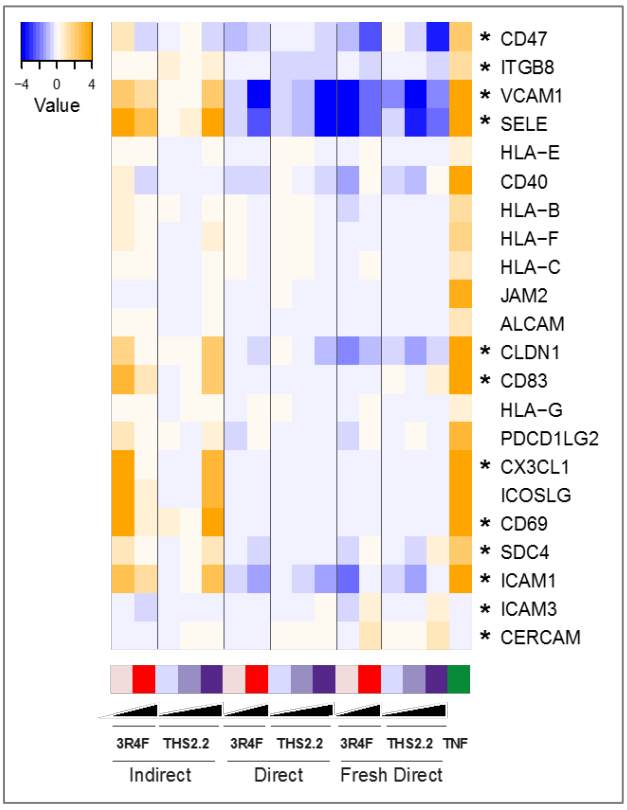


Figure 5. Altered expression levels of genes encoding cellular adhesion molecules (CAMs) in human coronary artery endothelial cells treated with 3R4F cigarette smoke and THS2.2 aerosol aqueous extracts

The heatmap depicts changes in gene expression for CAM-encoding genes (gene symbols listed on the left) relative to corresponding medium controls expressed as $\log_2$[fold change (value; fc)]. Upregulation and downregulation of gene expression levels are represented by orange and blue shades, respectively, with darker colors indicating greater absolute fold changes according to the color key. Statistically significant fold changes for at least one comparison excluding the tumor necrosis factor alpha (TNF) control, are highlighted by * (false discovery rate-adjusted $p<0.05$).

Subsequent gene set enrichment analysis revealed enriched gene sets related to TNF, cytokine signaling, NFκB, and CAMs, all of which are representative of an inflammatory response in the endothelium. Consistent with the network perturbation patterns, gene set

enrichment analysis also showed concentration-dependent increases with indirect treatment and no evident alterations with direct and fresh direct treatment modes.

Measurement of inflammatory marker proteins in the conditioned media of MM6 cells further confirmed the involvement of monocyte-derived factors in the activation of endothelial cells. Treatment with 3R4F CSE resulted in an increase in TNFα, soluble tumor necrosis factor receptor 2, and IL-8 (at the low concentration only), while concentrations of other mediators decreased. Treatment of MM6 cells with THS2.2 AE at low and medium concentrations had little or no effect on the production of pro-inflammatory mediator release, whereas treatment with THS2.2 AE at the high concentration also increased TNFα and soluble tumor necrosis factor receptor 2 secretion (Figure 6), suggesting that TNF signaling is a major driver of endothelial cell activation and monocyte adhesion.

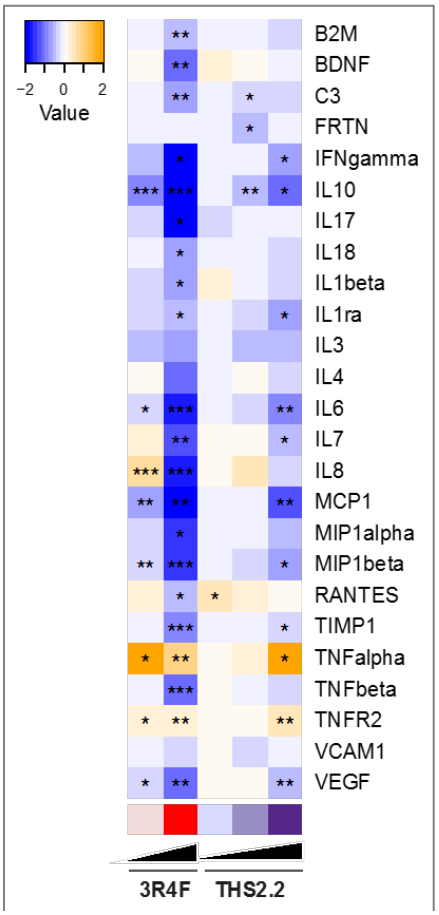


Figure 6. Alterations in inflammatory protein markers released into MM6 cell culture supernatants following treatment with 3R4F cigarette smoke and THS2.2 aerosol aqueous extracts

The heatmap depicts changes in inflammatory protein concentrations (protein symbols listed on the right) relative to corresponding medium controls expressed as $\log_2$[fold change (value; fc)]. Upregulation and downregulation of protein levels are represented by orange and blue shades, respectively, with darker colors indicating greater absolute fold changes according to the color key. * $p<0.05$, ** $p<0.01$, *** $p<0.001$ (unadjusted p-values are reported).

Examining the SRPs of MM6 cells, a concentration-dependent increase in DEGs with both THS2.2 AE and 3R4F CSE was observed. While a greater number of DEGs was identified following treatment of MM6 cells with 3R4F CSE, there were either no or only a few genes significantly deregulated in MM6 cells treated with the low and intermediate concentrations of THS2.2 AE, respectively. Only treatment with an approximately 20-times higher concentration of THS2.2 extract led to a similar number of DEGs as that observed with the low concentration of 3R4F CSE. Of note, MM6 cell viability decreased by ~25–30% at the high concentration for both reference and test items, indicative of cytotoxic effects.

The strongest biological impact was elicited in MM6 cells treated with 3R4F CSE at the low concentration (RBIF = 100%; REF). In comparison, the impact of MM6 cell treatment with THS2.2 AE was less severe, and even though it increased in a dose-dependent manner, it remained smaller than that observed with the low concentration of 3R4F CSE.

Nearly all networks were affected by the treatment of MM6 cells with 3R4F CSE, with significant perturbations seen in the networks capturing cell fate, proliferation, stress and inflammatory mechanisms. In MM6 cells treated with THS2.2 AE at low and intermediate concentrations, significant perturbations were noted in the Senescence, Necroptosis, Cell Stress and Cell Proliferation networks, and these had a noticeably lower amplitude than those seen in MM6 cells treated at matching 3R4F CSE concentrations. However, treatment of MM6 cells with THS2.2 AE at the highest concentration caused more wide-spread network perturbations, additionally leading to significant perturbations in networks reflecting the biology of macrophage activation and differentiation (Figure 7).

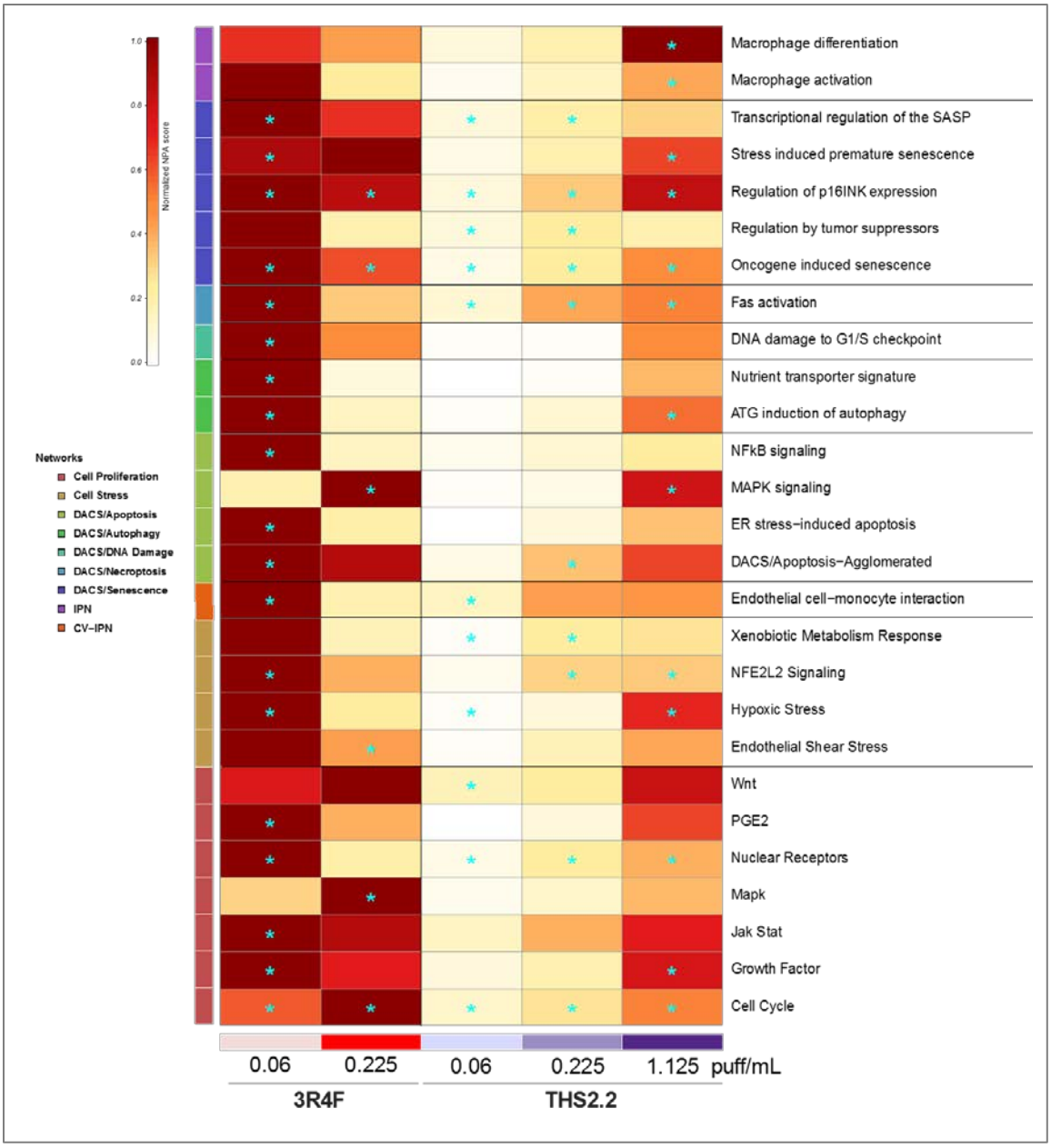


Figure 7. Network perturbations in MM6 cells following treatment with 3R4F cigarette smoke and THS2.2 aerosol aqueous extracts

Heatmap of network perturbation amplitude (NPA) scores summarizing subnetworks that were significantly perturbed in at least one treatment. A network is considered perturbed if, in addition to the significance of the NPA score with respect to the experimental variation, the two companion statistics (O and K) derived to inform on the specificity of the NPA score with respect to the biology described in the network, are significant. Significantly perturbed networks are indicated by * (i.e. O and K statistic *p*-values <0.05 and significant with respect to the experimental variation). Abbreviations: DACS, DNA damage, autophagy, cell death, and senescence; IPN, Inflammatory Process Network; CV-IPN, Cardiovascular Inflammatory Process Network.

In summary, 3R4F CSE promoted the adhesion of monocytic cells to endothelial cells via distinct mechanisms. At matching concentrations, THS2.2 aerosol extract did not trigger MM6 cell–HCAEC adhesion and clearly showed reduced impact on HCAECs and MM6 cells at the molecular level. MM6 cell–HCAEC adhesion accompanied by molecular changes in both cell types reached similar magnitude increases as those induced by 3R4F CSE only when concentrations of THS2.2 aerosol extract were 10- and 20-times higher for fresh direct and indirect exposure modes, respectively (Poussin et al, 2016).

3.3.1.2 Transendothelial Migration Assay

The *in vitro* transendothelial migration (TEM) assay was used to examine the differential effects of 3R4F CSE and THS2.2 AE on the capability of monocytic THP-1 cells to traverse an endothelial cell layer. Two different approaches were used in this study. In the first approach, serum-starved THP-1 cells were pre-stimulated for 4 hours with freshly prepared aqueous extracts. THP-1 cells were then washed and subjected to a series of CXCL12-mediated chemotaxis assays. In the second approach, confluent monolayers of HCAECs grown on the membranes of conventional Boyden or cell invasion/migration (CIM) chambers were pre-stimulated for 4 hours with freshly prepared extracts. The HCAEC monolayer was subsequently washed, followed by examination of conventional and real-time impedance-based CXCL12-mediated TEM of the THP-1 cells.

In the absence of HCAECs, concentration-dependent migration towards CXCL12 was induced without THP-1 cells adhering to the lower side of the CIM membrane, as indicated by the lack of an impedance signal. In the presence of a HCAEC monolayer, THP-1 cells transmigrated through the endothelial cell layer, traversed the CIM membrane, and adhered to its lower side thereby increasing impedance signals. These findings indicated that adhesion to endothelial cells preceded the passage of monocytes through the endothelial cell layer. IL-8 and TNFα levels increased in culture supernatants of treated THP-1 cells in a dose-dependent manner, albeit at a lower rate in THS2.2 AE compared with 3R4F CSE treatments, suggesting that monocytes acquired a pro-inflammatory phenotype (Figure 8).

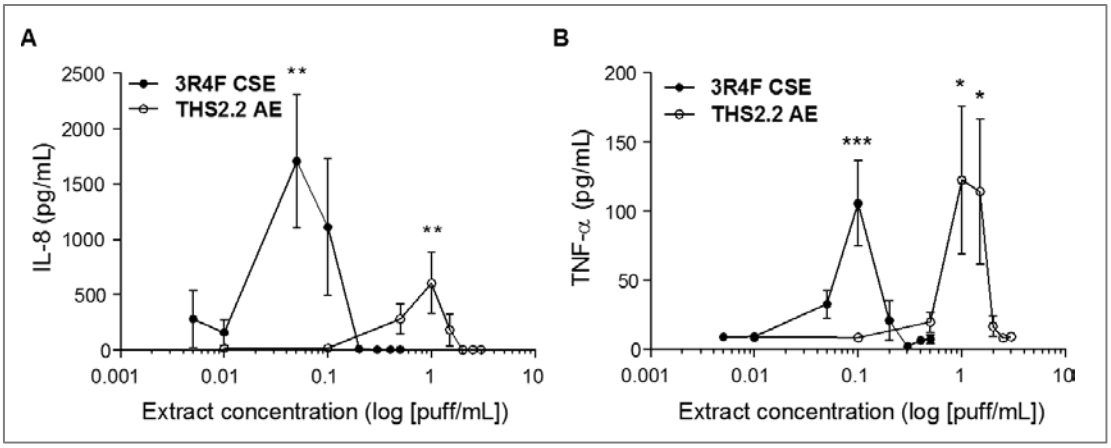


Figure 8. Altered cytokine levels in the supernatants of THP-1 cells treated with 3R4F cigarette smoke and THS2.2 aerosol aqueous extracts

Levels of (A) IL-8 and (B) TNFα in the supernatants of THP-1 cells treated with 3R4F CSE (filled circles) and THS2.2 AE (open circles). Data are mean ± SEM of four independent experiments. ∗ $p<0.05$, ∗∗ $p<0.01$, ∗∗∗ $p<0.001$ (relative to control) using the Dunnett's multiple comparison test.

Pre-treatment of THP-1 cells with either extract significantly inhibited CXCL12-stimulated chemotaxis in a concentration-dependent manner. Pre-treatment of THP-1 cells also decreased TEM rate in a concentration-dependent manner (Figure 9), similar to previous observations (Giunzioni et al, 2014; van der Toorn et al, 2015b). However, THS2.2 AE was approximately 50-times less effective than 3R4F CSE in inhibiting chemotaxis and about 18-times less effective in slowing TEM. Experimental data also indicated rapid concentration-dependent disruption of endothelial barrier integrity, with 3R4F CSE being more potent than THS2.2 extract in reducing impedance.

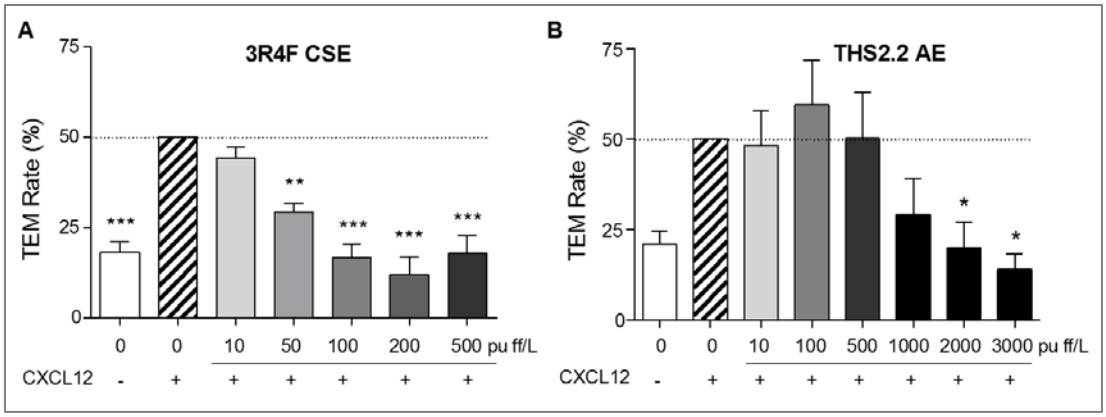


Figure 9. Effect of 3R4F cigarette smoke and THS2.2 aerosol extract on THP-1 monocyte transendothelial migration

Transendothelial migration of THP-1 cells treated with (A) 3R4F CSE or (B) THS2.2 AE in cell invasion/migration chambers. The CXCL12 concentration that induced 50% migration, indicated by the dotted line, was used in these assays (EC_{50}). Data are mean ± SEM of four independent experiments. ∗ $p<0.05$, ∗∗ $p<0.01$, ∗∗∗ $p<0.001$ (relative to control) using the Dunnett's multiple comparison test.

In summary, these results indicated that both CXCL12 and a functional monolayer of HCAECs are required for monocytes to differentiate and acquire an adhesive phenotype. Furthermore, extracts from 3R4F reference CS or THS2.2 aerosol induced concentration-dependent responses in endothelial barrier function, chemotaxis, and transendothelial migration. However, the effect of THS2.2 AE treatment was considerably weaker than that of 3R4F CSE treatment (van der Toorn et al, 2015a).

3.3.1.3 THS2.2 Aerosol Fraction Impact Assessment Study

Multiple parameters indicative of cell health, genotoxicity and cell stress were tested in normal human bronchial epithelial cells (NHBECs) grown in submerged culture and treated with a range of different doses of aqueous extract (CSE/AE), total particulate matter (TPM), or gas-vapor phase (GVP) from 3R4F reference cigarettes and THS2.2 heat sticks using real-time impedance and high-content screening. The different fractions were then further evaluated with respect to their impact on the NHBEC transcriptome.

Exposure of NHBECs to 3R4F CSE for 4 hours gradually increased the number of DEGs in a dose-dependent manner. In contrast, a 4-hour exposure to THS2.2 aerosol extract at comparable doses did not significantly change gene expression, and only 28 DEGs were identified for NHBECs treated with THS2.2 AE at a concentration 3.5-fold higher than the highest 3R4F dose tested. Prolonged exposure to 3R4F CSE for 24 hours did not significantly alter gene expression nor did treatment with THS2.2 AE at comparable doses. Only treatment at the highest THS2.2 AE concentration caused changes to the expression of a small number of genes. The numbers of DEGs in cells treated with 3R4F GVP at low and high concentrations also increased, while 4-hour treatment with the medium concentration only elicited a small effect. In contrast, short treatment with THS2.2 GVP at the low concentration induced fewer gene expression changes, and no DEGs were found following a 4-hour treatment with higher doses of THS2.2 GVP. However, in NHBECs treated with THS2.2 GVP at a concentration 3.5-times that of the

highest 3R4F GVP concentration for 4 hours, a few DEGs were seen. After 24 hours of exposure to 3R4F GVP, no significant changes in gene expression were detected (excluding the highest concentration because of high cytotoxicity). Similar observations were made in NHBECs treated with medium and high doses of THS2.2 GVP, while results with the lowest concentration paralleled those of the 4-hour treatment. Furthermore, SRPs from NHBECs treated with TPM indicated a dose-dependent increase in significantly altered genes following 3R4F treatment for 4 hours, and prolonged 3R4F exposure further increased the number of DEGs. In comparison, treatment of NHBECs with THS2.2 TPM for 4 hours only resulted in two significantly altered genes, while there were no DEGs at the 24-hour time point.

Examining these data further using the threshold-free network approach highlighted the strongest biological impact for the 4-hour treatment with the highest concentration of 3R4F TPM (RBIF = 100%; REF). At comparable doses, treatment with 3R4F CSE for 4 hours elicited a stronger impact than treatment with THS2.2 AE, causing perturbations in proliferation, cell stress, and senescence networks. Such perturbations were also noted for the lower 3R4F CSE concentrations, albeit with a much weaker impact. At 24 hours, RBIF values for both reference and test items were lower than at the 4-hour time point. Nevertheless, the biological impact of exposure to THS2.2 extract was lower than that of exposure to 3R4F CSE at this time point (Figure 10).

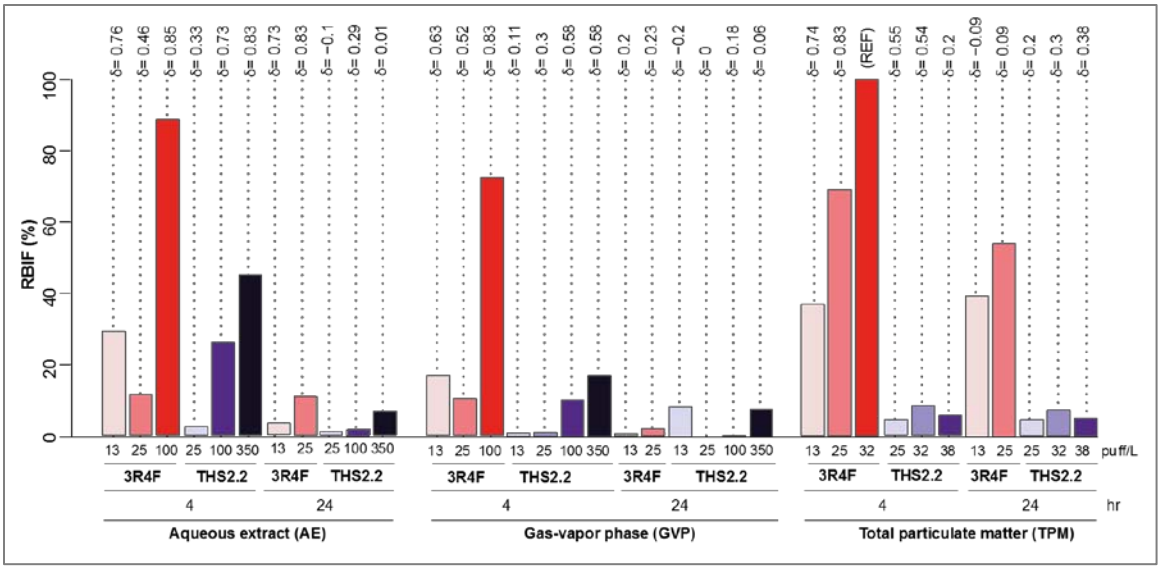


Figure 10. Network model-based analysis of the biological impact factor (BIF) in normal human bronchial epithelial cells following exposure to 3R4F cigarette smoke and THS2.2 aerosol fractions

The bar plot depicts BIF values relative to the maximum response (RBIF = 100%, REF). The δ values (−1 to 1) indicate how similar the underlying network perturbations are with respect to the REF. Scores were computed using transcriptomics profiling data from NHBE cells exposed to vehicle, aqueous extracts (AE), gas-vapor phase (GVP), or total particulate matter (TPM) from 3R4F cigarette smoke (red bars) or THS2.2 aerosol (purple bars) for 4 or 24 hours.

Network perturbations that contributed most to the observed impact of 3R4F GVP at 4 hours predominantly occurred in networks describing cell stress, proliferation, and senescence biology. In cells treated for 24 hours with this fraction, Cell Stress and Proliferation networks continued to be most perturbed, albeit to a smaller extent. By comparison, the impact of THS2.2 GVP on NHBECs was considerably less than that observed for 3R4F GVP at comparable concentrations, independent of the treatment time. Similar, but far more moderate, perturbations were noted in THS2.2 GVP-treated NHBECs. Perturbations in the Epithelial Mucus Hypersecretion and Epithelial Innate Immune Activation subnetworks contributed the most to the IPN perturbations in NHBECs treated with either GVP fraction for 4 hours, with the underlying biology being very similar between 3R4F and THS2.2 GVP. Prolonged treatment with GVP, however, did not further increase these network perturbations (Figure 11).

Short-term treatment with 3R4F TPM at the low dose significantly perturbed all networks except the Necroptosis subnetwork. Networks capturing the mechanisms of cell proliferation, inflammation, and cell stress responses contributed the most to the TPM-induced biology. Among the IPN subnetworks, Epithelial Mucus Hypersecretion and Epithelial Innate Immune Activation contributed the most to the IPN perturbations. Prolonged treatment with 3R4F TPM did not result in further amplification; instead, the Tissue Damage subnetwork was also significantly impacted. In comparison, in THS2.2 TPM-treated NHBECs, independent of treatment duration, IPN, Cell Stress and Cell Fate

networks were the most perturbed, albeit to a smaller extent than in 3R4F TPM-treated cells (Figure 11).

Treatment with 3R4F CSE elicited a strong impact on networks capturing mechanisms related to cell fate, cell proliferation and cell stress in addition to impacting all IPN subnetworks, most notably at the highest concentration and the shorter treatment duration. Extended treatment with 3R4F CSE, however, only had a small effect on network biology. At comparable concentrations, treatment with THS2.2 AE caused similar perturbations of a considerably lower amplitude. Treatment of NHBECs with THS2.2 AE at a concentration 10-times that of 3R4F CSE had an increased impact on the networks, still exhibiting the same underlying mechanisms found to drive 3R4F CSE-related network perturbations. Twenty-four-hour treatment with THS2.2 AE also did not amplify those perturbations further, but reduced them (Figure 11).

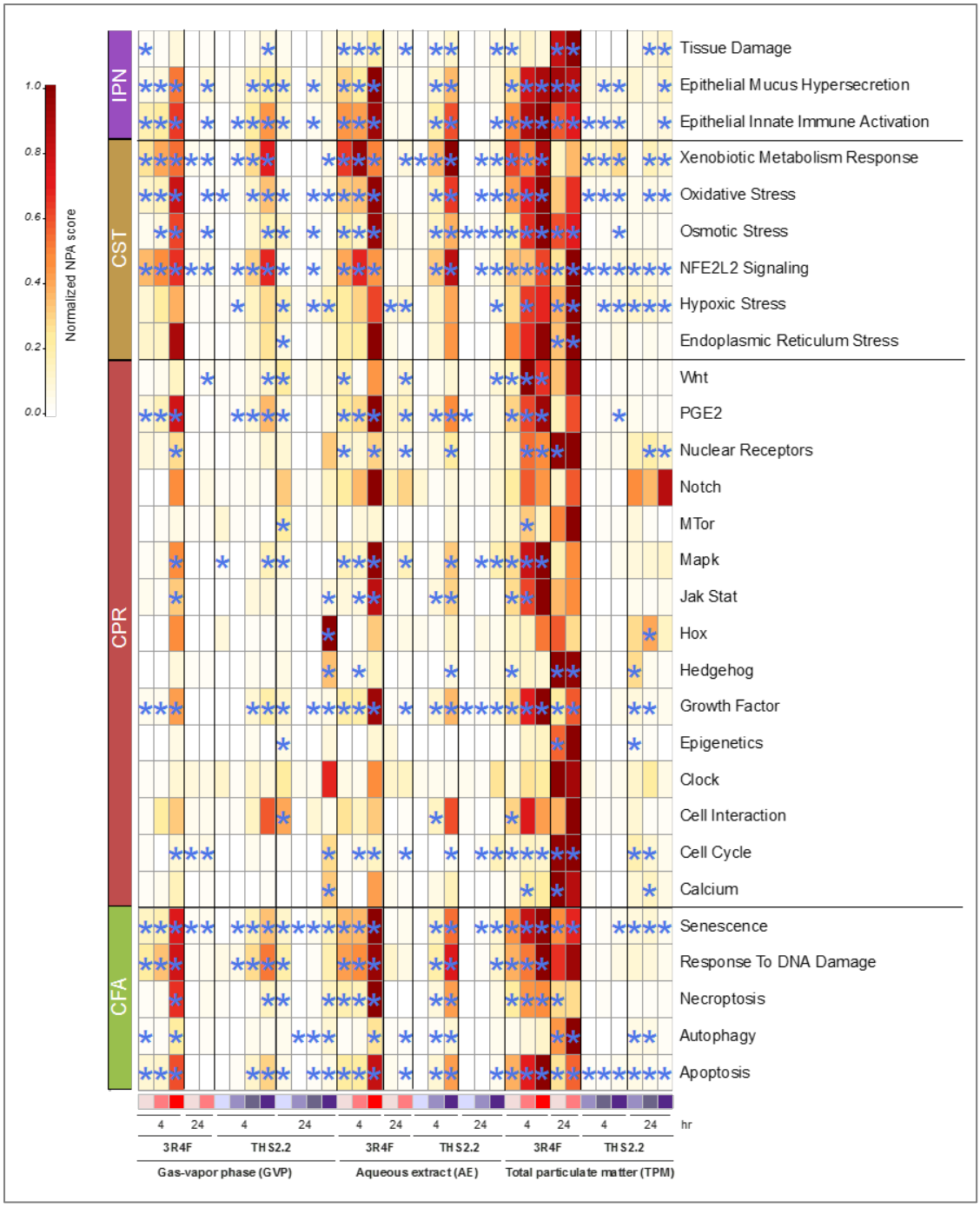


Figure 11. Network perturbations in normal human bronchial epithelial cells following exposure to 3R4F smoke and THS2.2 aerosol fractions

Heatmap of network perturbation amplitude (NPA) scores summarizing subnetworks that were significantly perturbed in at least one treatment. A network is considered perturbed if, in addition to the significance of the NPA score with respect to the experimental variation, the two companion statistics (O and K) derived to inform on the specificity of the NPA score with respect to the biology described in the network, are significant. Significantly perturbed networks are indicated by * (i.e. O and K statistic *p*-values <0.05 and significant with respect to the experimental variation). Abbreviations: CFA, Cell Fate; CPR, Cell Proliferation; CST, Cell Stress; IPN, Inflammatory Process Network.

Taken together, these results showed that fractions of 3R4F CS have a much greater potential to induce cytotoxicity and various stress responses including a sustained inflammatory response in NHBECs compared with fractions derived from THS2.2 aerosol. 3R4F cigarette smoke-derived TPM exerted the highest biological impact on primary human airway epithelial cells, while 3R4F GVP and CSE had a comparably lower biological impact. While this tendency was also observed for the different THS2.2 aerosol-derived fractions, the overall impact these fractions elicited on NHBECs was markedly smaller than the impact seen following treatment with the 3R4F fractions (Gonzalez-Suarez et al, 2016).

3.3.1.4 Oral Organotypic Study

To understand and compare the biological impacts of THS aerosol and 3R4F CS exposures in physiologically relevant systems representative of the human upper airway, human organotypic EpiOral™ cultures (MatTek Corp., Ashland, MA, USA) were exposed for 28 minutes to air; to 15% or 24% (v/v in air) 3R4F mainstream smoke, equivalent to a target concentration of 0.32 or 0.54 mg/L nicotine, respectively; or to 25%, 34%, or 69% (v/v in air) aerosol from THS, corresponding to target nicotine concentrations of 0.31, 0.46, or 1.09 mg/L, respectively. Cytotoxicity and SRPs were assessed at 4, 24, 48 and 72 hours following exposure. Several inflammatory mediators released into the culture supernatants were quantified at 24, 48 and 72 hours and tissue integrity was evaluated at 48 and 72 hours post-exposure.

Exposure of EpiOral™ tissues to 3R4F CS resulted in tissue injury, as evidenced by keratinization and desquamation, which was most prominent at the higher concentration and later time point. In contrast, THS2.2 aerosol-exposed cultures showed a strongly attenuated response. The cytotoxicity assay gave comparable results. Cultures exposed to 3R4F CS secreted higher levels of inflammatory mediators than those exposed to air. Far fewer and less pronounced changes in levels of these mediators were observed in oral tissues exposed to THS2.2 aerosol at comparable or even higher nicotine levels.

At the 72-hour post-exposure time point, 3R4F CS exposure at the lowest dose produced the highest impact on the cultures (RBIF = 100%; REF). Shorter post-exposure times also elicited a high biological impact, which initially declined during the post-exposure period, but rose again at 72 hours post-exposure. Overall lower BIF values were observed for all THS2.2 concentrations at the different post-exposure time points compared with the corresponding 3R4F exposure groups (Figure 12).

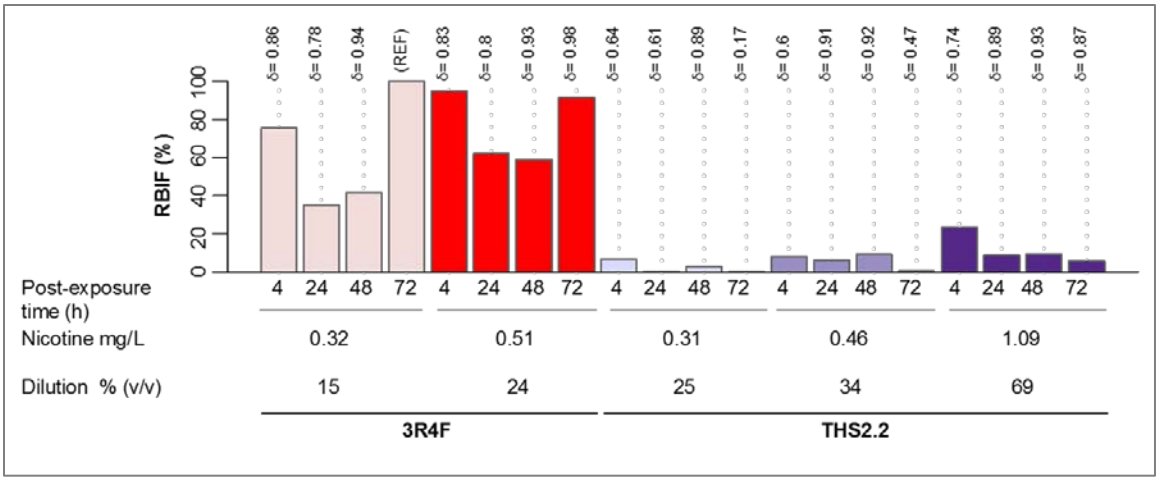


Figure 12. Network model-based analysis of the biological impact factor (BIF) in EpiOral™ tissues following exposure to 3R4F cigarette smoke and THS2.2 aerosol compared with air controls

The bar plot depicts BIF values relative to the maximum response (RBIF = 100%, REF). The δ values (−1 to 1) indicate how similar the underlying network perturbations are with respect to the REF. Scores were computed using transcriptomics profiling data from EpiOral™ tissues that were exposed to air, 3R4F cigarette smoke (red bars), or THS2.2 aerosol (purple bars) for 28 minutes and collected at 4, 24, 48 or 72 hours post-exposure.

Examining the affected networks contributing to the observed biological impact of exposure to 3R4F CS indicated perturbations in the majority of networks. Mirroring the BIF pattern, the impact of 3R4F CS exposure, independent of concentration, decreased at 24 and 48 hours post-exposure, and increased again at 72 hours. Exposure of EpiOral™ tissues to 3R4F CS affected all Cell Fate subnetworks describing the biology of senescence, necroptosis and apoptosis, but also had an effect on some of the IPN subnetworks. The Cell Proliferation network family was less affected, with fewer statistically significantly altered subnetworks. Of note, with the exception of the Endoplasmic Reticulum Stress subnetwork, CS exposure also impacted all Cell Stress subnetworks including Oxidative Stress and NFE2L2 signaling (Figure 13). By contrast, THS2.2 aerosol exposure at comparable nicotine concentrations did not result in substantial perturbations of the same networks. In general, the observed perturbations exhibited a markedly lower amplitude (NPA score), and EpiOral™ tissues exhibited broad network perturbations only at the highest nicotine concentration at all post-exposure time points. Nevertheless, the extent of those perturbations was lower compared with the impact of the highest concentration 3R4F CS at corresponding post-exposure time points (Figure 13).

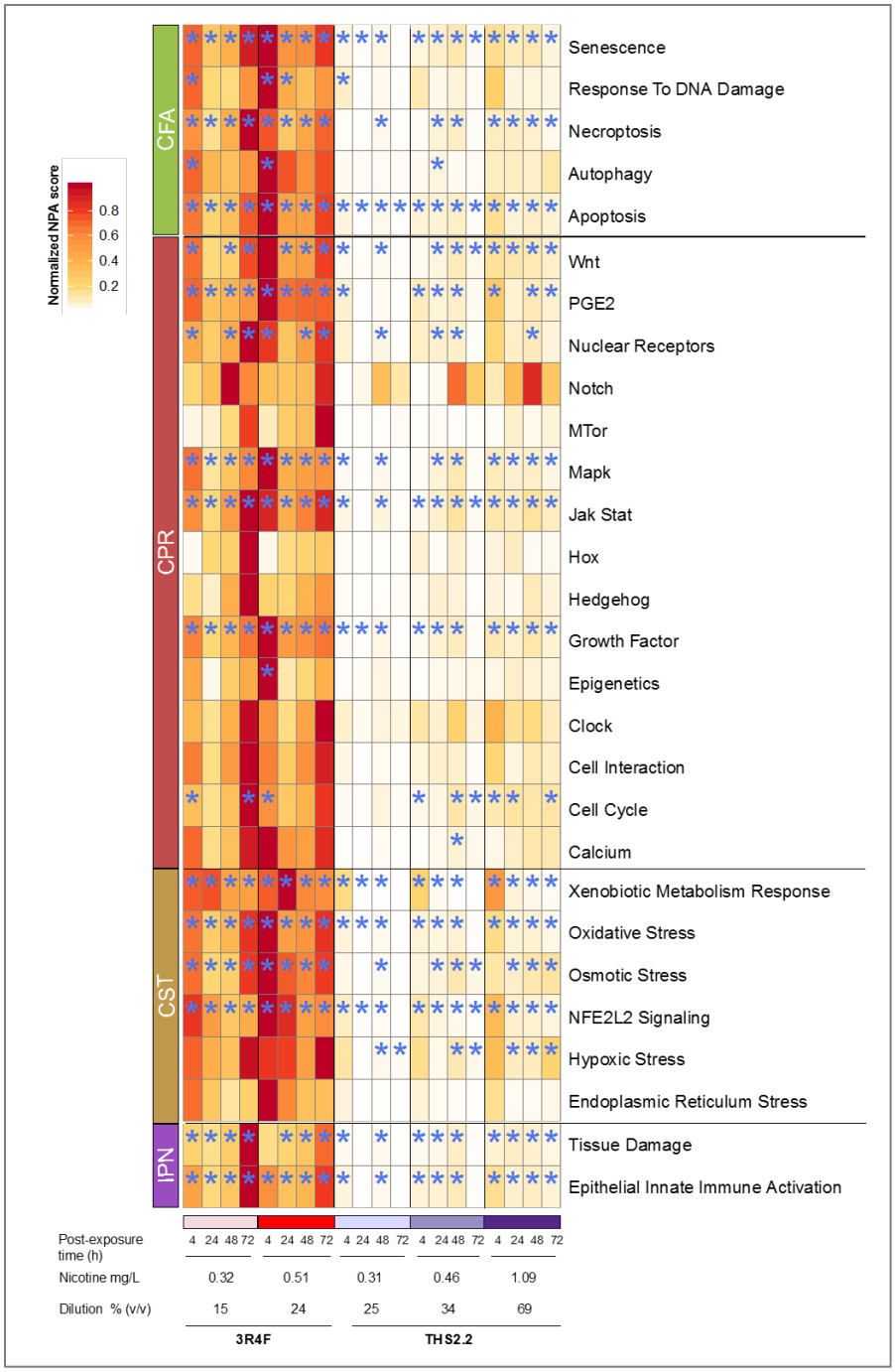


Figure 13. Network perturbations in EpiOral™ tissues following exposure to 3R4F cigarette smoke and THS2.2 aerosol compared with air controls

Heatmap of network perturbation amplitude (NPA) scores summarizing subnetworks that were significantly perturbed in at least one treatment. A network is considered perturbed if, in addition to the significance of the NPA score with respect to the experimental variation, the two companion statistics (O and K) derived to inform on the specificity of the NPA score with respect to the biology described in the network, are significant. Significantly perturbed networks are indicated by * (i.e. O and K statistic *p*-values <0.05 and significant with respect to the experimental variation). Abbreviations: CFA, Cell Fate; CPR, Cell Proliferation; CST, Cell Stress; IPN, Inflammatory Process Network.

The IPN subnetworks Tissue Damage and Epithelial Innate Immune Activation were most strongly affected by 3R4F CS, while THS2.2 aerosol exposure had a much lower impact on these mechanisms. The high amplitude of perturbation, in particular at 72 hours following 3R4F CS exposure, also indicated that the CS-related effects did not subside over time which was in agreement with histopathological findings of advanced tissue injury. In contrast, at that time point, the small impact of THS2.2 aerosol exposure had even further decreased, suggesting that inflammatory processes were not sustained over a long period of time (Figure 14).

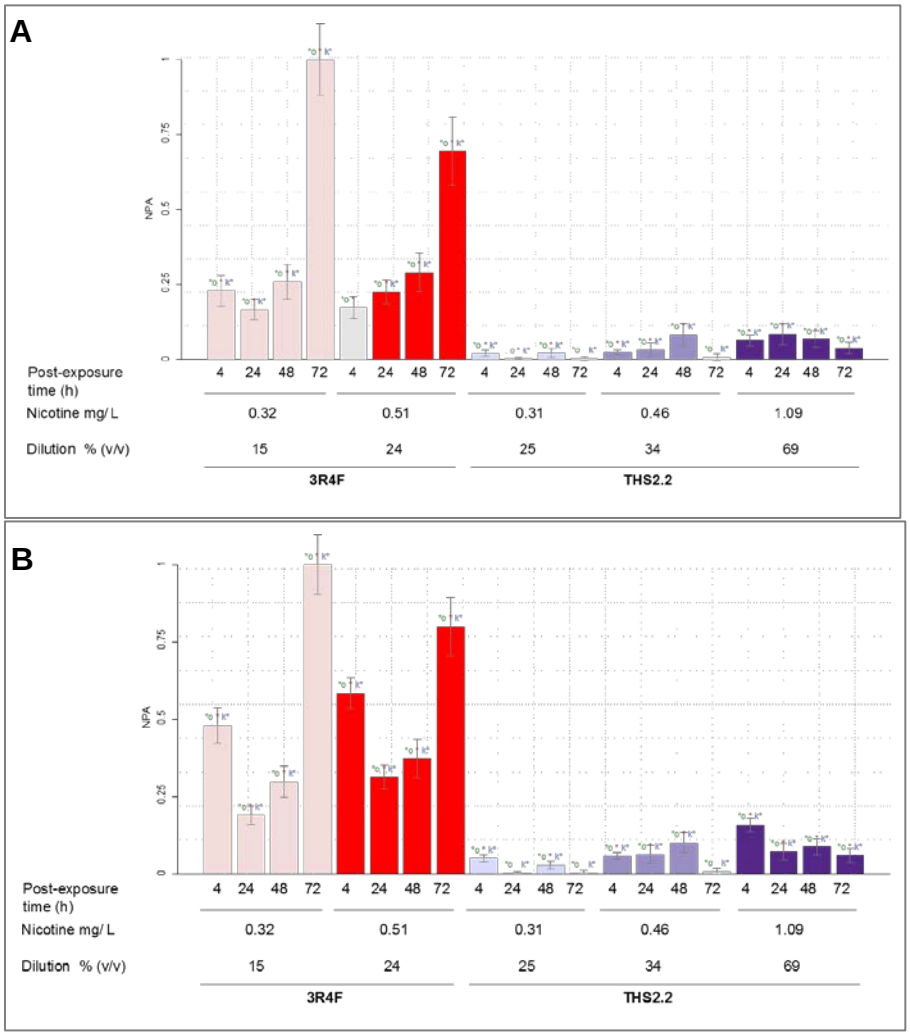


Figure 14. Relative network perturbation amplitude (NPA) scores of specific Inflammatory Process Network (IPN) subnetworks in EpiOral™ tissues following exposure to 3R4F cigarette smoke and THS2.2 aerosol

The relative NPA scores for the (A) Tissue Damage and (B) Epithelial Innate Immune Activation subnetwork models are shown with their confidence interval accounting for experimental variation. The percentages give the relative NPA score for the subnetworks compared with the reference (treatment comparison showing the highest perturbation). In addition, companion statistics derived to inform on the specificity of the NPA score with respect to the biology described in the respective subnetwork models are shown as *O and K*, respectively, if their p-values are below the significance level. Symbol legend: *, O and K statistic *p*-values <0.05; .O and K., *p*-values between 0.05 and 0.1.

3R4F CS-exposure substantially altered expression levels of genes implicated in the epithelial inflammatory response, including *IL1A*, *IL1B*, *CTGF* (connective tissue growth factor), *PTGS2* (prostaglandin-endoperoxide synthase 2; Cox-2), *MMP1* (matrix metalloprotease 1), *MMP10*, and *CXCL14*. In contrast, at comparable nicotine concentrations, THS2.2 aerosol exposure minimally influenced the expression of these genes, if at all, and significant changes were observed only for *IL1A* and *IL1B* at the early post-exposure time point and for *MMP1* and *MMP10* 48 hours post-exposure. Exposure of EpiOral™ tissues to the high nicotine concentration of THS2.2 aerosol also increased mRNA levels of these genes, albeit at a lower degree compared with 3R4F CS-exposed cultures. In addition, a small number of other genes whose expression levels were modified following 3R4F CS exposure (e.g., *CTGF*, *PTGS2*, and *CXCL14*) were also deregulated by THS2.2 aerosol exposure at the high dose (Figure 15).

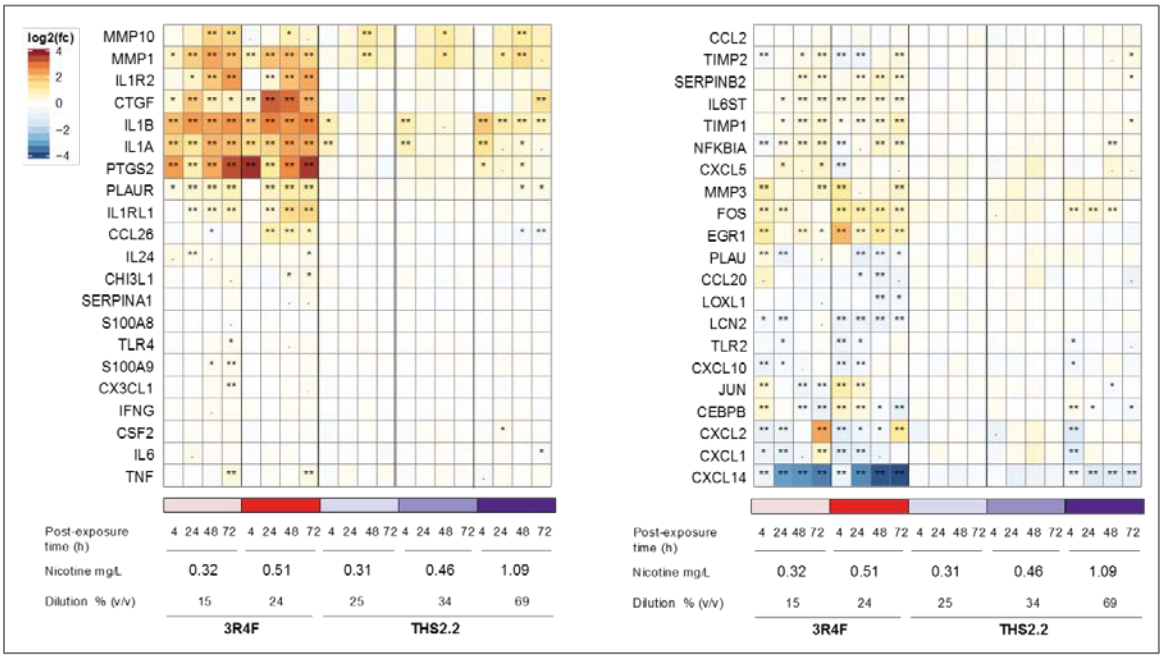


Figure 15. Altered expression levels of genes linked to inflammation in EpiOral™ tissues following exposure to 3R4F cigarette smoke and THS2.2 aerosol

The heatmap depicts changes in gene expression of inflammation-related genes (gene symbols listed on the left) relative to corresponding air-exposed controls expressed as $\log_2$[fold change (value; fc)]. Upregulation and downregulation of gene expression levels are represented by orange and blue shades, respectively, with darker colors indicating greater absolute fold changes. Statistically significant fold changes are highlighted by ** (adjusted $p<0.05$) and * (adjusted $p<0.1$).

Analysis of soluble mediator concentrations in the basolateral medium of 3R4F CS-exposed EpiOral™ tissues revealed increased IL-1β and MMP-1 production in addition to increased VEGFA and transforming growth factor alpha levels, providing further evidence of an inflammatory response to exposure. While these mediators also increased

in conditioned media of THS2.2 aerosol-exposed cultures (at comparable nicotine concentrations), changes relative to controls were generally less than 2-fold. In addition, levels of IL-6, CXCL8 (IL-8), colony-stimulating factor (CSF)2, and CXCL10 decreased in 3R4F CS-exposed oral tissues, while THS2.2 aerosol exposure at nicotine concentrations above 0.31 mg/mL only reduced CXCL10 concentrations (Figure 16).

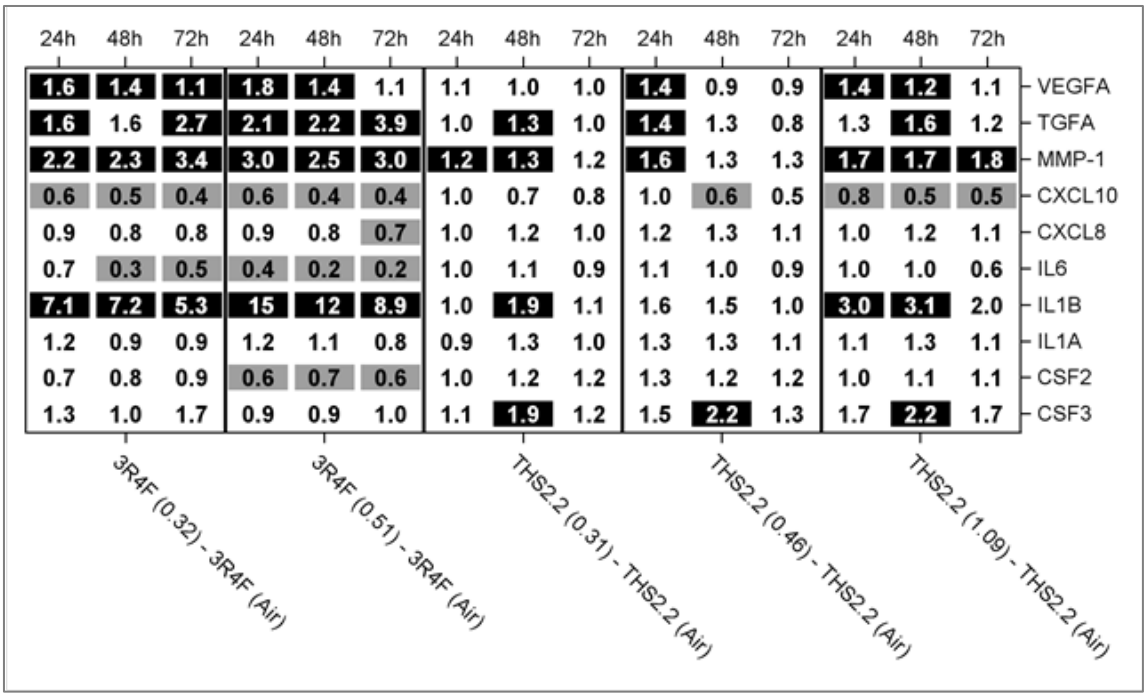


Figure 16. Altered levels of inflammation protein markers in conditioned media of EpiOral™ tissues following exposure to 3R4F cigarette smoke and THS2.2 aerosol

The heatmap depicts fold changes in the amounts of soluble inflammation protein markers (symbols listed on the left) relative to corresponding air-exposed controls expressed as $\log_2$[fold change (value; fc)]. Dark and light grey shading indicates significant increases and decreases, respectively, between the comparisons ($p<0.05$).

In summary, these results showed that exposure of human oral organotypic tissues to 3R4F CS resulted in time- and dose-dependent cytotoxicity, tissue damage and an inflammatory response. In contrast, the effects of exposure to matching concentrations of THS2.2 aerosol were only transient, eliciting far less extensive responses (Zanetti et al, 2016).

3.3.1.5 Nasal Organotypic Study

In addition to studies using oral 3D cultures, the impact of exposure to 3R4F CS and THS2.2 aerosol was also investigated using 3D organotypic models of the nose. For this purpose, human nasal MucilAir™ organotypic tissue cultures (Epithelix Sarl, Geneva, Switzerland) were exposed to 8% and 15% (v/v in air) 3R4F mainstream smoke

equivalent to a target concentration of 0.15 or 0.25 mg/L nicotine, respectively, or to 15%, 24%, and 31% (v/v in air) aerosol from THS2.2 corresponding to target nicotine concentrations of 0.15, 0.27, and 0.44 mg/L, respectively, for 28 minutes. Cytotoxicity, tissue integrity and transcriptome profiles were assessed at 4, 24, 48 and 72 hours following exposure, and the release of inflammatory mediators into cell culture supernatants was evaluated at 24, 48 and 72 hours post-exposure.

While exposure to 8% 3R4F CS induced no or only little cytotoxicity, exposure to 15% 3R4F CS elicited extensive tissue damage at 24, 48, and 72 hours post-exposure. Similar to fresh air exposure, exposure to various concentrations of THS2.2 aerosol did not induce any cytotoxicity. Histological examination confirmed that exposure to 3R4F CS resulted in more tissue damage than did exposure to THS2.2 aerosol, and that the exposed tissues exhibited less extensive damage at 48 hours than at 72 hours post-exposure. Since exposure to a high concentration of 3R4F CS (15%) was detrimental to nasal organotypic cultures and led to tissue loss, detachment from the membrane, and development of regions of a squamous phenotype at 48 and 72 hours post-exposure, these tissues were excluded from further systems biology analysis.

Using a threshold-free computational network approach, the strongest biological impact was detected 4 hours post-exposure in nasal MucilAir™ tissues exposed to 8% 3R4F CS (RBIF = 100%; REF), and this impact decreased over the 72-hour post-exposure period. In contrast, the impact on nasal tissues at 4 hours following exposure to THS2.2 aerosol at matched nicotine concentrations was only a fraction of that seen following exposure to 3R4F CS, and the effects diminished rapidly with further post-exposure. When nasal tissues were exposed to higher concentrations of THS2.2 aerosol, the biological impact observed at 4 hours post-exposure was somewhat more extensive than at the lower dose, reaching RBIF values of 28% and 41% at THS2.2 aerosol doses of 24% and 31%, respectively. Again, the RBIF values decreased rapidly and markedly when post-exposure was prolonged (Figure 17).

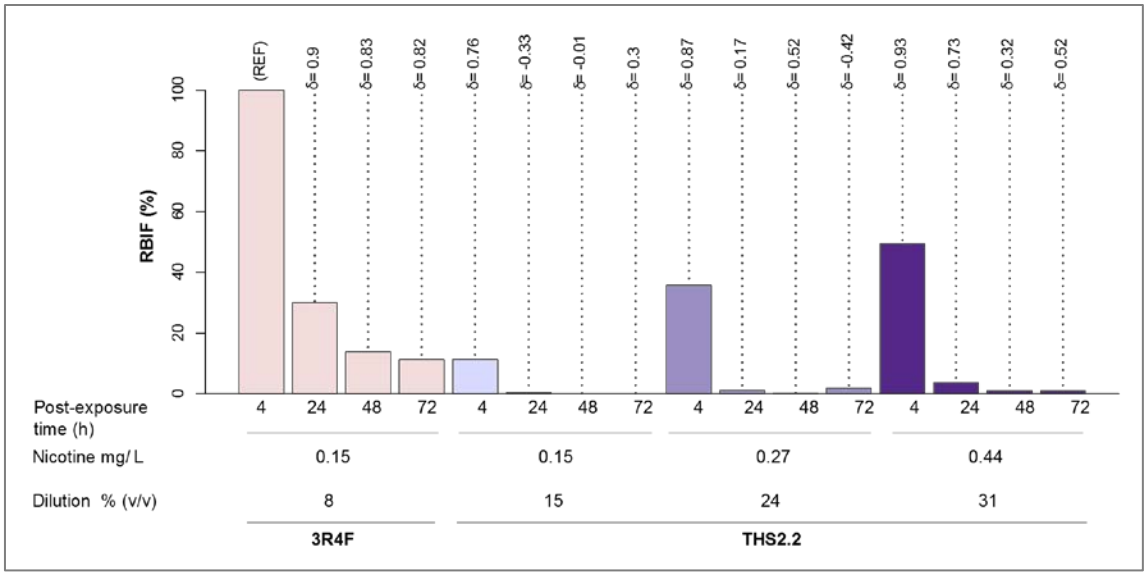


Figure 17. Network model-based analysis of the biological impact factor (BIF) in nasal MucilAir™ tissues following exposure to 3R4F cigarette smoke and THS2.2 aerosol compared with air controls

The bar plot depicts BIF values relative to the maximum response (RBIF = 100%, REF). The δ values (−1 to 1) indicate how similar the underlying network perturbations are with respect to the REF. Scores were computed using transcriptomics profiling data from nasal MucilAir™ tissues that were exposed to air, 3R4F cigarette smoke (red bars), or THS2.2 aerosol (purple bars) for 28 minutes and collected at 4, 24, 48 or 72 hours post-exposure.

Exposure to 3R4F CS caused significant perturbations predominantly in networks capturing the biology of senescence, apoptosis, DNA damage, MAPK and Jak/Stat-mediated cell proliferation, cell stress responses and those reflecting inflammatory processes in the epithelium. Of note, at matching nicotine concentrations, exposure of nasal MucilAir™ tissues to THS2.2 aerosol affected far fewer networks, and significant perturbations in the Cell Fate network and IPN were restricted to the early post-exposure time point. At the highest THS2.2 aerosol concentrations, network perturbations similar to those caused by exposure to 3R4F were observed, and they also persisted throughout the post-exposure period. However, with very few exceptions, the extent of these perturbations was noticeably smaller than that of the network perturbations seen with 3RF CS exposure (Figure 18).

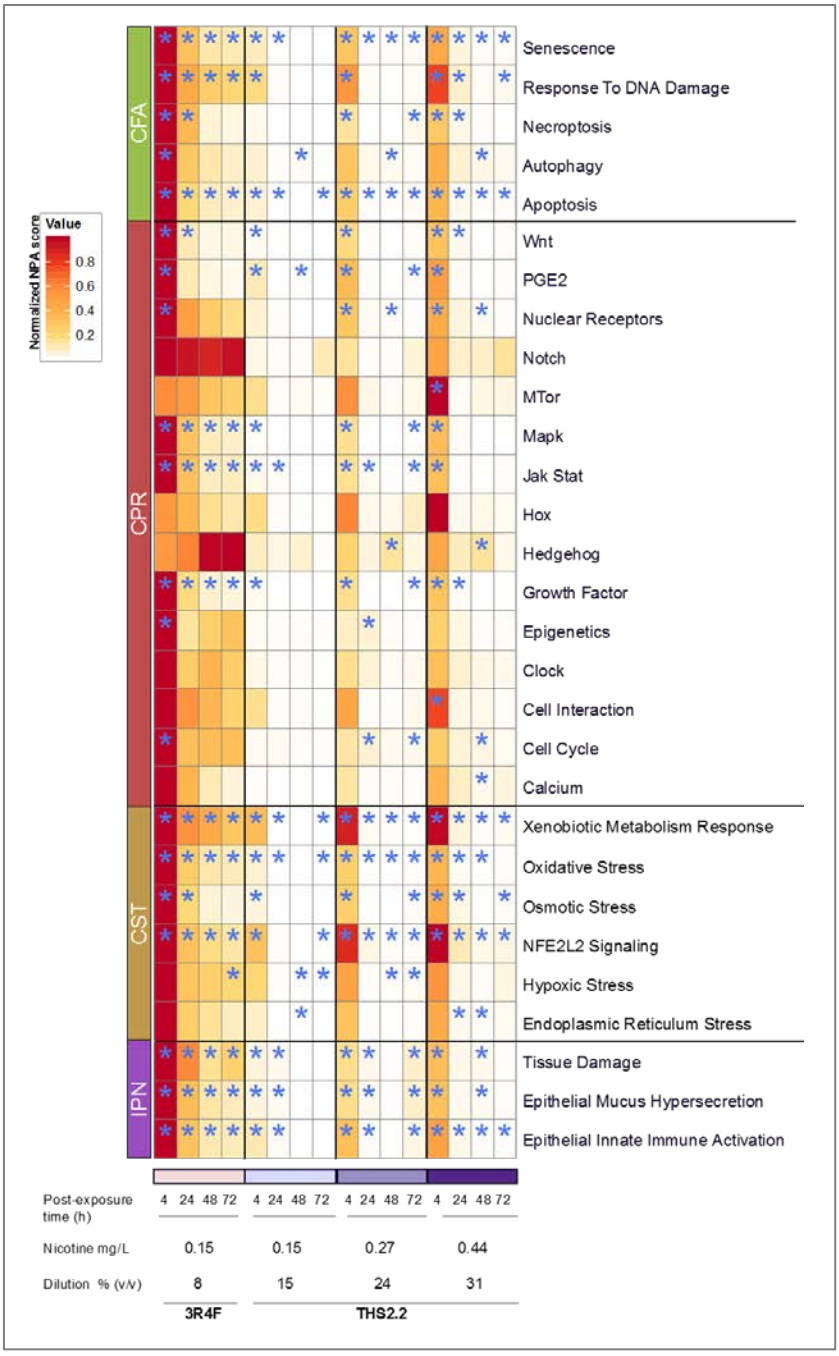


Figure 18. Network perturbations in nasal MucilAir™ tissues following exposure to 3R4F cigarette smoke and THS2.2 aerosol compared with air controls

Heatmap of network perturbation amplitude (NPA) scores summarizing subnetworks that were significantly perturbed in at least one treatment. A network is considered perturbed if, in addition to the significance of the NPA score with respect to the experimental variation, the two companion statistics (O and K) derived to inform on the specificity of the NPA score with respect to the biology described in the network, are significant. Significantly perturbed networks are indicated by * (i.e. O and K statistic *p*-values <0.05 and significant with respect to the experimental variation). Abbreviations: CFA, Cell Fate; CPR, Cell Proliferation; CST, Cell Stress; IPN, Inflammatory Process Network.

All three IPN subnetworks included in the analysis, Tissue Damage, Epithelial Mucus Hypersecretion and Epithelial Innate Immune Activation, were significantly perturbed in 3R4F CS-exposed MucilAir™ cultures throughout the post-exposure period. In contrast, THS2.2 aerosol exposure at comparable nicotine concentrations had a less pronounced impact on the mechanisms captured by these subnetworks, and perturbations had subsided at 48 hours post-exposure. Higher THS2.2 aerosol doses exerted a higher impact, particularly at the 4-hour time point. However, the amplitudes of the perturbations were still smaller than those observed in 3R4F CS-exposed cultures, and perturbations were also not sustained over time (Figure 19).

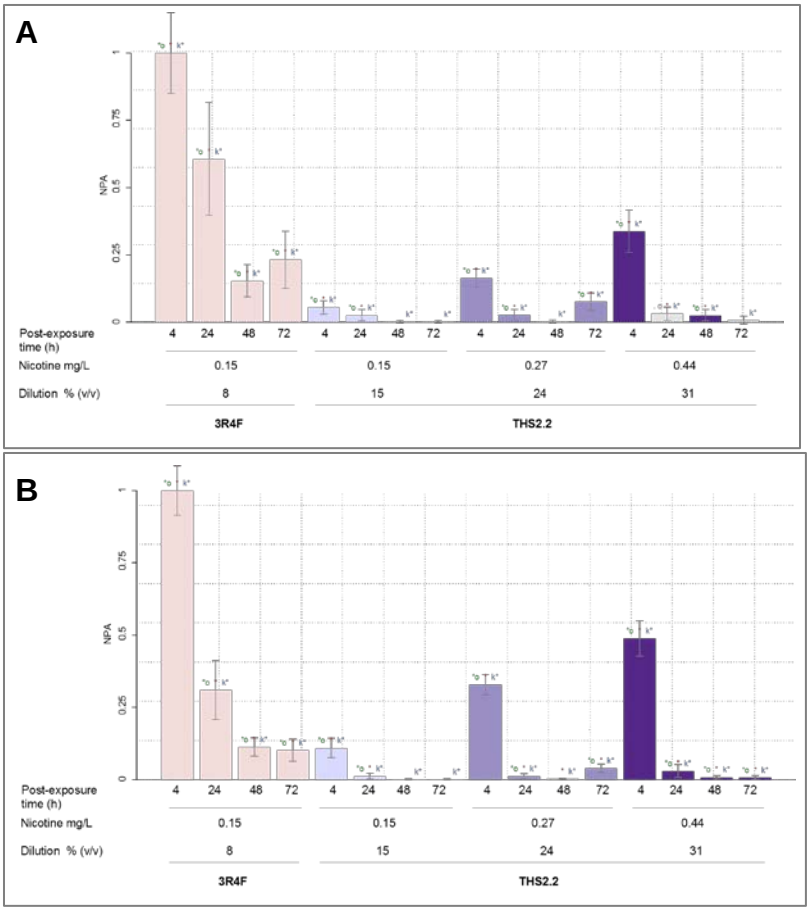


Figure 19. Relative network perturbation amplitude (NPA) scores of specific Inflammatory Process Network (IPN) subnetworks in nasal MucilAir™ tissues following exposure to 3R4F cigarette smoke and THS2.2 aerosol

The relative NPA scores for the (A) Tissue Damage and (B) Epithelial Innate Immune Activation subnetwork models are shown with their confidence interval accounting for experimental variation. Percentages give the relative NPA score for the subnetworks compared with the reference (treatment comparison showing the highest perturbation). In addition, companion statistics derived to inform on the specificity of the NPA score with respect to the biology described in the respective subnetwork models are shown as *O and K*, respectively, if their *p*-values are below the significance level. Symbol legend: *, O and K statistic *p*-values <0.05; .O and K., *p*-values between 0.05 and 0.1.

Closer examination of changes in expression levels of genes linked to inflammation showed limited effects for both 3R4F CS and THS2.2 aerosol exposure. While transcriptional levels of *IL1A*, *IL1B*, *PTGS2*, *TIMP1*, *S100A8* (S100 calcium binding protein A8), and *S100A9* were elevated throughout the post-exposure period in 3R4F CS-exposed nasal tissues, the expression of these genes was only significantly deregulated at 4 hours post-exposure in THS2.2 aerosol-exposed cultures (Figure 20).

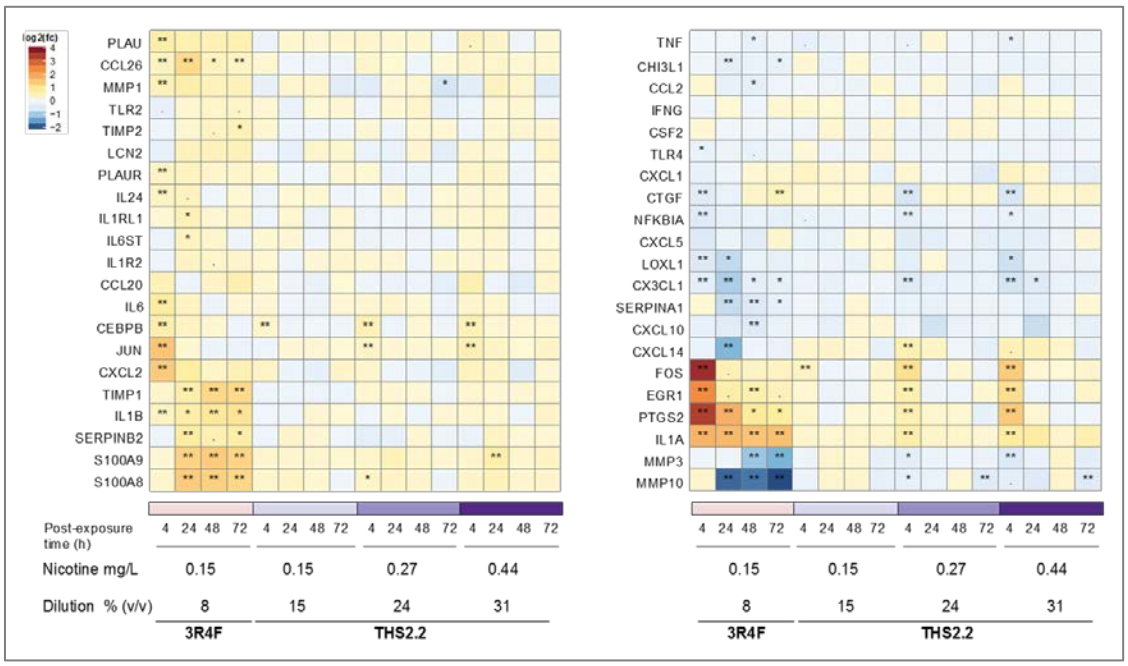


Figure 20. Altered expression levels of genes linked to inflammation in nasal MucilAir™ tissues following exposure to 3R4F cigarette smoke and THS2.2 aerosol

The heatmap depicts changes in gene expression of inflammation-related genes (gene symbols listed on the left) relative to corresponding air-exposed controls expressed as $\log_2$(fold change (fc)). Upregulation and downregulation of gene expression levels are represented by orange and blue shades, respectively, with darker colors indicating greater absolute fold changes. Statistically significant fold changes are highlighted by ** (adjusted $p<0.05$) and * (adjusted $p<0.1$).

Similar to previous reports of increased levels of IL-8, VEGF, and MMP-1 in the CS-injured lung (Comandini et al, 2009; Thorley & Tetley, 2007b), basolateral media of 3R4F CS-exposed nasal organotypic cultures had increased levels of CXCL8, EGF, MMP-1, TIMP-1 and VEGFA. Exposure to a higher dose of 3R4F CS additionally increased production of a number of other soluble mediators including TNFα, CCL20 and sICAM-1, providing further support for an epithelial inflammatory response contributing to the extensive tissue damage seen on histopathologic examination. In contrast, in THS2.2 aerosol-exposed cultures, VEGFA only increased at nicotine concentrations nearly twice those of the high 3RF CS dose. Marked elevations in sICAM-1, MMP-1 and TIMP-1 levels above controls were also only noted in nasal MucilAir™ tissues exposed to the high THS2.2 aerosol concentration (Figure 21).

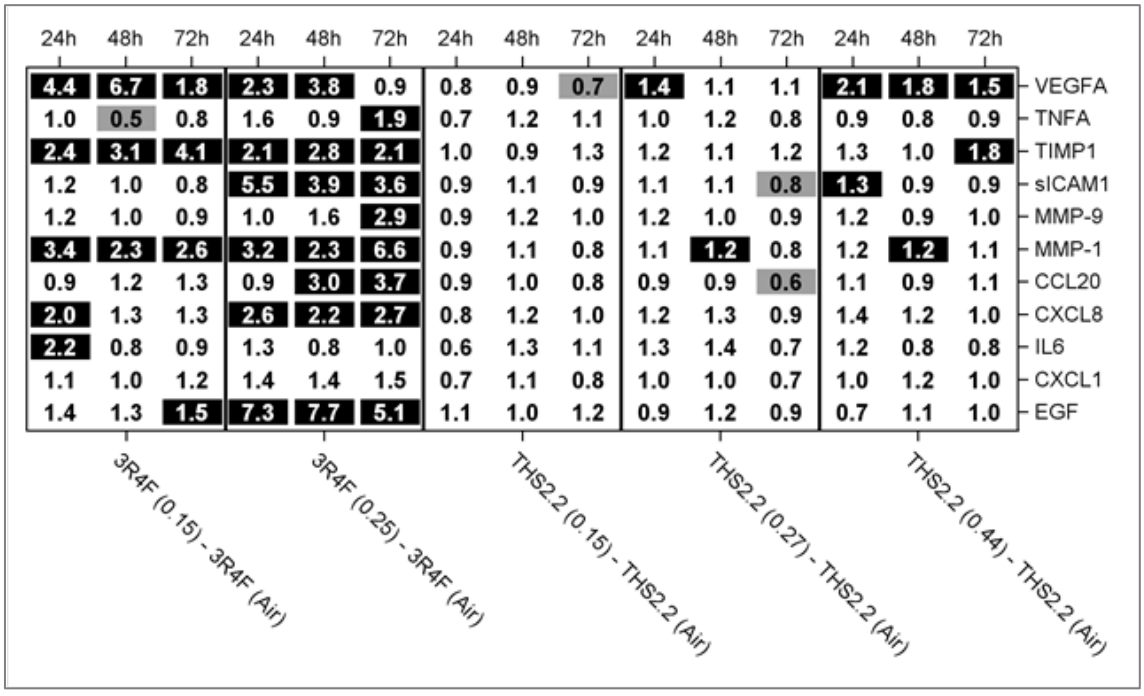


Figure 21. Altered levels of inflammation protein markers in conditioned media of nasal MucilAir™ tissues following exposure to 3R4F cigarette smoke and THS2.2 aerosol

The heatmap depicts fold changes in amounts of soluble inflammation protein markers (symbols listed on the right) relative to corresponding air-exposed controls at 24, 48, and 72 hours post-exposure. Dark and light grey shading indicates significant increases and decreases, respectively, between the comparisons (p<0.05).

Together these results demonstrated that exposure to THS2.2 aerosol causes little cytotoxicity and markedly less tissue damage and inflammation in nasal tissues *in vitro* (Iskandar et al, 2016).

3.3.1.6 Bronchial Organotypic Study

Similar to studies using 3D organotypic nasal tissues, 3D organotypic bronchial tissues (bronchial MucilAir™) were exposed to air; 7% and 13% (v/v in air) 3R4F CS equivalent to a target concentration of 0.13 or 0.25 mg/L nicotine, respectively; and 14%, 24%, and 31% (v/v in air) THS2.2 aerosol corresponding to target nicotine concentrations of 0.14, 0.24, and 0.31 mg/L, respectively, for 28 minutes. Exposure-related effects including cytotoxicity, tissue damage, release of inflammatory mediators and biological impact were evaluated at 4, 24, 48 and 72 hours post-exposure.

At the earliest time point following exposure, no cytotoxicity was noted, independent of the type of exposure. However, 3R4F CS exposure resulted in increased cytotoxicity from 24 hours post-exposure onwards, with significant damage to the tissues elicited by the high CS dose. THS2.2 aerosol exposure did not cause cytotoxicity in bronchial MucilAir™ tissues, independent of dose and post-exposure time point. These results were confirmed by histological evaluation of the 3D tissues, demonstrating that THS2.2 aerosol-exposed cultures resembled those exposed to air in morphology. Since exposure to a high concentration of 3R4F CS (25%) severely damaged the bronchial organotypic cultures, these tissues were excluded from further systems biology analysis.

Network model-based analysis showed that 3R4F CS exposure had the strongest impact on bronchial MucilAir™ cultures at 4 hours post-exposure (RBIF = 100%), and this impact declined over the post-exposure period. At comparable nicotine concentration, the impact of THS2.2 aerosol exposure on the tissues was always lower than that of 3R4F CS exposure, independent of the post-exposure time point. The impact of THS2.2 aerosol exposure decreased sharply with increasing post-exposure duration. In addition, there was a dose-dependent effect of THS2.2 aerosol exposure on the RBIF at 4 hours post-exposure (Figure 22).

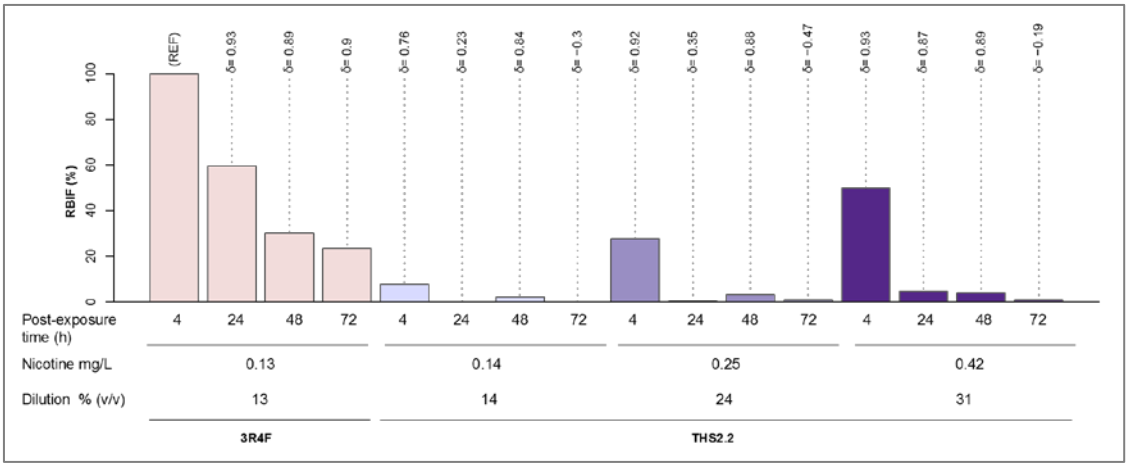


Figure 22. Network model-based analysis of the biological impact factor (BIF) in bronchial MucilAir™ tissues following exposure to 3R4F cigarette smoke and THS2.2 aerosol compared with air controls

The bar plot depicts BIF values relative to the maximum response (RBIF = 100%, REF). The δ values (−1 to 1) indicate how similar the underlying network perturbations are with respect to the REF. Scores were computed using transcriptomics profiling data from bronchial MucilAir™ tissues that were exposed to air, 3R4F cigarette smoke (red bars), or THS2.2 aerosol (purple bars) for 28 minutes and collected at 4, 24, 48 or 72 hours post-exposure.

Network analysis of the transcriptomic changes induced by exposure to 3R4F CS indicated that significant perturbations occurred at all post-exposure time points in networks incorporating senescence, necroptosis, and apoptosis biology, mechanisms of cell proliferation associated with growth factor, Wnt, nuclear receptor, MAPK and Jak/Stat signaling, inflammatory and other cellular stress responses. With very few exceptions, THS2.2 aerosol exposure affected the same networks, but perturbations were typically of lower amplitude and often not sustained over the entire post-exposure period. For both, 3R4F CS and THS2.2 aerosol exposures, network perturbations initially peaked at 4 hours post-exposure, gradually decreasing until the 72-hour time point (Figure 23).

Among the biological processes captured in the IPN, Tissue Damage, Epithelial Innate Immune Activation, Epithelial Mucus Hypersecretion exhibited significant perturbations in exposed bronchial MucilAir™ tissues. The impact on these subnetworks was always highest at 4 hours post-exposure and gradually decreased as post-exposure time increased. Although the drivers of the underlying perturbations were not different between the two exposures, the extent of perturbations in THS2.2 aerosol-exposed bronchial cultures was always smaller than that seen with 3R4F CS exposure (Figure 24).

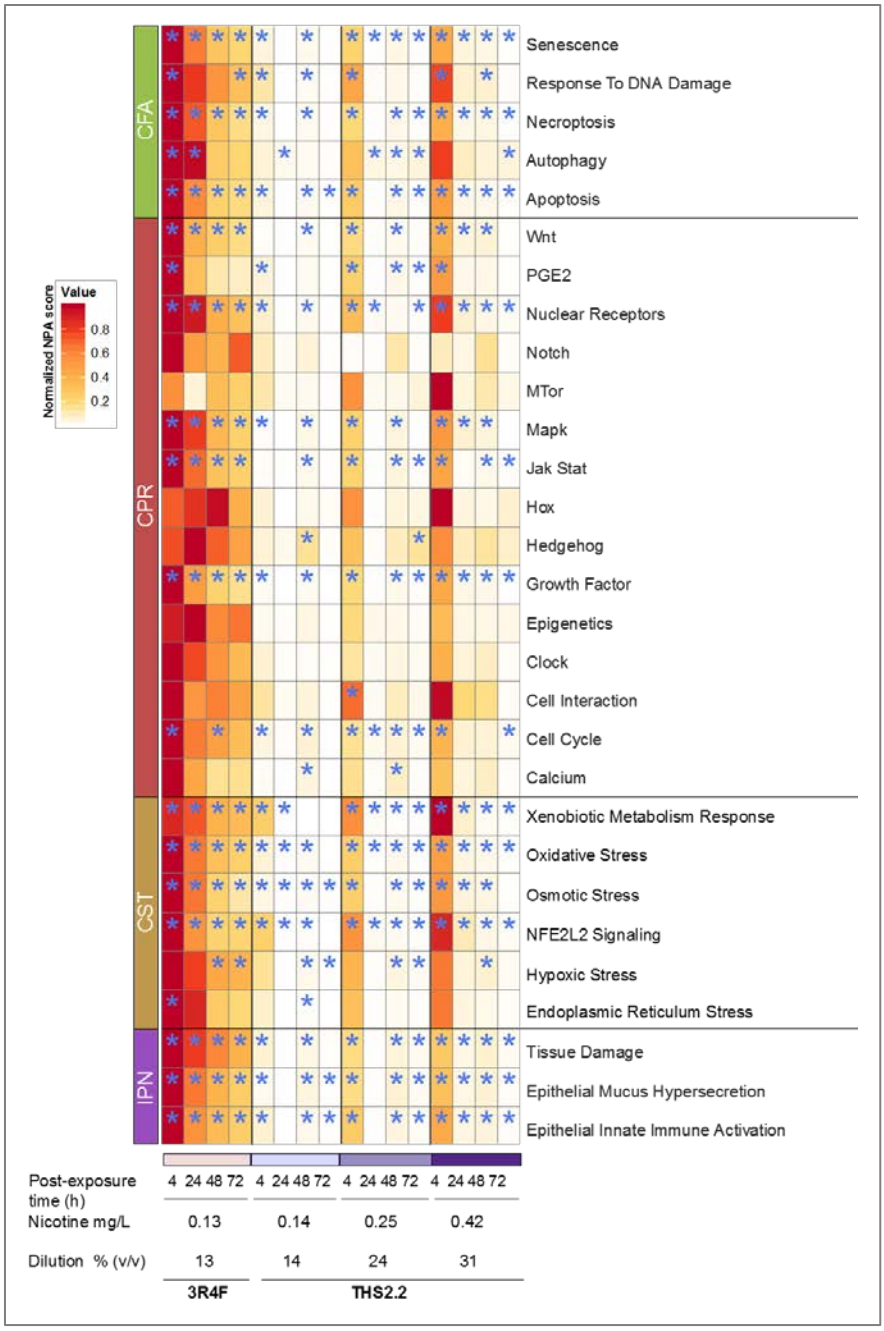


Figure 23. Network perturbations in bronchial MucilAir™ tissues following exposure to 3R4F cigarette smoke and THS2.2 aerosol compared with air controls

Heatmap of network perturbation amplitude (NPA) scores summarizing subnetworks that were significantly perturbed in at least one treatment. A network is considered perturbed if, in addition to the significance of the NPA score with respect to the experimental variation, the two companion statistics (O and K) derived to inform on the specificity of the NPA score with respect to the biology described in the network, are significant. Significantly perturbed networks are indicated by * (i.e. O and K statistic *p*-values <0.05 and significant with respect to the experimental variation). Abbreviations: CFA, Cell Fate; CPR, Cell Proliferation; CST, Cell Stress; IPN, Inflammatory Process Network.

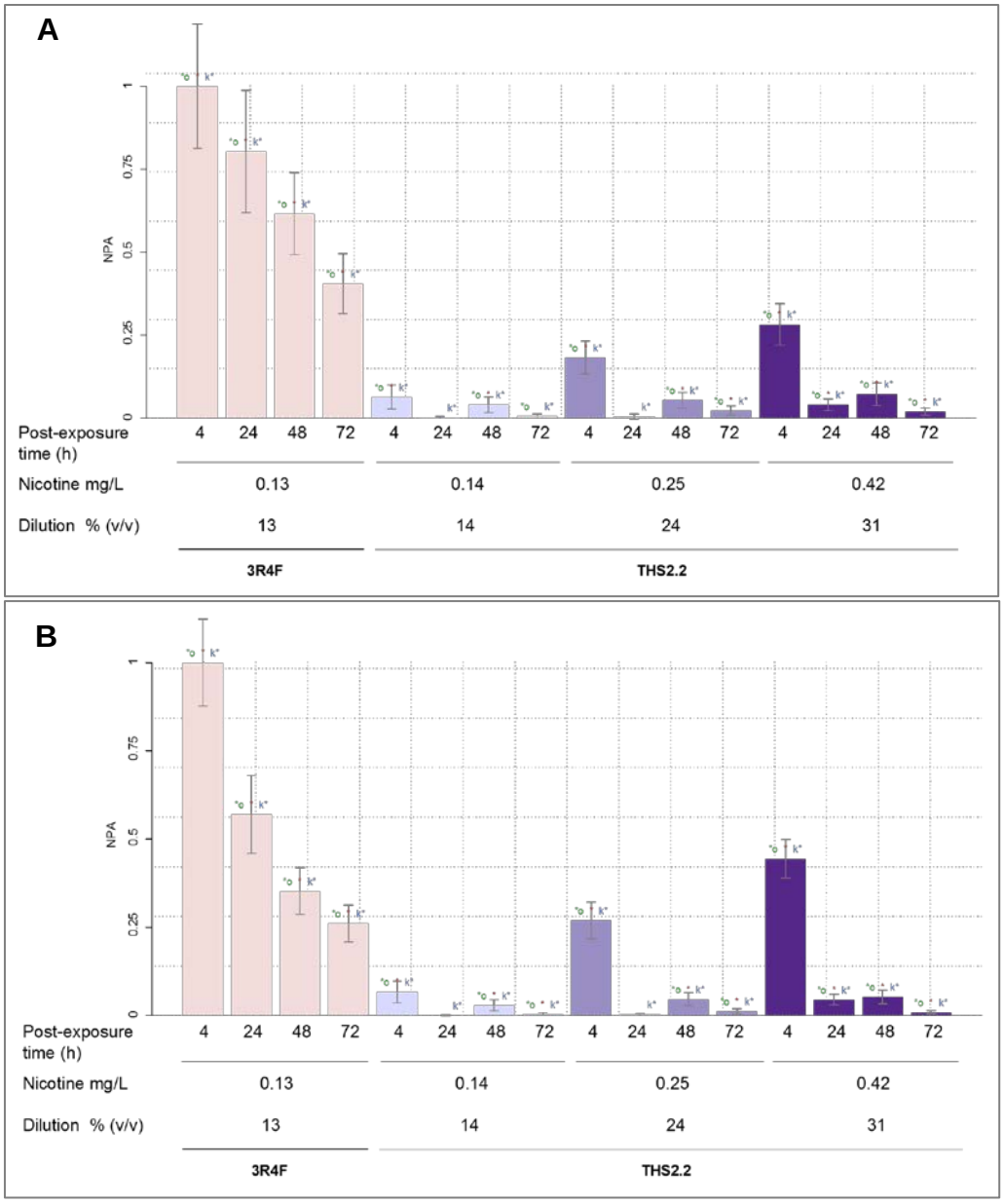


Figure 24. Relative network perturbation amplitude (NPA) scores of specific Inflammatory Process Network (IPN) subnetworks in bronchial MucilAir™ tissues following exposure to 3R4F cigarette smoke and THS2.2 aerosol

The relative NPA scores for the (A) Tissue Damage and (B) Epithelial Innate Immune Activation subnetwork models are shown with their confidence interval accounting for experimental variation. Percentages give the relative NPA score for the subnetworks compared with the reference (treatment comparison showing the highest perturbation). In addition, companion statistics derived to inform on the specificity of the NPA score with respect to the biology described in the respective subnetwork models are shown as *O and K*, respectively, if their *p*-values are below the significance level. Symbol legend: *, O and K statistic *p*-values <0.05; .O and K., *p*-values between 0.05 and 0.1.

Similar to observations in exposed nasal MucilAir™ tissues, several genes linked to inflammation were strongly deregulated in 3R4F CS-exposed bronchial cultures. These included *IL1A*, *IL1B*, *PTGS2* and *MMP1*, among others. In addition, expression levels of other genes (e.g., *TIMP1*, *S100A8*, *S100A9* and *CXCL2*) that were not affected in nasal tissues also increased in response to 3R4F CS exposure. Of note, increased expression of these genes was sustained throughout the post-exposure period. In contrast, the expression of fewer genes was significantly affected by THS2.2 aerosol exposure, in particular, at the high nicotine concentration and at the early post-exposure time point. With very few exceptions, gene expression was no longer altered in THS2.2 aerosol-exposed bronchial MucilAir™ tissues at the later post-exposure time points (Figure 25).

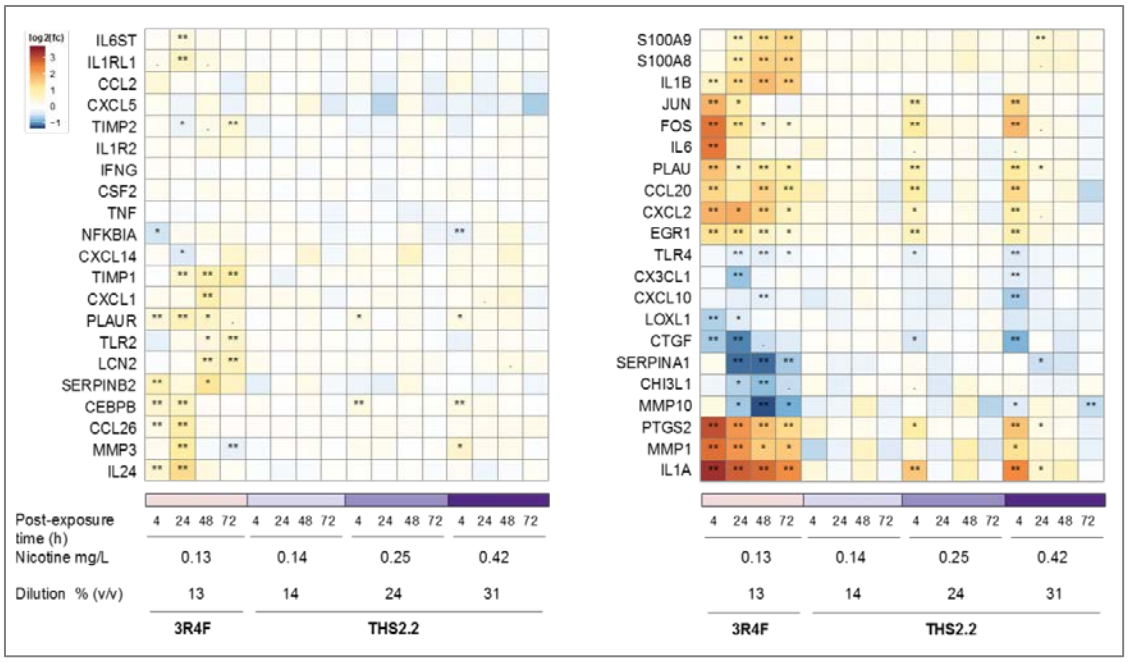


Figure 25. Altered expression levels of genes linked to inflammation in bronchial MucilAir™ tissues following exposure to 3R4F cigarette smoke and THS2.2 aerosol

The heatmap depicts changes in gene expression of inflammation-related genes (gene symbols listed on the left) relative to corresponding air-exposed controls expressed as $\log_2$[fold change (value; fc)]. Upregulation and downregulation of gene expression levels are represented by orange and blue shades, respectively, with darker colors indicating greater absolute fold changes. Statistically significant fold changes are highlighted by ** (adjusted $p<0.05$) and * (adjusted $p<0.1$).

The contribution of an active inflammatory response to the observed tissue damage in 3R4F CS-exposed bronchial tissues was further supported by increased secretion of CXCL8, VEGFA, MMP-1, and TIMP-1 levels into the culture media. This was further augmented by exposure to the higher 3R4F CS concentration, additionally resulting in increased production of IL-1α, IL-6, TNFα, sICAM1, CCL5, CXCL10, MMP-9, and GM-CSF (CSF2). Increased amounts of CXCL8, VEGFA, MMP-1 and TIMP-1 were

also secreted into the basolateral media of THS2.2 aerosol-exposed MucilAir™ tissues at one or more post-exposure time points, qualitatively resembling the effect seen in 3R4F CS-exposed tissue, though at a lower level. Induction of additional soluble mediators by THS2.2 aerosol exposure was not observed, suggesting that the ensuing inflammatory response was limited in extent (Figure 26).

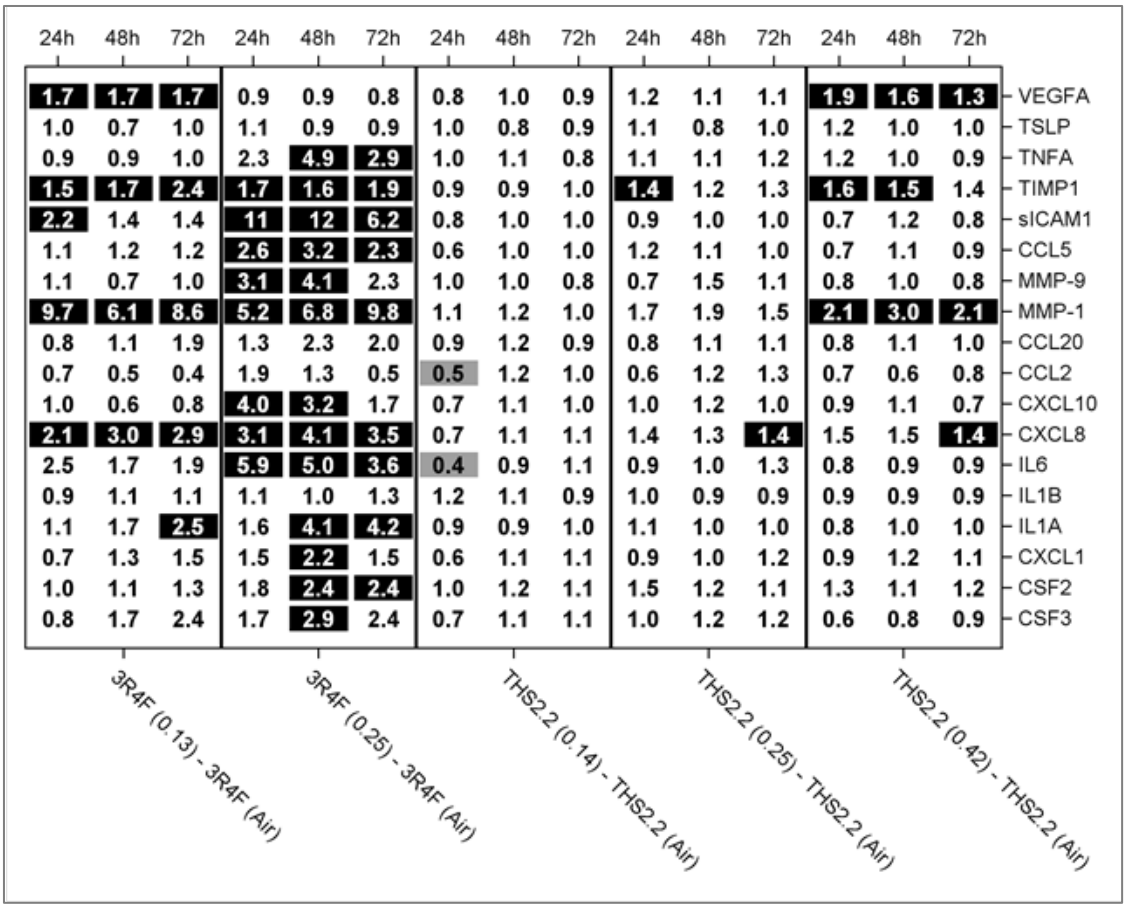


Figure 26. Altered levels of inflammation protein markers in conditioned media of bronchial MucilAir™ tissues following exposure to 3R4F cigarette smoke and THS2.2 aerosol

The heatmap depicts fold changes in amounts of soluble inflammation protein markers (symbols listed on the right) relative to corresponding air-exposed controls at 24, 48 and 72 hours post-exposure. Dark and light grey shading indicates significant increases and decreases, respectively, between the comparisons (p<0.05).

In summary, these results demonstrate that exposure to THS2.2 aerosol, in contrast to 3R4F CS exposure, causes little to no cytotoxicity, tissue damage and inflammation in 3D bronchial organotypic tissues *in vitro*.

3.3.2 Results from *In Vivo* Studies

3.3.2.1 Rat OECD Studies

Two independent 90-day inhalation studies were conducted with THS2.2 (Rat-THS-TG413) and THS2.2 Menthol (Rat-THSM-TG413) according to OECD Test Guideline 413 (TG413), comparing the toxicity of CS from 3R4F with aerosol from the THS and its mentholated version (THSM). For this purpose, male and female Sprague Dawley rats were nose-only exposed to filtered fresh air (sham), three target nicotine concentrations of 3R4F CS (8, 15 or 23 µg/L), or aerosol from THS/THS menthol (15, 23 or 50 µg/L) for 6 hours per day, 5 days per week for 13 weeks. Additional groups of animals were included for exposure to THS aerosol at the highest nicotine concentration for 13 weeks, followed by a 42-day recovery period, to investigate the reversibility or persistence of test substance-related effects. In addition to the OECD endpoints, pulmonary inflammation was assessed by BALF cell counts and quantification of BALF inflammatory mediators at the end of exposure (90 days) and following the post-exposure period (90 + 42 days). Furthermore, potential molecular changes as a consequence of exposure were evaluated using transcriptomics, proteomics and lipidomics analyses.

The results of OECD TG413 toxicological assessments in rats have been described in another section of this dossier (link to 6.1.2 Preclinical Safety). This part of the document will focus on the results of the oxidative stress-related endpoints that were obtained from the additional integrative systems toxicological evaluation of samples from the OECD inhalation studies (the 'OECD Plus' part).

3.3.2.1.1 Rat OECD THS2.2 Study

Exposure to 3R4F CS over a 90-day period resulted in the development of adaptive changes in rat nasal epithelium including moderate-to-marked reserve cell hyperplasia, marked squamous metaplasia with and without cornification, particularly in animals exposed to high concentrations, and loss of goblet cells. In addition, slight infiltration by neutrophilic granulocytes indicated mild inflammation. Reserve cell hyperplasia and squamous metaplasia were also observed in rats exposed to THS2.2 aerosol. However, lesions in these animals showed remarkably less cornification and loss of goblet cells than those seen in the 3R4F groups. There was no difference in the incidence and severity of lesions between the two genders, independent of exposure. With the exception of squamous metaplasia, lesion severity decreased following a 42-day post-exposure period, indicating that the observed changes represented local adaptation to irritant inhalation.

Histopathological evaluation at nose level 2 also identified reserve cell hyperplasia and squamous metaplasia in the respiratory and olfactory nasal epithelia of animals exposed to medium and high doses of 3R4F CS which were, at least in part, fully reversible following post-exposure. In contrast, exposure to THS2.2 aerosol led to limited reserve cell hyperplasia in some, but not all animals, and did not result in the development of squamous metaplasia in either the respiratory or olfactory epithelium of exposed rats. Similarly, mixed inflammatory cell infiltrates were seen in the olfactory nasal epithelium following 3R4F CS exposure, which largely persisted throughout the post-exposure period. This finding was incidental and less severe in THS2.2 aerosol-exposed rats and was also less common at the post-exposure time point.

Examination of laryngeal tissues showed marked squamous metaplasia with extensive cornification in male and female rats exposed to 3R4F CS, and less severe metaplastic lesions that were not cornified following a 42-day post-exposure period in animals from the 3R4F high-dose group. Squamous metaplasia was also seen at the base of the epiglottis and floor of the larynx in rats of both genders exposed to THS2.2 aerosol. In contrast to findings in 3R4F CS-exposed rats, these lesions were less severe and exhibited a lower extent of cornification. In addition, 42 days after the last exposure, the lesions had noticeably regressed.

Exposure to 3R4F CS resulted in the development of goblet cell hyperplasia in bronchial epithelium, with a dose-dependent increase in lesion severity that was more pronounced in male rats than in female rats. In contrast, the bronchial epithelium of rats exposed to THS2.2 aerosol did not present with extensive goblet cell hyperplasia in either male or female rats. Of note, these lesions appeared to regress noticeably in animals that were permitted a post-exposure recovery. Furthermore, inflammatory changes in lung parenchyma were observed in 3R4F-exposed groups. For example, accumulation of pigmented and unpigmented macrophages in the alveolar lumen increased in extent in a concentration-dependent manner following 3R4F CS exposure. In THS2.2 aerosol-exposed rats, only the high concentration resulted in a weak increase in unpigmented and pigmented macrophages. For unpigmented macrophages, complete clearance was seen after the 42-day recovery period, while pigmented macrophages partially remained. 3R4F CS at medium and high concentrations also elicited a concentration-dependent increase in pigmented macrophage nests that did not decrease after the 42-day recovery period. Marginal increases in response to THS2.2 aerosol exposure lacked statistical significance for this endpoint. In alveolar epithelium, a weak infiltration with neutrophilic granulocytes was observed following 3R4F CS exposure, which was completely reversed after the 42-day recovery period, in agreement with previous reports (Friedrichs et al, 2006; Stevenson et al, 2007). 3R4F CS exposure-related lung inflammation was further evidenced by the increase in the total cell number recovered in BALF. This was primarily driven by increases in macrophage and neutrophil numbers in both female and male animals. While macrophage counts remained elevated following the 42-day recovery period, neutrophil numbers decreased in BALF of 3R4F CS-exposed rats. In contrast, exposure to THS2.2 aerosol did not affect the total number of free lung cells in BALF, even at the highest nicotine concentration. A strong but incomplete reduction in the number of neutrophils in BALF of CS-exposed rats was also previously reported after a 35-day exposure and a 28-day recovery (Friedrichs et al, 2006), and after a 182-day (6 month) exposure and a 56-day recovery (Stevenson et al, 2007).

Gene expression profiles of respiratory nasal epithelia from exposed rats of both genders were analyzed and demonstrated a clear concentration-dependent response with respect to the number of statistically significant DEGs in 3R4F CS-exposed animals, and, to a lesser extent, in THS2.2 aerosol-exposed animals. There was a clear difference in the magnitude of the changes in respiratory nasal epithelial samples between matching nicotine concentrations of 3R4F CS and THS2.2 aerosol exposures. After the 42-day recovery period, gene expression changes were much reduced in all groups, except in nasal epithelia from rats exposed to the medium and high 3R4F CS concentrations.

Systems toxicological evaluation of the nasal epithelial transcriptome from 3R4F CS-exposed rats further highlighted extensive perturbations in nearly all networks, with

significant perturbations becoming apparent at a dose equivalent to 15 µg/L nicotine. By contrast, not even the highest THS2.2 aerosol dose elicited as strong an impact on the networks of interest (Figure 27).

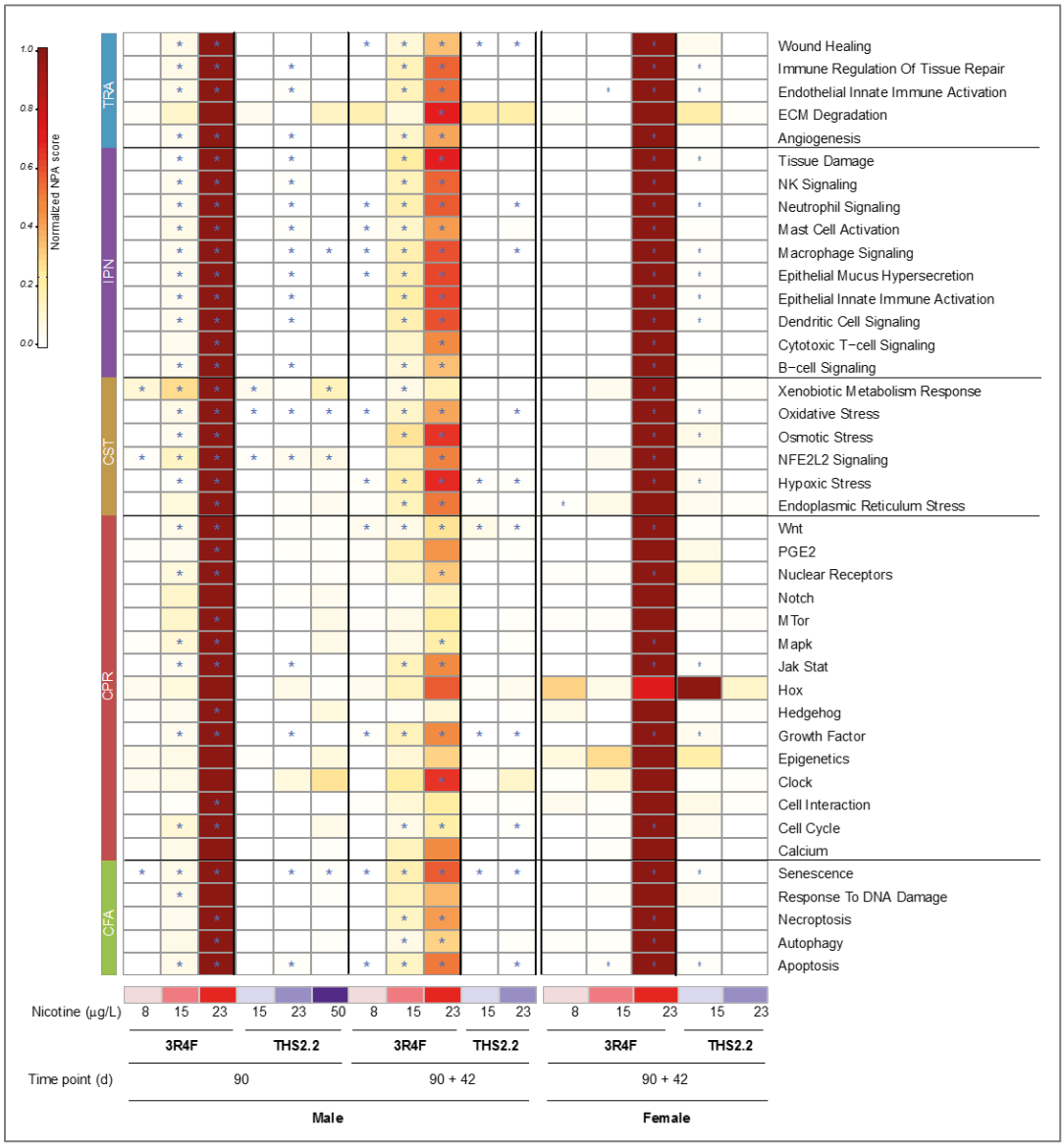


Figure 27. Network perturbations in rat nasal epithelial tissues following exposure to 3R4F cigarette smoke and THS2.2 aerosol compared with air controls

Heatmap of network perturbation amplitude (NPA) scores summarizing subnetworks that were significantly perturbed in at least one treatment. A network is considered perturbed if, in addition to the significance of the NPA score with respect to the experimental variation, the two companion statistics (O and K) derived to inform on the specificity of the NPA score with respect to the biology described in the network, are significant. Significantly perturbed networks are indicated by * (i.e. O and K statistic *p*-values <0.05 and significant with respect to the experimental variation). Abbreviations: CFA, Cell Fate; CPR, Cell Proliferation; CST, Cell Stress; IPN, Inflammatory Process Network; TRA, Tissue Repair and Angiogenesis. Note: Only RNA extracted from nasal epithelia of female rats at 90 + 42 days passed quality check criteria for subsequent gene expression and network analyses.

Using the network-based approach, a quantitative measure of the perturbed biological processes was obtained. There was a steep dose response to 3R4F CS exposure that was not seen for THS2.2 aerosol exposure at any concentration and time point examined. Mechanisms governing tissue damage related to epithelial pro-inflammatory signaling, neutrophil chemotaxis and neutrophil response, macrophage, Th1, mast, and NK cell activation, Th17 cell differentiation and mucus hypersecretion contributed to overall inflammation in nasal epithelia of 3R4F CS-exposed rats (Figure 28). Following the 42-day recovery period, inflammation subsided in nasal epithelium of rats exposed to the medium 3R4F CS concentration, whereas there was only a weak reduction in the inflammatory state following exposure to the high concentration. These findings indicated that subchronic exposure to 3R4F CS caused some inflammatory perturbations that did not resolve during a 6-week recovery period.

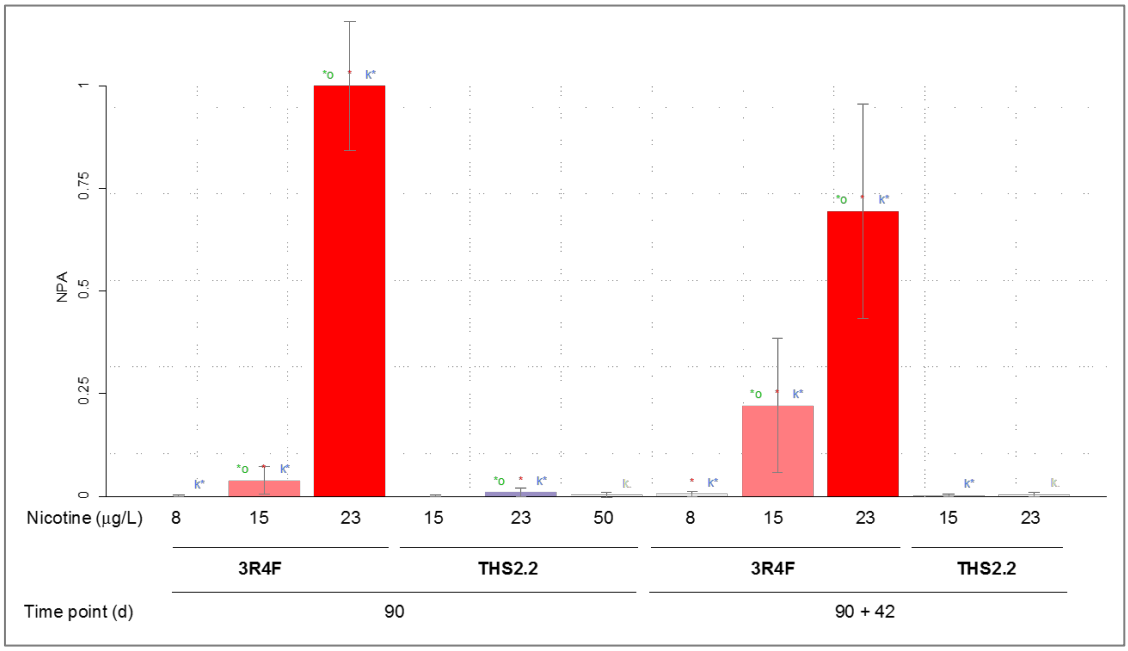


Figure 28. Relative network perturbation amplitude (NPA) scores of the Tissue Damage subnetwork in nasal respiratory epithelia of male rats exposed to 3R4F cigarette smoke and THS2.2 aerosol

The relative NPA scores for the Tissue Damage subnetwork model are shown with their confidence interval accounting for experimental variation. Percentages give the relative NPA score for the subnetworks compared with the reference (treatment comparison showing the highest perturbation). In addition, companion statistics derived to inform on the specificity of the NPA score with respect to the biology described in the respective subnetwork models are shown as *O and K*, respectively, if their *p*-values are below the significance level. Symbol legend: *, O and K statistic *p*-values <0.05; .O and K., *p*-values between 0.05 and 0.1.

Examining the expression of several genes encoding inflammatory mediators revealed altered levels of mRNA for chemokines (e.g., *CXCL1*, *CXCL6*, *CCL3*, *CCL20*), cytokines (e.g., *IL1A* and *IL1B*) and tissue remodeling factors (e.g., *MMP3*, *MMP10*, *TIMP1*,

PLAUR) in nasal epithelia of 3R4F CS-exposed but not THS2.2 aerosol-exposed male rats. These changes were only significant for the high CS concentration and did not persist during post-exposure, suggesting a rapid inflammatory response that, considering the histopathological findings, is predominantly aimed at tissue repair (Figure 29).

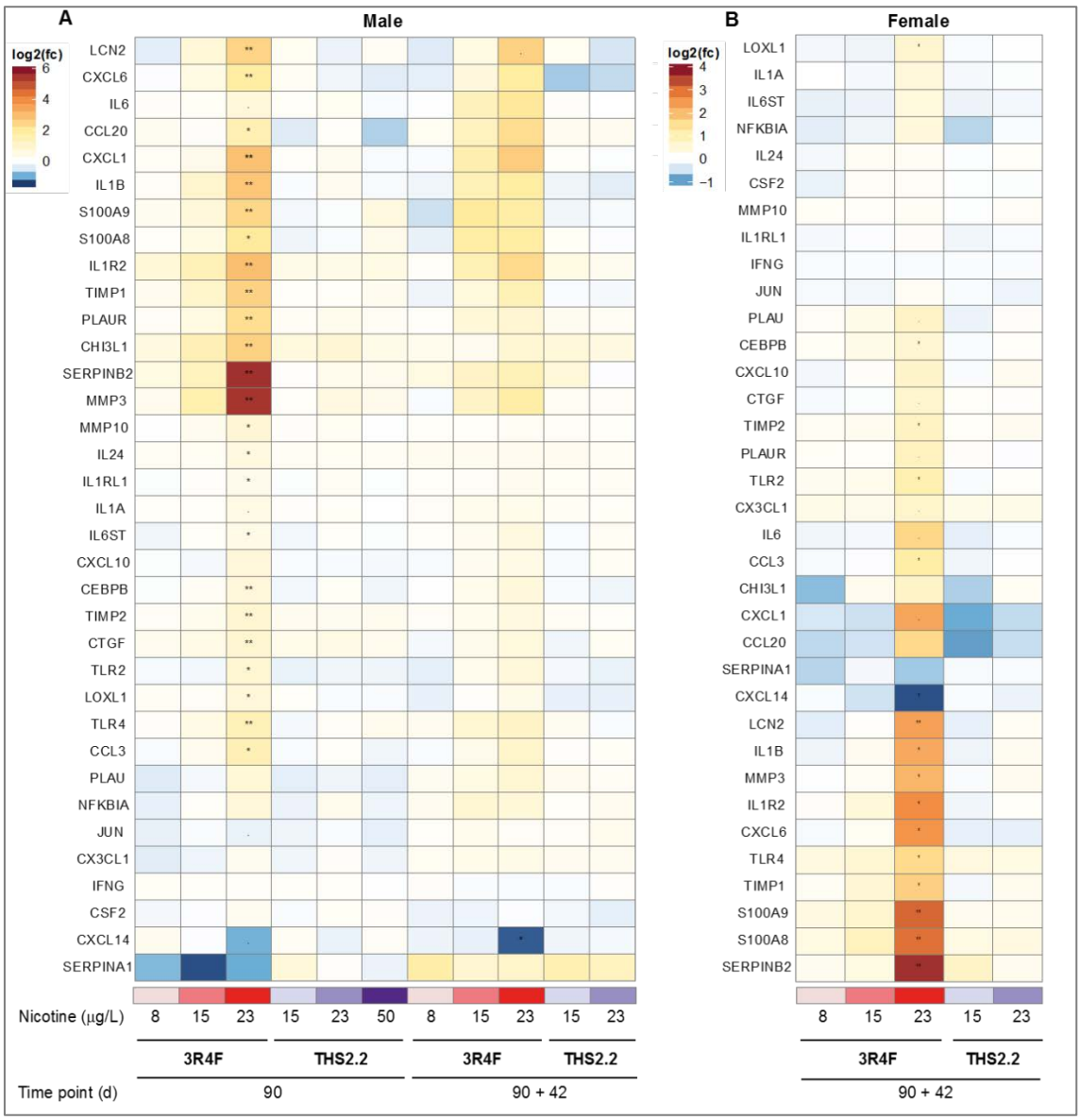


Figure 29. Altered expression levels of genes linked to inflammation in nasal epithelial tissues of male rats following exposure to 3R4F cigarette smoke and THS2.2 aerosol

The heatmap depicts changes in gene expression for oxidative stress-related genes (gene symbols listed on the left) relative to corresponding air-exposed controls in nasal epithelia of (A) male and (B) female rats expressed as $\log_2$[fold change (value; fc)]. Upregulation and downregulation of gene expression levels are represented by orange and blue shades, respectively, with darker colors indicating greater absolute fold changes. Statistically significant fold changes are highlighted by ** (adjusted $p<0.05$) and * (adjusted $p<0.1$).

Evaluation of lung SRPs from exposed male and female rats indicated that only a few genes showed significant deregulation following exposure to 3R4F CS. This response was dose-dependent, and, at least in part, reversible in animals that were allowed a 42-day post-exposure recovery, and there was no obvious difference between male and female rats' SRPs. By comparison, exposure to THS2.2 aerosol induced a markedly less pronounced systems response, even at the highest concentration. In addition, gene expression changes following THS2.2 aerosol exposure fully reverted during the post-exposure period. Systems toxicological analysis of transcriptomics data revealed significant perturbations in all network families in the lungs of 3R4F CS-exposed rats. In particular, the majority of subnetworks belonging to the IPN and Tissue Repair and Angiogenesis networks were affected by the exposure, and this impact was sustained throughout the recovery period. The IPN network also exhibited significant perturbations following THS2.2 aerosol exposure. However, these perturbations were generally of markedly smaller amplitude and the exposure effects did not persist (Figure 30).

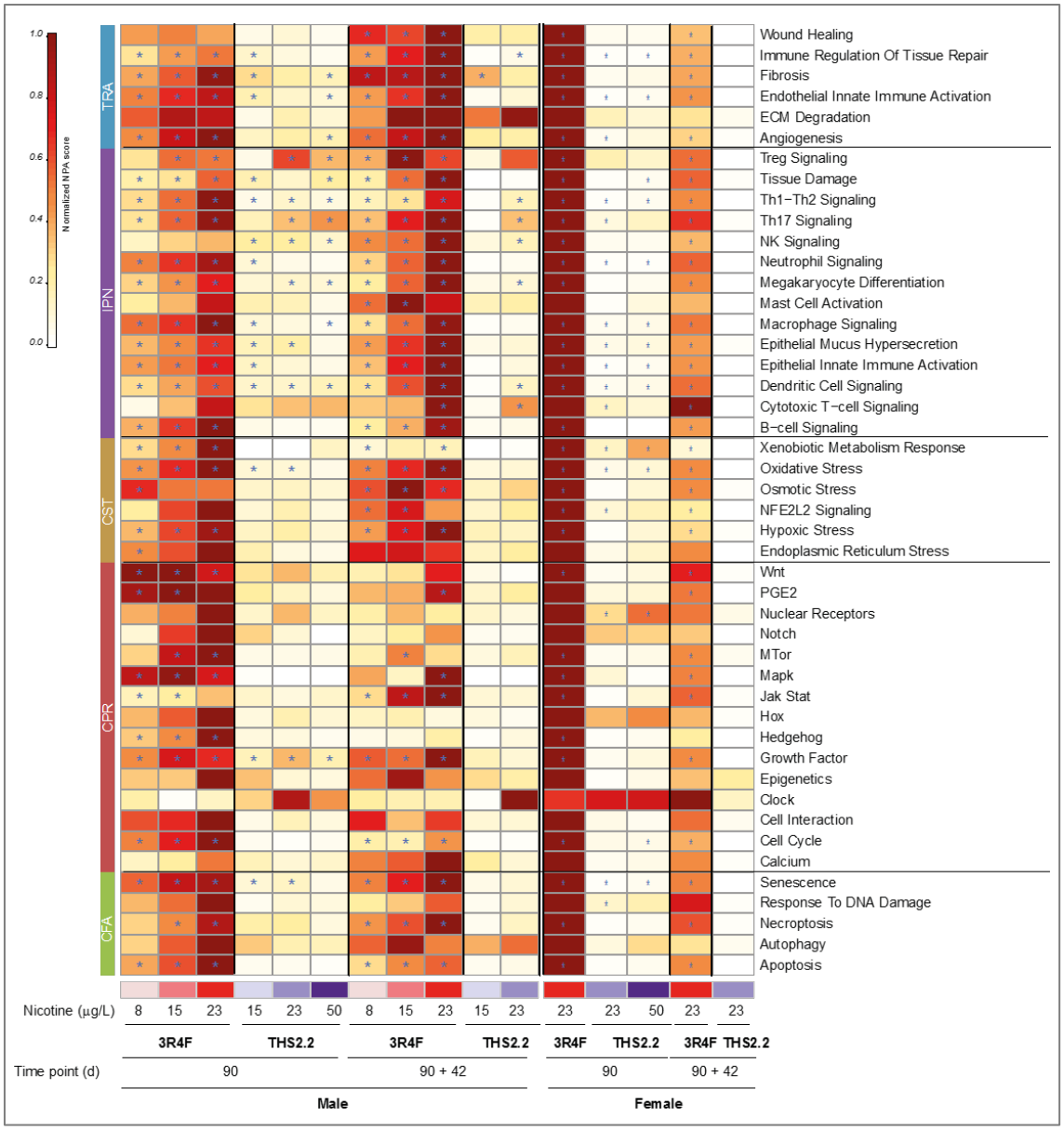


Figure 30. Network perturbations in rat lung tissues following exposure to 3R4F cigarette smoke and THS2.2 aerosol compared with air controls

Heatmap of network perturbation amplitude (NPA) scores summarizing subnetworks that were significantly perturbed in at least one treatment. A network is considered perturbed if, in addition to the significance of the NPA score with respect to the experimental variation, the two companion statistics (O and K) derived to inform on the specificity of the NPA score with respect to the biology described in the network, are significant. Significantly perturbed networks are indicated by * (i.e. O and K statistic *p*-values <0.05 and significant with respect to the experimental variation). Abbreviations: CFA, Cell Fate; CPR, Cell Proliferation; CST, Cell Stress; IPN, Inflammatory Process Network; TRA, Tissue Repair and Angiogenesis.

Several genes linked to inflammation including *CCL3*, *CXCL1*, *IL1R2*, *LCN2* and *S100A9* were significantly deregulated in the lungs of both male and female rats exposed to 3R4F CS. In contrast, only *LCN2* gene expression increased in THS2.2 aerosol-exposed female animals; no other gene was affected (Figure 31).

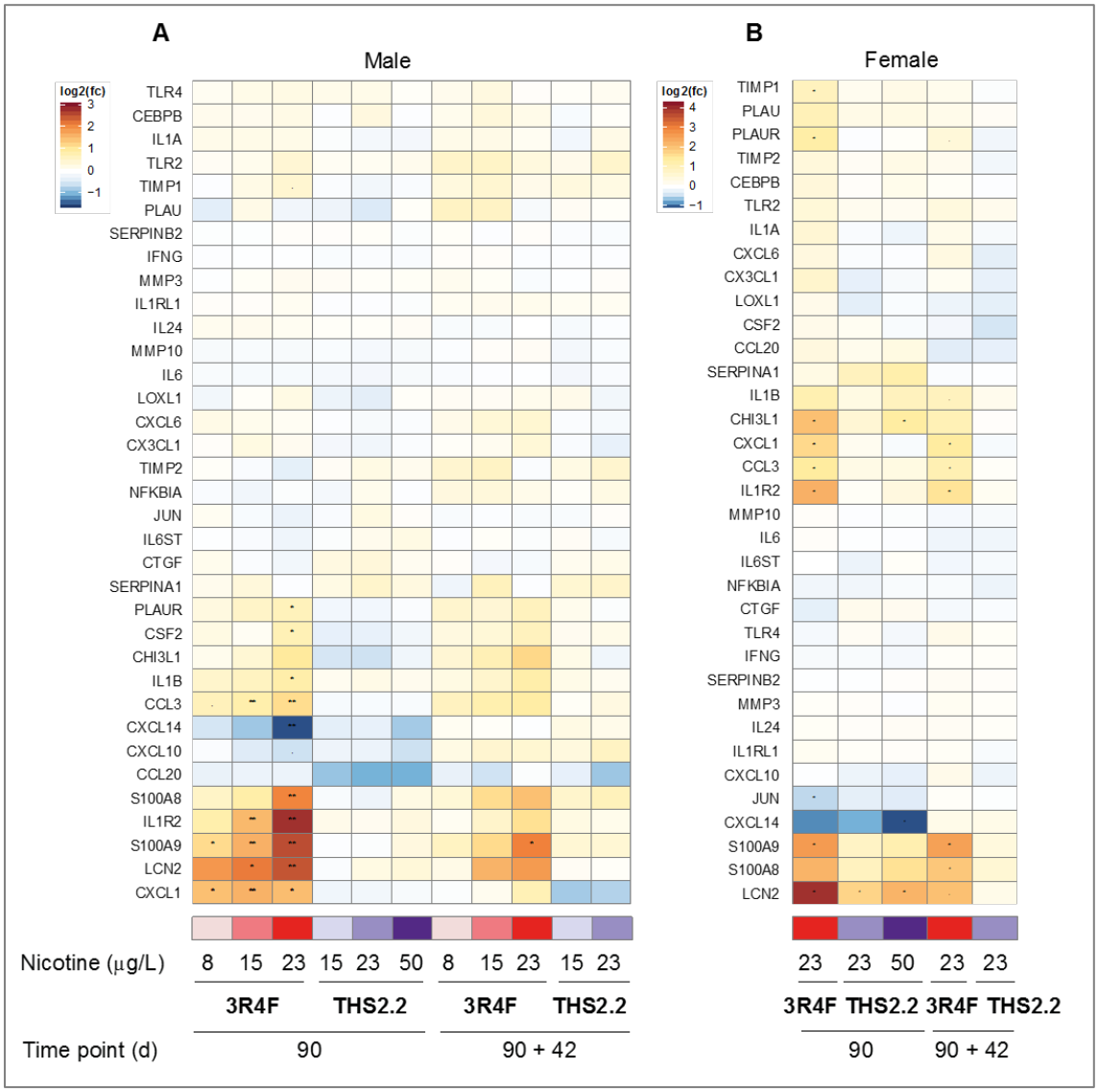


Figure 31. Altered expression levels of genes linked to inflammation in lung tissues of male rats following exposure to 3R4F cigarette smoke and THS2.2 aerosol

The heatmap depicts changes in gene expression for oxidative stress-related genes (gene symbols listed on the left) relative to corresponding air-exposed controls in nasal epithelia of (A) male and (B) female rats expressed as $\log_2$[fold change (value; fc)]. Upregulation and downregulation of gene expression levels are represented by orange and blue shades, respectively, with darker colors indicating greater absolute fold changes. Statistically significant fold changes are highlighted by ** (adjusted $p<0.05$) and * (adjusted $p<0.1$).

Corresponding to this state of heightened inflammation in the lung, the levels of several cytokines and growth factors increased following the 90-day inhalation period. BALF concentrations of CCL2, CCL4, CCL7, CCL22, CSF1, myeloperoxidase, and fibroblast growth factor 9 were elevated in 3R4F CS-exposed rats in a dose-dependent manner in both genders. Of these, only CCL4 was increased in BALF from THS2.2-exposed male rats at the same or even higher nicotine concentrations. Other soluble mediators including CD40 ligand (CD40-L), CCL11, CXCL2, CXCL10, resistin, PAI-1, VCAM-1, VEGFA, and lymphotactin-1 were also found at elevated concentrations for all or most 3R4F CS-exposure concentrations in both genders, but lacked a consistent concentration relationship. Of note, CXCL10, CXCL2, resistin, and PAI-1 BALF levels were slightly increased in THS2.2 aerosol-exposed animals, but they did not usually reach the levels seen following 3R4F CS exposure. Furthermore, haptoglobin was slightly increased in female rats exposed to THS2.2 aerosol at high but not low and medium concentrations. In BALF from 3R4F CS-exposed rats, increases in haptoglobin levels were only seen in males, independent of the concentration. Following the 42-day recovery period, CCL2, CCL4, CCL7, CSF1 and PAI-1 levels decreased in BALF of CS-exposed rats. In female animals, a decline in BALF levels was additionally noted for VEGFA, CCL22, CXCL-10, fibrinogen and CD40-L although levels remained above those seen in sham animals. This incomplete ‘normalization’ is in accordance with the incomplete remission in the numbers of neutrophils and macrophages described above. For THS2.2 aerosol-exposed rats, full or partial remission was seen for most inflammatory protein markers in BALF. Of note, after the recovery period, the amounts of CXCL5, fibroblast growth factor 2, IL-11 (both genders), C-reactive protein, and IL-12 (in females only) increased above the levels seen upon completion of the 90-day inhalation in 3R4F CS-exposed rats, particularly at the high concentration, providing further evidence for the persistence of inflammation in the lung injured by CS exposure (Figure 32, Figure 33).

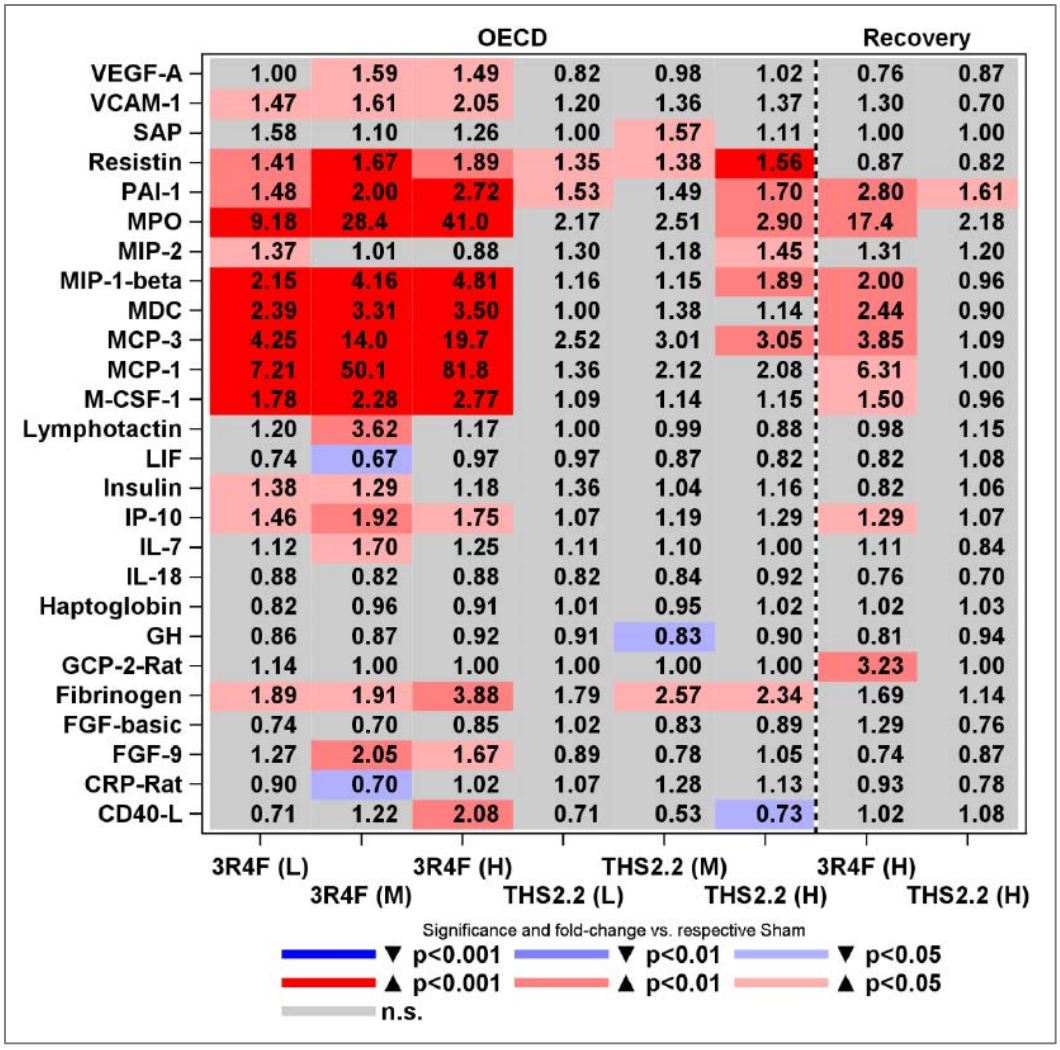


Figure 32. Alterations in levels of soluble inflammation mediators in bronchoalveolar lavage fluid of male rats exposed to 3R4F cigarette smoke or THS2.2 aerosol

The heatmap depicts fold changes in mediator concentrations in bronchoalveolar lavage fluid of rats exposed to 3R4F cigarette smoke or THS2.2 aerosol for 90 days (OECD), or for the same duration followed by a 42-day recovery period (Recovery). Colors indicate a statistically significant increase (▲, shades of red) or decrease (▼, blue shades).

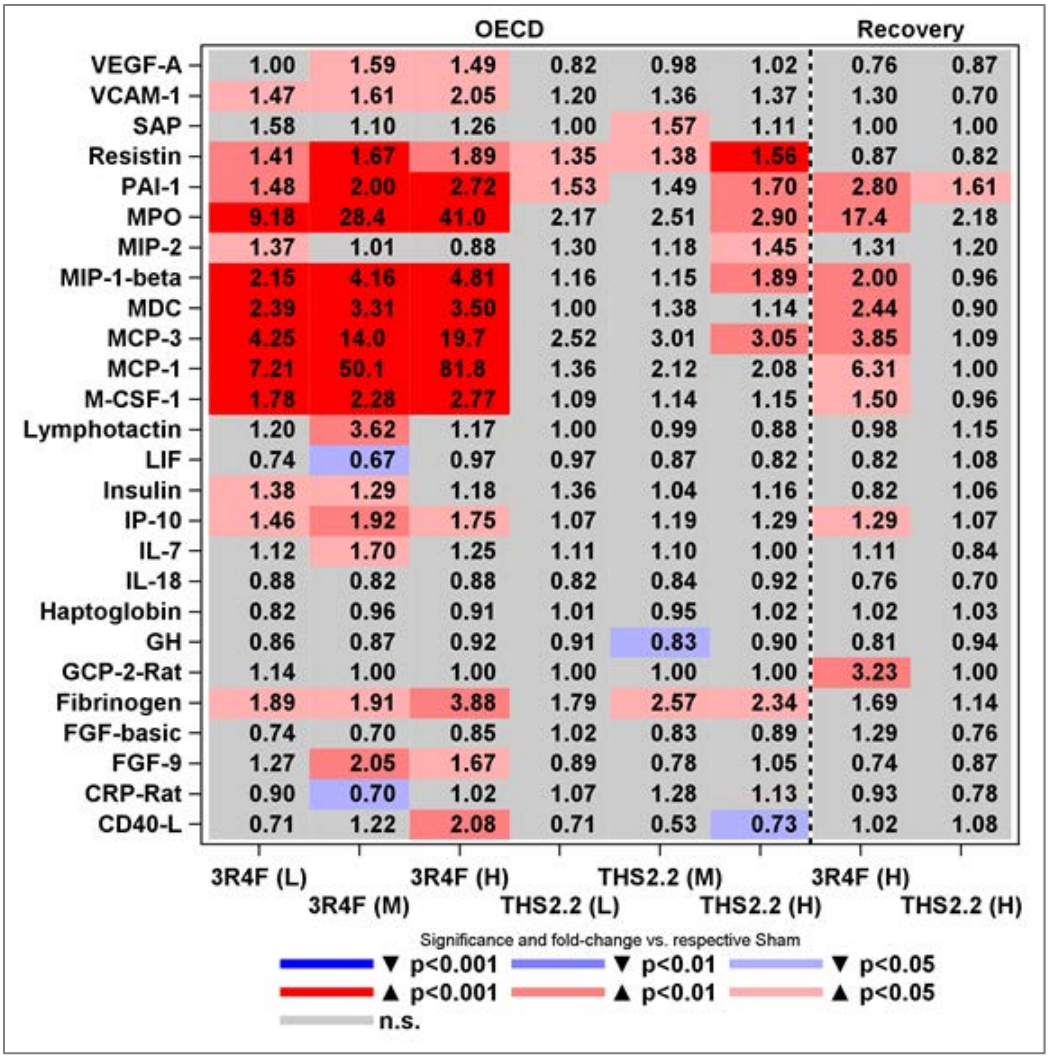


Figure 33. Alterations in levels of soluble inflammation mediators in bronchoalveolar lavage fluid of female rats exposed to 3R4F cigarette smoke or THS2.2 aerosol

The heat map depicts fold changes in mediator concentrations in bronchoalveolar lavage fluid of rats exposed to 3R4F cigarette smoke or THS2.2 aerosol for 90 days (OECD), or for the same duration followed by a 42-day recovery period (Recovery). Colors indicate a statistically significant increase (▲, shades of red) or decrease (▼, blue shades).

In summary, this study analyzed the biological effects of inhaled THS2.2 aerosol compared with smoke from the 3R4F reference cigarette. Lung inflammation and histopathological changes of respiratory tract organs in THS2.2 aerosol-exposed rats were markedly reduced compared with 3R4F CS-exposed rats. In line with this finding, transcriptomics-based mechanistic studies of nasal and lung tissues also indicated reduced perturbation of inflammatory processes as well as of other toxicity mechanisms linked to tissue repair and cell fate in animals exposed to THS2.2 aerosol.

3.3.2.1.2 Rat OECD THS2.2 Menthol Study

The second 90-day inhalation study was conducted with a mentholated version of the THS2.2 modified risk tobacco product prototype (THSM), comparing the toxicity of cigarette smoke from 3R4F to the aerosol from THS2.2 Menthol. In this study, rats were exposed to filtered fresh air (sham), to cigarette smoke from 3R4F, and to two mentholated reference cigarettes (MRC), all corresponding to 23 µg/L nicotine, or to a low, medium, or high concentration of the aerosol from THS2.2 Menthol corresponding to 15, 23, and 50 µg/L nicotine, respectively. MRC low menthol (LM) and MRC high menthol (HM) were designed to meet the tar, nicotine, carbon monoxide, and cigarette diameter specifications of 3R4F reference cigarettes and to produce approximately 1.2 mg and 2.4 mg menthol in smoke, respectively, when smoked according to International Organization for Standardization (ISO) standard 3308:2012. As in the previous OECD study, respiratory tract organs from animals of all exposure groups were subjected to histopathological evaluation following the 90-day inhalation, and pulmonary inflammation was assessed at the end of exposure (90 days) and following the 42-day post-exposure period (90 + 42 days). Furthermore, potential molecular changes as a consequence of exposure were evaluated using transcriptomics, proteomics, and lipidomics analyses.

Changes in the nasal respiratory epithelium were observed in rats following exposure to CS and THS2.2M aerosol over a 90-day period and consisted of squamous cell metaplasia, goblet cell hyperplasia with and without loss of goblet cells and reserve cell hyperplasia. Squamous metaplasia was predominantly seen in animals exposed to smoke from reference cigarettes without marked differences in the severity of lesions between the three items. Squamous metaplasia was also incidentally found in animals exposed to a high concentration of THS2.2M aerosol. However, squamous metaplastic changes in nasal respiratory epithelia of the THS2.2M High group animals were less severe than in animals in the 3R4F and MRC HM groups. Reserve cell hyperplasia was also less severe in animals from the THS2.2M groups than in rats exposed to smoke from the reference cigarettes, independent of the presence or concentration of menthol in smoke. Importantly, there was nearly complete regression of these adaptive epithelial changes following a recovery period of 42 days, independent of the exposure, suggesting that they represented local adaptive changes to irritant inhalation. In contrast, goblet cell hyperplasia was observed in all exposed female animals relative to the sham group, and although the changes were not severe or extensive, they persisted throughout the post-exposure period and even worsened in severity. However, goblet cell hyperplasia was still less severe in THS2.2M-exposed rats compared with those animals exposed to any of the reference cigarettes.

Squamous metaplasia and reserve cell hyperplasia were also noted in nasal olfactory epithelium in animals exposed to smoke from any of the reference cigarettes. The severity of these adaptive lesions decreased in female rats during the recovery period. By contrast, THS2.2M-exposed animals only exhibited squamous metaplasia and reserve cell hyperplasia at this location incidentally and also did not display any major abnormalities in distal nasal epithelium. Furthermore, squamous metaplasia was one of the morphological features observed in laryngeal epithelium, at the base of the epiglottis and arytenoid projections in all exposed animals. Generally, lesions were more severe in rats exposed to smoke from the reference cigarettes than in those exposed to THS2.2M

aerosol, and grading was similar in male and female rats. Lesions regressed in animals allowed a recovery period, suggesting that they were predominantly adaptive and reversible epithelial changes.

The bronchial epithelium of rats exposed to THS2.2M aerosol did not exhibit any marked increase in goblet cells or squamous metaplastic lesions. However, exposure to reference cigarette smoke, independent of the presence of menthol, resulted in the development of goblet cell hyperplasia in bronchial epithelium that was more advanced than that observed in THS2.2M aerosol-exposed animals. Of note, incidental goblet cell hyperplasia in bronchial epithelium regressed noticeably in female animals that were permitted a post-exposure recovery. Lungs of CS-exposed rats exhibited mild-to-moderate inflammation, as evidenced by increased numbers of unpigmented and pigmented macrophages and the presence of macrophage nests, which were not seen in THS2.2M aerosol-exposed animals. Lung inflammation in CS-exposed rats was further reflected in increased counts of total free cells in BALF, which, at least in part, declined after post-exposure recovery. In contrast, total free lung cell counts in THS2.2M aerosol-exposed animals were not markedly elevated above those seen in sham animals.

Examining the biological impact of exposure on nasal epithelium using a mechanistic network approach identified exposure to MRC LM as having the biggest biological impact on male as well as female rats (RBIF = 100%; REF). Of note, this was nearly identical to the biological impact of exposure to MRC HM in female rats, closely followed by the impact elicited by 3R4F CS exposure. In noses of male rats exposed to MRC HM, the impact was approximately half that seen following MRC LM exposure, and 3R4F CS exposure had a biological impact falling between the exposures to the two MRC. A marked effect of THS2.2M aerosol exposure on the biological networks was only seen at the highest concentration. In addition, while the impact caused by THS2.2M aerosol exposure almost entirely abated following post-exposure recovery, the effects of 3R4F CS and MRC HM CS exposure only diminished, suggesting that they were partially irreversible.

Examining the affected network families further, a range of biological processes and mechanisms in the nose were found to be affected by exposure to reference cigarette smoke including those related to cell proliferation, stress responses, programmed cell death and senescence, tissue repair and angiogenesis, and innate and adaptive immune responses. There was no gender-specific difference in the pattern of network perturbations. Furthermore, in female rats exposed to smoke from any of the reference cigarettes, all of these perturbations were sustained throughout the post-exposure period, albeit with a smaller amplitude. By comparison, exposure to aerosol from THS2.2M led to few perturbations, most of which reflected cellular stress responses, and, at medium and high concentrations, cell death mechanisms, tissue repair and epithelial immune responses. However, perturbations due to THS2.2M exposure, independent of dose, never reached the same amplitude as that observed following exposure to any of the reference products and diminished to a large degree during the 42-day post-exposure period (Figure 34).

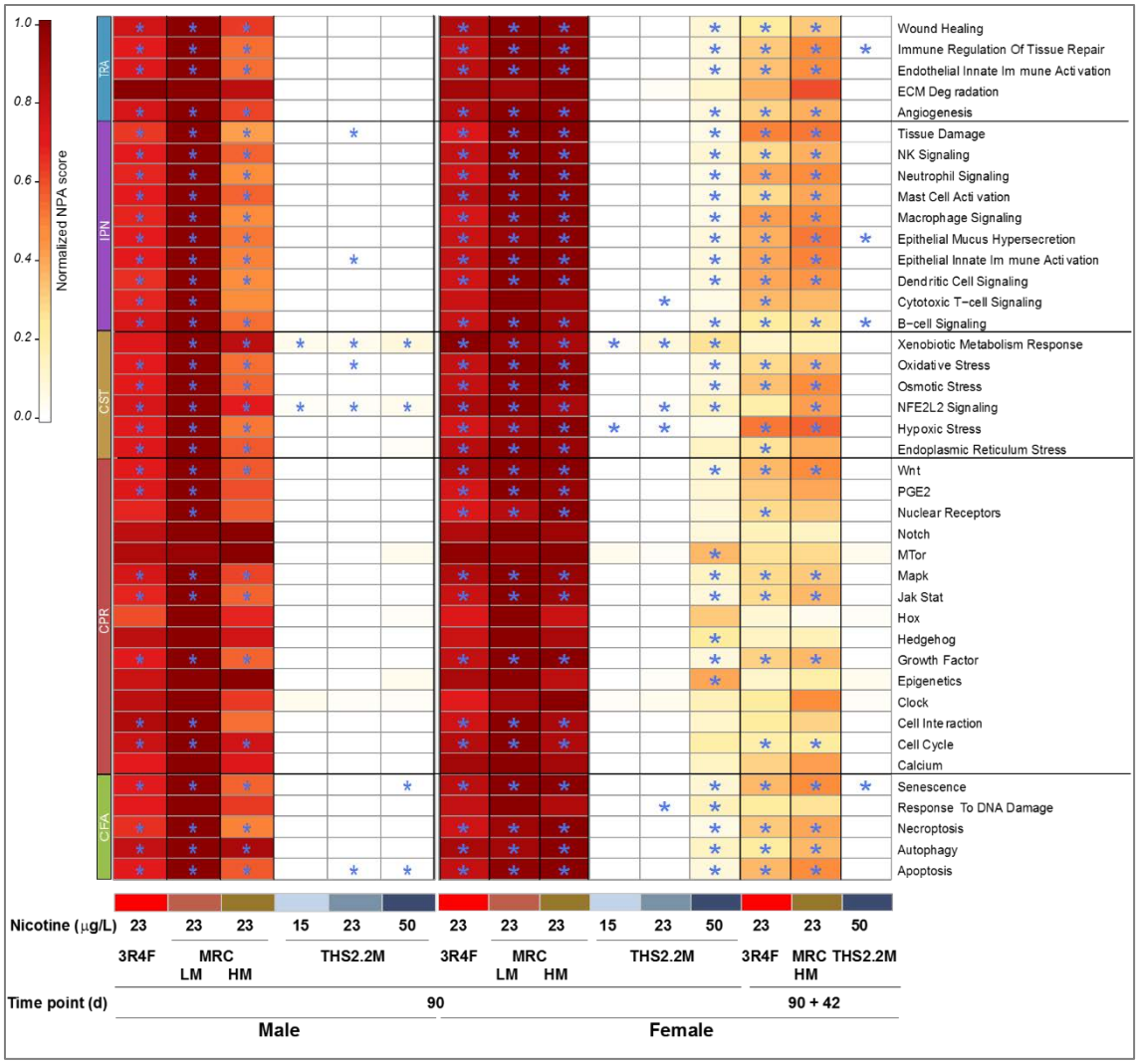


Figure 34. Network perturbations in rat nasal epithelial tissues following exposure to reference cigarette smoke and THS2.2M aerosol compared with air controls

Heatmap of network perturbation amplitude (NPA) scores summarizing subnetworks that were significantly perturbed in at least one treatment. A network is considered perturbed if, in addition to the significance of the NPA score with respect to the experimental variation, the two companion statistics (O and K) derived to inform on the specificity of the NPA score with respect to the biology described in the network, are significant. Significantly perturbed networks are indicated by * (i.e. O and K statistic *p*-values <0.05 and significant with respect to the experimental variation). Abbreviations: CFA, Cell Fate; CPR, Cell Proliferation; CST, Cell Stress; IPN, Inflammatory Process Network; TRA, Tissue Repair and Angiogenesis.

With few exceptions, network perturbations in the IPN subnetworks followed the same patterns: in male rats, exposure to smoke from MRC LM had a bigger impact across all IPN subnetworks than that from MRC HM or 3R4F. In contrast, THS2.2M aerosol exposure only elicited minor perturbations in the Tissue Damage and Epithelial Immune Activation subnetworks. In female rats, smoke from the mentholated reference cigarettes (independent of menthol concentration) had the biggest impact on the mechanisms

associated with the epithelial inflammatory response to tissue injury including the activation of various immune cells (macrophages, neutrophils, mast cells). The same underlying biology was affected by 3R4F CS exposure, although perturbation amplitudes were somewhat smaller than those seen with exposure to smoke from MRC. In addition, in rats exposed to CS, perturbations abated only slightly after 42 days. A similar pattern of IPN subnetwork perturbations was also observed in nasal epithelia from female THS2.2M aerosol-exposed rats, but only at the high concentration. Nevertheless, the extent of those perturbations was always lower compared with the impact of CS exposure, and only a minor effect on the Epithelial Mucus Hypersecretion subnetwork persisted after post-exposure recovery, while all other perturbations subsided (Figure 35).

Of note, expression levels of several genes linked to inflammation were strongly deregulated in the nasal respiratory epithelium of CS-exposed rats, resulting in upregulation of mRNA in most cases. With very few exceptions, exposure to mentholated CS affected the same genes as 3R4F CS. In contrast, THS2.2M aerosol exposure did not cause any significant changes in expression of genes linked to inflammation in male rats, while transcriptional levels of a small number of genes were significantly altered in nasal epithelia of female animals (Figure 36).

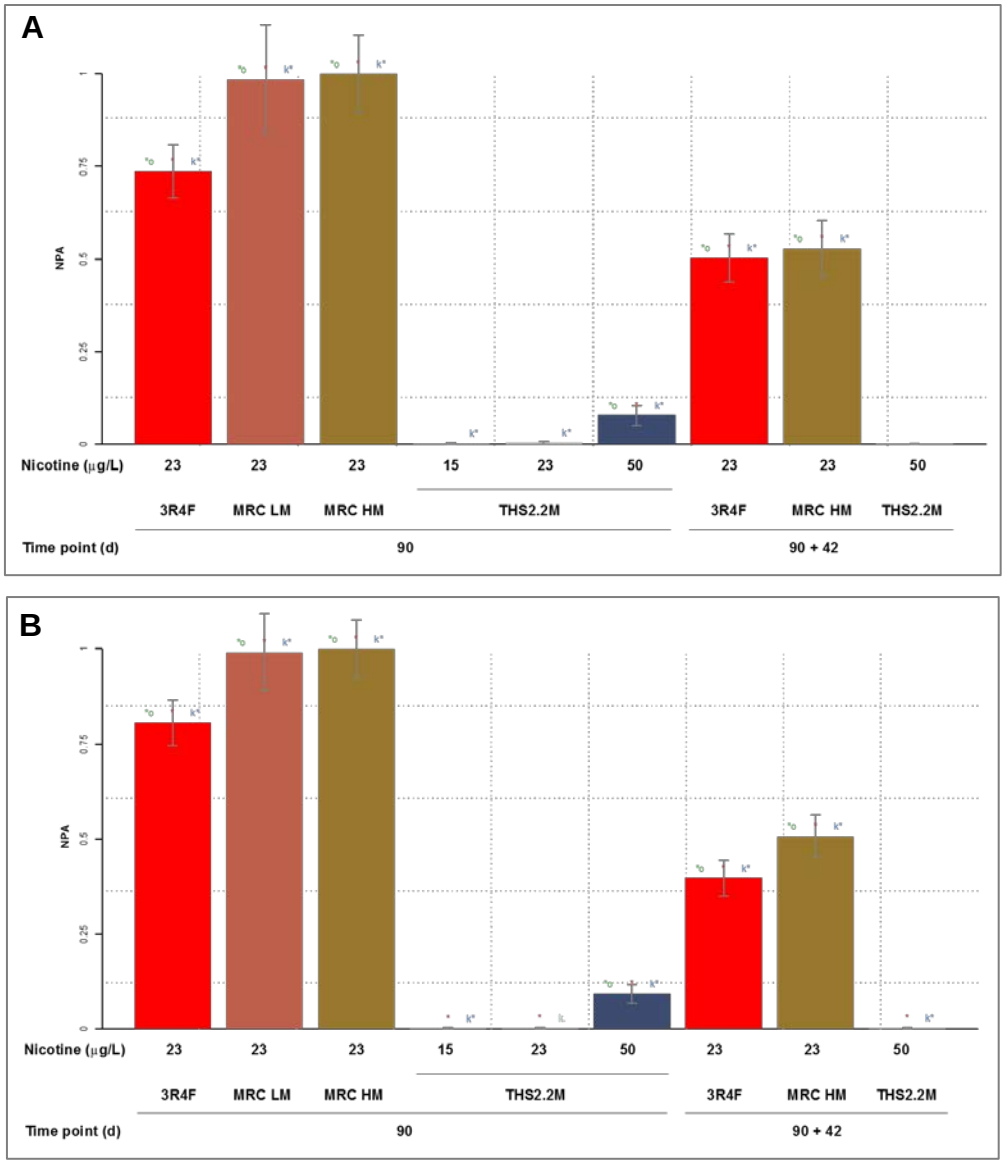


Figure 35. Relative network perturbation amplitude (NPA) scores of specific Inflammatory Process Network (IPN) subnetworks in nasal epithelial tissues of female rats exposed to reference cigarette smoke and THS2.2M aerosol

The relative NPA scores for the (A) Tissue Damage and (B) Epithelial Innate Immune Activation subnetwork models are shown with their confidence interval accounting for experimental variation. Percentages give the relative NPA score for the subnetworks compared with the reference (treatment comparison showing the highest perturbation). In addition, companion statistics derived to inform on the specificity of the NPA score with respect to the biology described in the respective subnetwork models are shown as *O and K*, respectively, if their *p*-values are below the significance level. Symbol legend: *, O and K statistic *p*-values <0.05; .O and K., *p*-values between 0.05 and 0.1.

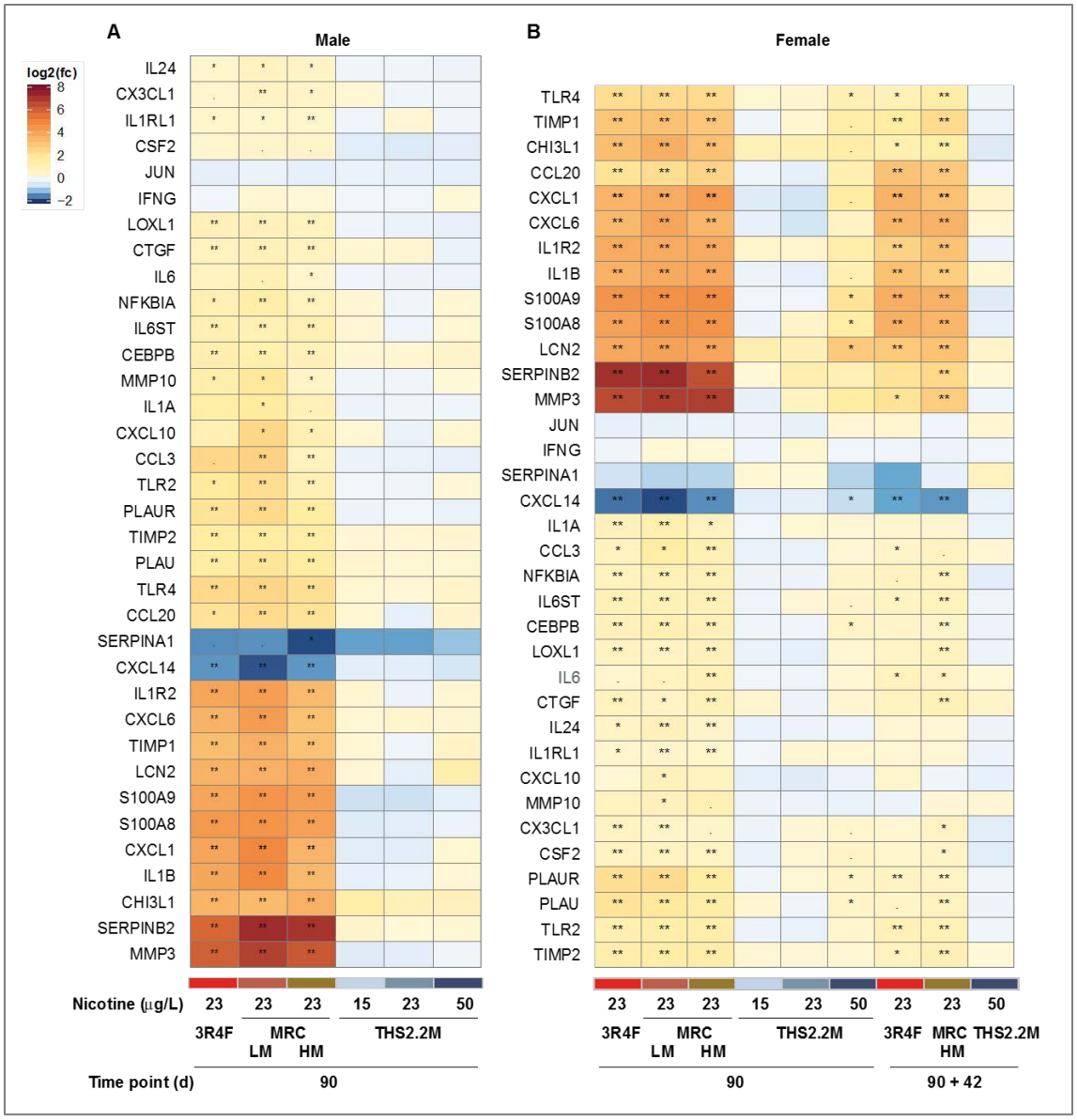


Figure 36. Altered expression levels of genes linked to inflammation in rat nasal epithelial tissues following exposure to reference cigarette smoke and THS2.2M aerosol

The heatmap depicts changes in gene expression of inflammation-related genes (gene symbols listed on the left) relative to corresponding air-exposed controls in the lungs of (A) male and (B) female rats expressed as $\log_2$[fold change (value; fc)]. Upregulation and downregulation of gene expression levels are represented by orange and blue shades, respectively, with darker colors indicating greater absolute fold changes. Statistically significant fold changes are highlighted by ** (adjusted $p<0.05$) and * (adjusted $p<0.1$).

Evaluation of lung SRPs from exposed male and female rats indicated that only a few genes showed significant deregulation following exposure to 3R4F CS. This response was dose-dependent, and, at least in part, reversible in animals that were allowed a 42-day post-exposure recovery, and there was no obvious difference between male and female rats' SRPs. By comparison, exposure to THS2.2M aerosol induced a markedly less pronounced systems response, even at the highest concentration. In addition, gene expression changes following THS2.2M aerosol exposure fully reverted during the post-exposure period.

Systems toxicological analysis of transcriptomics data revealed significant perturbations in all network families in the lungs of CS-exposed rats, and this impact, in particular on the IPN and Tissue Repair and Angiogenesis networks, was sustained throughout the recovery period. Exposure of male rats to THS2.2M aerosol, however, had an overall lower impact on the lung, affecting fewer mechanisms and to a lower degree. Lungs of female rats exposed to THS2.2M aerosol exhibited more perturbations than those of exposed male animals, with significant effects on more than half of the inflammatory processes capturing T cell biology and innate immune responses. However, these perturbations were generally of smaller amplitude, and, in contrast to CS exposure, the exposure effects largely subsided (Figure 37).

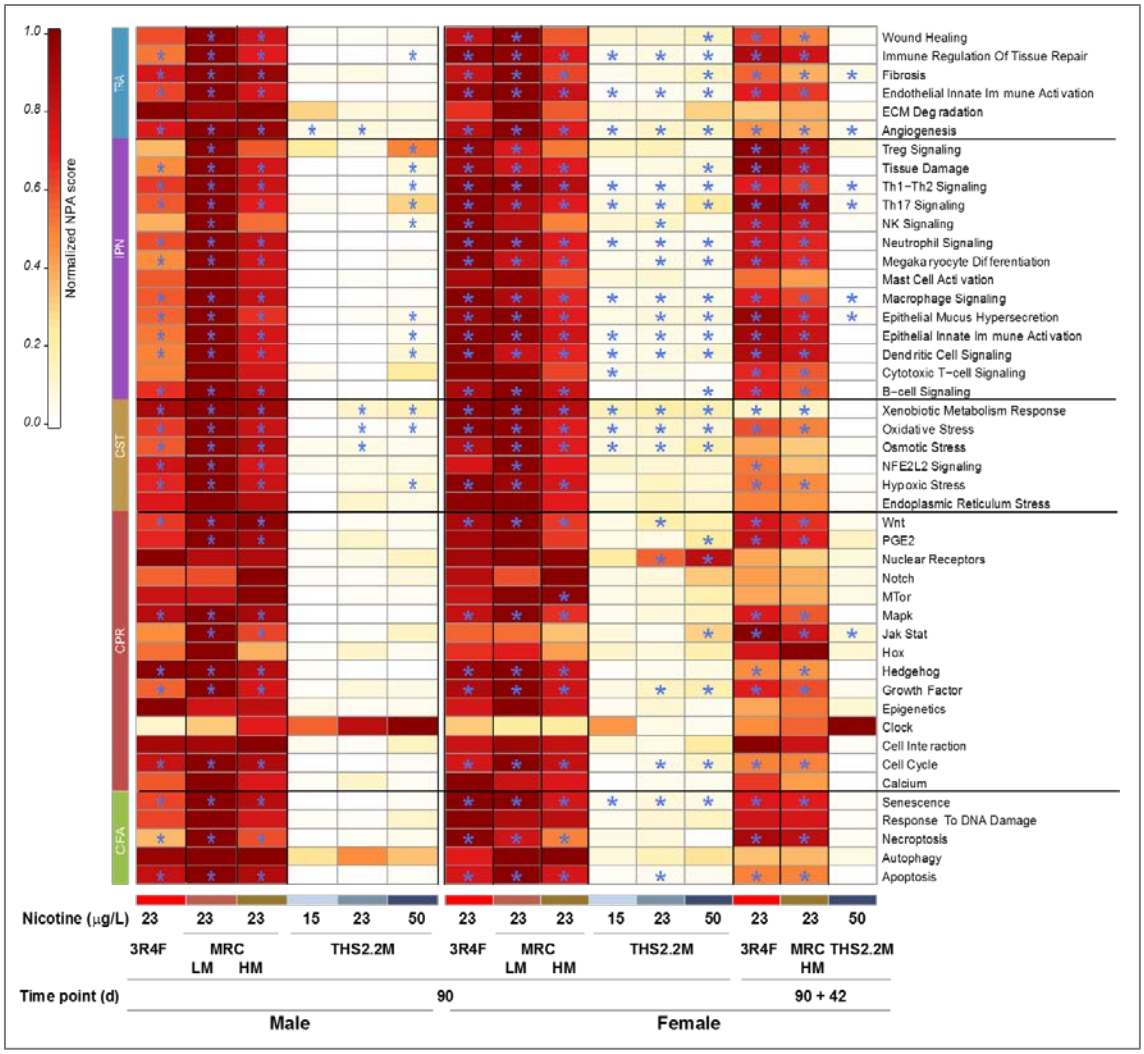


Figure 37. Network perturbations in rat lung tissues following exposure to reference cigarette smoke and THS2.2M aerosol compared with air controls

Heatmap of network perturbation amplitude (NPA) scores summarizing subnetworks that were significantly perturbed in at least one treatment. A network is considered perturbed if, in addition to the significance of the NPA score with respect to the experimental variation, the two companion statistics (O and K) derived to inform on the specificity of the NPA score with respect to the biology described in the network, are significant. Significantly perturbed networks are indicated by * (i.e. O and K statistic p-values <0.05 and significant with respect to the experimental variation). Abbreviations: CFA, Cell Fate; CPR, Cell Proliferation; CST, Cell Stress; IPN, Inflammatory Process Network; TRA, Tissue Repair and Angiogenesis.

Unlike in the nose, fewer genes known to play a role in inflammation were deregulated in the lungs of CS-exposed rats; e.g., *ILR2*, *LCN2*, *S100A8*, *S100A9*, *CXCL1*, *CCL3*, *CHI3L1* and *PLAUR* were strongly upregulated, while *CXCL14* levels significantly decreased in both male and female animals' lungs. In female rats, elevated transcript levels were sustained throughout the post-exposure period, confirming the observation of a persistent inflammatory response to exposure. In contrast, THS2.2M exposure

decreased *CXCL10* gene expression in the lungs of female animals only, and only at the high concentration, but did not elicit any other changes in the expression of these genes (Figure 38).

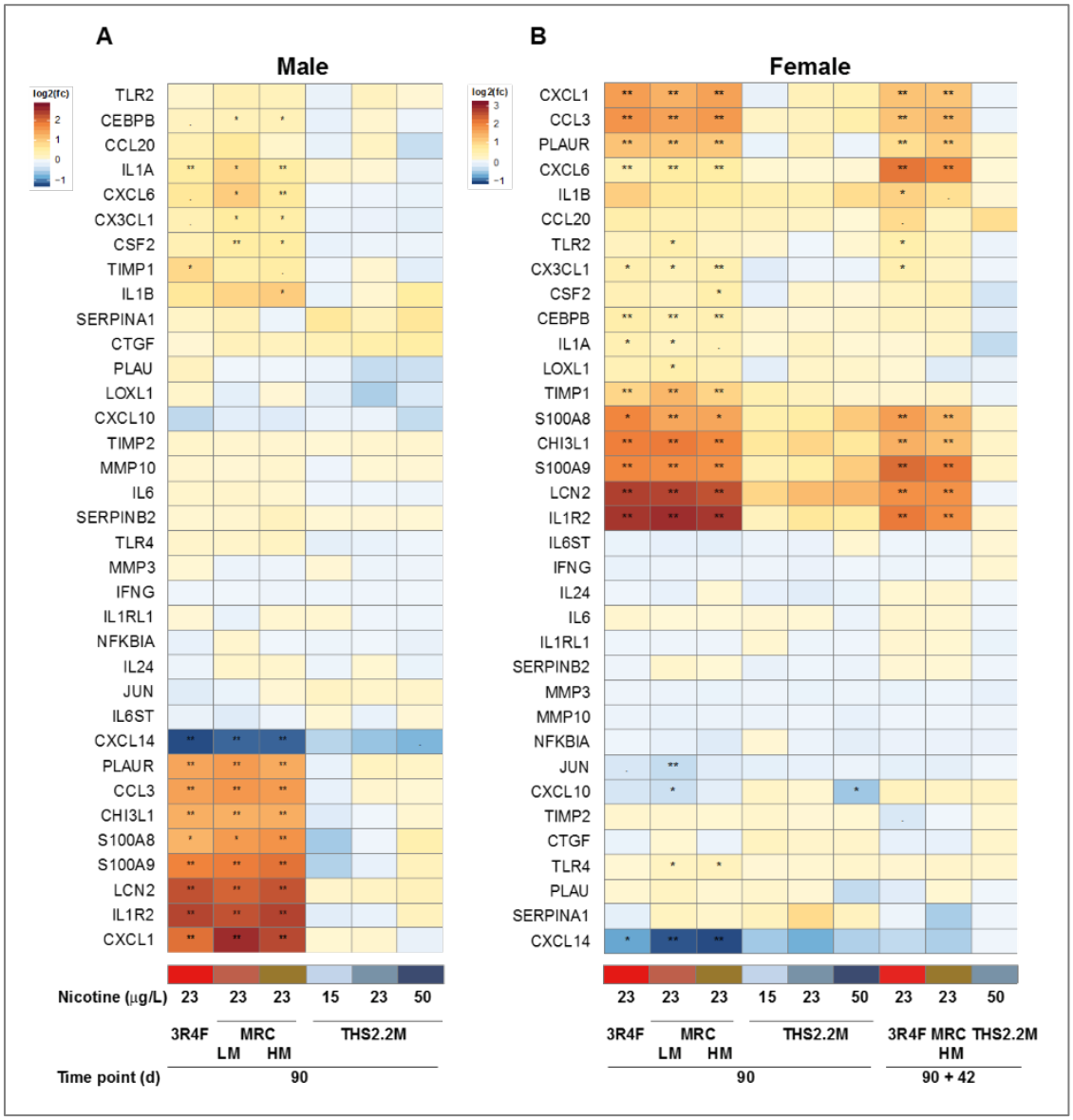


Figure 38. Altered expression levels of genes linked to inflammation in rat lung tissues following exposure to reference cigarette smoke and THS2.2M aerosol

The heatmap depicts changes in gene expression of inflammation-related genes (gene symbols listed on the left) relative to corresponding air-exposed controls in the lungs of (A) male and (B) female rats expressed as $\log_2$[fold change (value; fc)]. Upregulation and downregulation of gene expression levels are represented by orange and blue shades, respectively, with darker colors indicating greater absolute fold changes. Statistically significant fold changes are highlighted by ** (adjusted $p<0.05$) and * (adjusted $p<0.1$).

These observations of increased inflammation in the lungs of CS-exposed rats were further supported by increased levels of several pro-inflammatory mediators in BALF. Similar to the observations in the OECD inhalation study with non-mentholated THS2.2 aerosol, exposure to CS strongly elevated VCAM-1, CCL2, CCL4, CCL7, CCL22, CSF1, MMP-9 and PAI-1, while smaller increases were noted for fibrinogen, VEGFA, TIMP1, resistin and SCF, in particular when mentholated CS was used. Of note, in female rats exposed to CS, fibrinogen levels were higher than in males. Furthermore, VCAM-1 and MMP-9 levels remained high in 3R4F CS-exposed animals following the 42-day post-exposure period, while amounts of CCL2, CCL7, CCL22, and CSF1 in BALF declined. In contrast, exposure to THS2.2M aerosol resulted in fewer altered inflammatory marker levels; there was a slight elevation in amounts of TIMP-1, CCL4, CXCL2 and CSF1 (M-CSF-1) in male animals (only at the high concentration), and an increase in CCL7 and fibrinogen levels in females. None of these changes persisted throughout the post-exposure recovery (Figure 39, Figure 40).

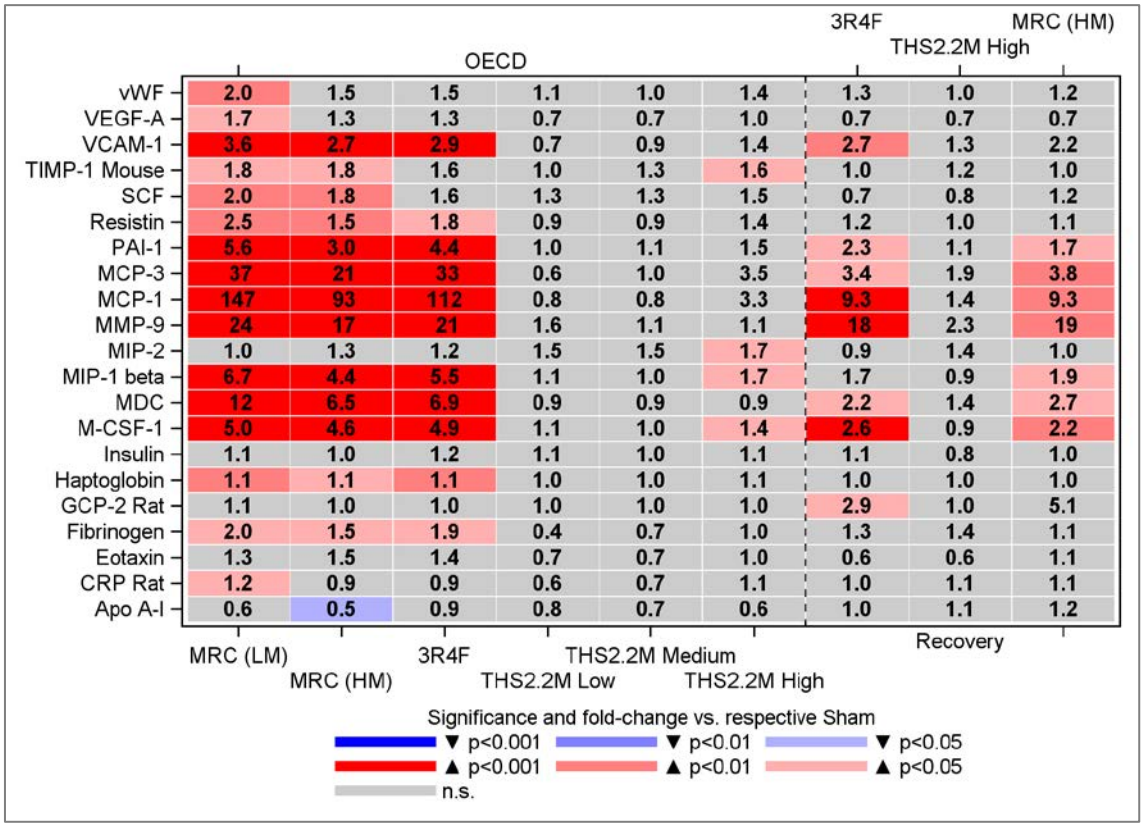


Figure 39. Alterations in levels of soluble inflammation mediators in bronchoalveolar lavage fluid of male rats exposed to 3R4F cigarette smoke or THS2.2M aerosol

The heatmap depicts fold changes in mediator concentrations in bronchoalveolar lavage fluid of rats exposed to 3R4F cigarette smoke or THS2.2M aerosols for 90 days (OECD), or for the same duration followed by a 42-day recovery period (Recovery). Colors indicate a statistically significant increase (▲, shades of red) or decrease (▼, blue shades).

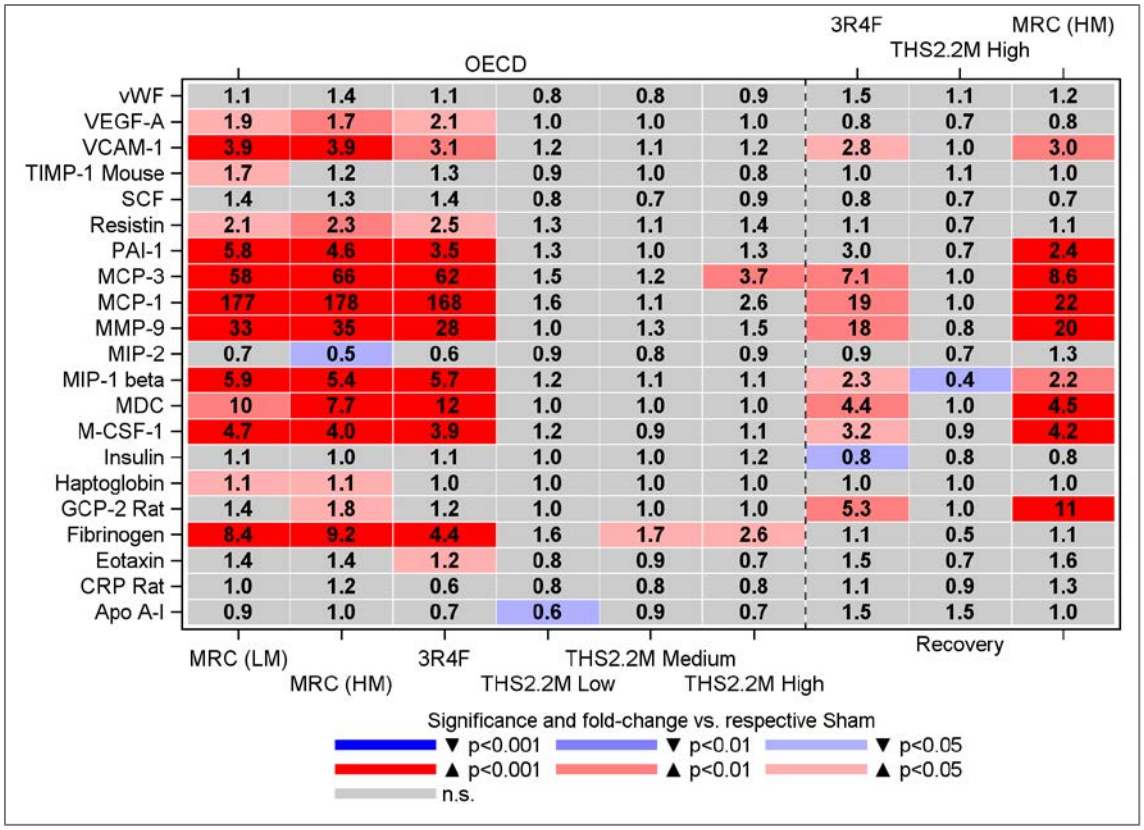


Figure 40. Alterations in levels of soluble inflammation mediators in bronchoalveolar lavage fluid of female rats exposed to 3R4F cigarette smoke or THS2.2M aerosol

The heatmap depicts fold changes in mediator concentrations in bronchoalveolar lavage fluid of rats exposed to 3R4F cigarette smoke or THS2.2M aerosols for 90 days (OECD), or for the same duration followed by a 42-day recovery period (Recovery). Colors indicate a statistically significant increase (▲, shades of red) or decrease (▼, blue shades).

In summary, adaptive epithelial changes were noted in the upper respiratory tract in rats exposed to 3R4F, MRC LM, and MRC HM CS, at comparable incidences and with comparable severity between the male and female animals exposed to any of the reference products. In contrast, there were only incidental exposure-related findings in the respiratory tracts of animals from the Low and Medium THS2.2M groups. While exposure to THS2.2M aerosol at high concentrations did produce epithelial alterations, these changes were typically mild in severity or rare in comparison to the reference items even though the aerosol nicotine concentration was more than twice as high as that of the reference cigarettes. The noses and lungs of rats exposed to CS exhibited a strong epithelial inflammatory response, which did not fully abate during post-exposure recovery. In contrast, exposure to THS2.2M aerosol induced limited inflammation in the upper respiratory tract, and this subsided once exposure ceased.

3.3.2.2 Apoe$^{-/-}$ THS Study

The development and progression of COPD and CVD were evaluated in *Apoe*$^{-/-}$ mice following chronic exposure to 3R4F mainstream cigarette smoke at a target nicotine concentration of 29.9 µg/L, to an aerosol from THS2.2 at a matched nicotine concentration, or to filtered fresh air for 3 hours per day, 5 days per week, for up to 8 months. After 2 months of exposure to 3R4F CS, designated groups of animals were switched to THS2.2 aerosol exposure (switching group) or exposed to filtered air (cessation group) for up to 6 months following the same daily exposure regimen. At designated time points (months 1, 2, 3, 6, and 8 after commencing exposure), animals were examined for multiple parameters to comprehensively assess the development and progression of COPD or CVD indicators. These included hematology and clinical chemistry, pulmonary inflammation measurements, assessment of pulmonary function, lung histopathology and morphometry, evaluation of atherosclerotic plaque formation in the aortic arch and descending aorta, and the examination of molecular changes in various tissues throughout the exposure period by transcriptomics, proteomics, and lipidomics.

Typical cigarette smoke exposure-related effects including reserve cell hyperplasia and squamous metaplasia were noted in nasal respiratory epithelium, with the incidence and severity of these lesions diminishing towards the more distal regions of the nose. Such marked effects were not seen in THS2.2 aerosol-exposed mice, although mild reserve cell hyperplasia was noted in nasal respiratory epithelium at month 6. This did not worsen over the exposure period. Within 1 and 3 months, both cessation and switching resulted in rapid repair of CS-related metaplastic and hyperplastic lesions, respectively, in nasal epithelium, indicative of their transient nature.

Bronchial epithelia displayed mild-to-moderate reserve cell hyperplasia in 3R4F CS-exposed animals which diminished in severity upon cessation and switching. In contrast, continuous exposure to THS2.2 aerosol caused reserve cell hyperplasia in some but not all animals, and alterations to bronchial epithelium were minimal. Similarly, the lungs of THS2.2 aerosol-exposed mice also lacked inflammatory cell infiltrates in the alveolar lumen and interstitium and the increase in pigmented and unpigmented macrophages over time that were the most pronounced histopathological findings in the lungs of *Apoe*$^{-/-}$ mice exposed to 3R4F CS and decreased in incidence and severity when animals were switched to fresh air or THS2.2 aerosol. This was further confirmed by increased total numbers of free lung cells in 3R4F CS-exposed mice, primarily because of a significant increase in BALF neutrophil counts followed by an increase in lymphocyte, dendritic cell, and macrophage numbers. In contrast, prolonged exposure to the THS2.2 aerosol had no effect on total free lung cell counts. Both cessation and switching resulted in the rapid decline in the total number of free lung cells, which almost reached that seen in sham or THS2.2 aerosol-exposed mice after just 1 month of cessation, and returned to counts observed in sham and THS2.2 aerosol-exposed mice by month 8. Histopathological and morphometric assessment of the lungs also confirmed the presence of emphysematous lesions in animals exposed to 3R4F CS, but not in those exposed to THS2.2 aerosol. Although very mild age-dependent emphysematous lesions were noted in all animals, both cessation and switching contributed noticeably to lung tissue regeneration and repair.

The size of atherosclerotic plaques increased following 3R4F CS exposure over time. Although animals in the THS2.2 group were exposed to matched aerosol nicotine levels, their plaque sizes demonstrated only minimal differences from those seen in sham animals. Moreover, cessation and switching appeared to halt plaque growth and to not further aggravate the CS exposure-related effects.

Analysis of transcriptomics data from nasal epithelia of exposed *Apoe*$^{-/-}$ mice using a systems toxicology approach showed the highest biological impact for the 8-month 3R4F CS exposure (RBIF = 100%; REF). Only a fraction of that was seen at the earlier time points or with continued THS2.2 aerosol exposure. Importantly, switching to fresh air or THS2.2 aerosol greatly reduced the biological impact of 3R4F CS exposure over time. Further examination of the mechanisms contributing to the observed biological impact on the nose of 3R4F CS-exposed *Apoe*$^{-/-}$ mice revealed significant perturbations of the Cell Cycle and Senescence networks in addition to a sustained xenobiotic metabolism response. The perturbations increased in amplitude over time, and, at 8 months, a number of additional subnetworks in all network families were found to be significantly impacted. In contrast, exposure to THS2.2 aerosol for 2 months elicited the strongest biological impact on the nose, affecting predominantly Cell Stress network and IPN and, to a lesser degree, other subnetworks capturing apoptosis, senescence, and cell proliferation biology. Of note, with the exception of the Cell Cycle, Senescence and Xenobiotic Metabolism Response subnetwork perturbations, THS2.2 aerosol exposure did not cause such a significant impact after this time point. Upon cessation, the majority of network perturbations quickly abated. While this was also the case for the switching group, some cell stress and inflammatory responses remained active in the nasal epithelium of *Apoe*$^{-/-}$ mice (Figure 41).

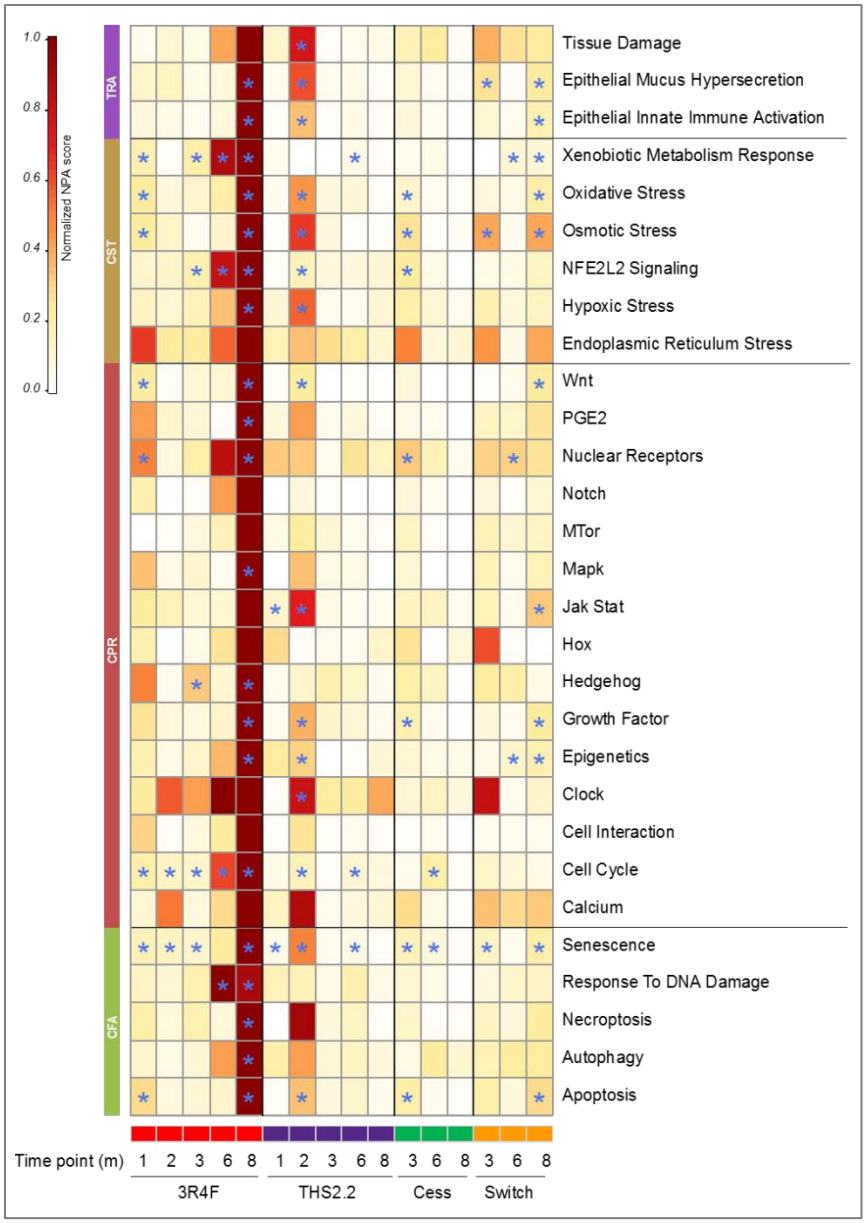


Figure 41. Network perturbations in *Apoe*$^{-/-}$ mouse nasal tissues following exposure to 3R4F cigarette smoke and THS2.2 aerosol compared with air controls

Heatmap of network perturbation amplitude (NPA) scores summarizing subnetworks that were significantly perturbed in at least one treatment. A network is considered perturbed if, in addition to the significance of the NPA score with respect to the experimental variation, the two companion statistics (O and K) derived to inform on the specificity of the NPA score with respect to the biology described in the network, are significant. Significantly perturbed networks are indicated by * (i.e. O and K statistic *p*-values <0.05 and significant with respect to the experimental variation). Abbreviations: Cess, cessation; Switch, switching; CFA, Cell Fate; CPR, Cell Proliferation; CST, Cell Stress; IPN, Inflammatory Process Network; TRA, Tissue Repair and Angiogenesis.

Similar to observations in nasal samples, lung SRPs revealed an increasing number of DEGs in 3R4F CS-exposed mice compared with sham mice over time, while no DEGs were identified in lung tissues from THS2.2 aerosol-exposed mice or animals from the cessation and switching groups. Biological impact analysis indicated a major impact for 3R4F CS at the first three time points, peaking at 6 months of exposure (RBIF = 100%; REF) before declining slightly. By comparison, continued THS2.2 aerosol exposure had a considerably smaller impact on the lungs of *Apoe*$^{-/-}$ mice. Both cessation and switching resulted in marked reductions of the 3R4F CS-exposure effects, suggesting that they were, at least in part, reversible.

Early drivers of THS2.2 aerosol exposure effects were restricted to the networks describing tissue repair and oxidative stress-related processes. A more extensive involvement of other cell stress as well as innate and adaptive immune responses did not become apparent until month 3. After this time point, however, very few networks remained significantly perturbed. In contrast, the mechanisms underlying the observed biological impact exerted by 3R4F CS exposure encompassed all network models, with predominant involvement of the Tissue Repair and Angiogenesis network and IPN families, followed by less extensive perturbations of the Cell Stress, Cell Proliferation and Cell Fate networks. Most of the affected networks remained significantly perturbed throughout the cessation period, although the extent of perturbations was noticeably smaller. This was different from what was seen in the lungs of animals from the switching group. In that group, the majority of network perturbations subsided until they were no longer significant, suggesting that switching to THS2.2 aerosol exposure for this period of time did not worsen the effects of prior 3R4F CS exposure and also did not cause any additional effects on the lungs (Figure 42).

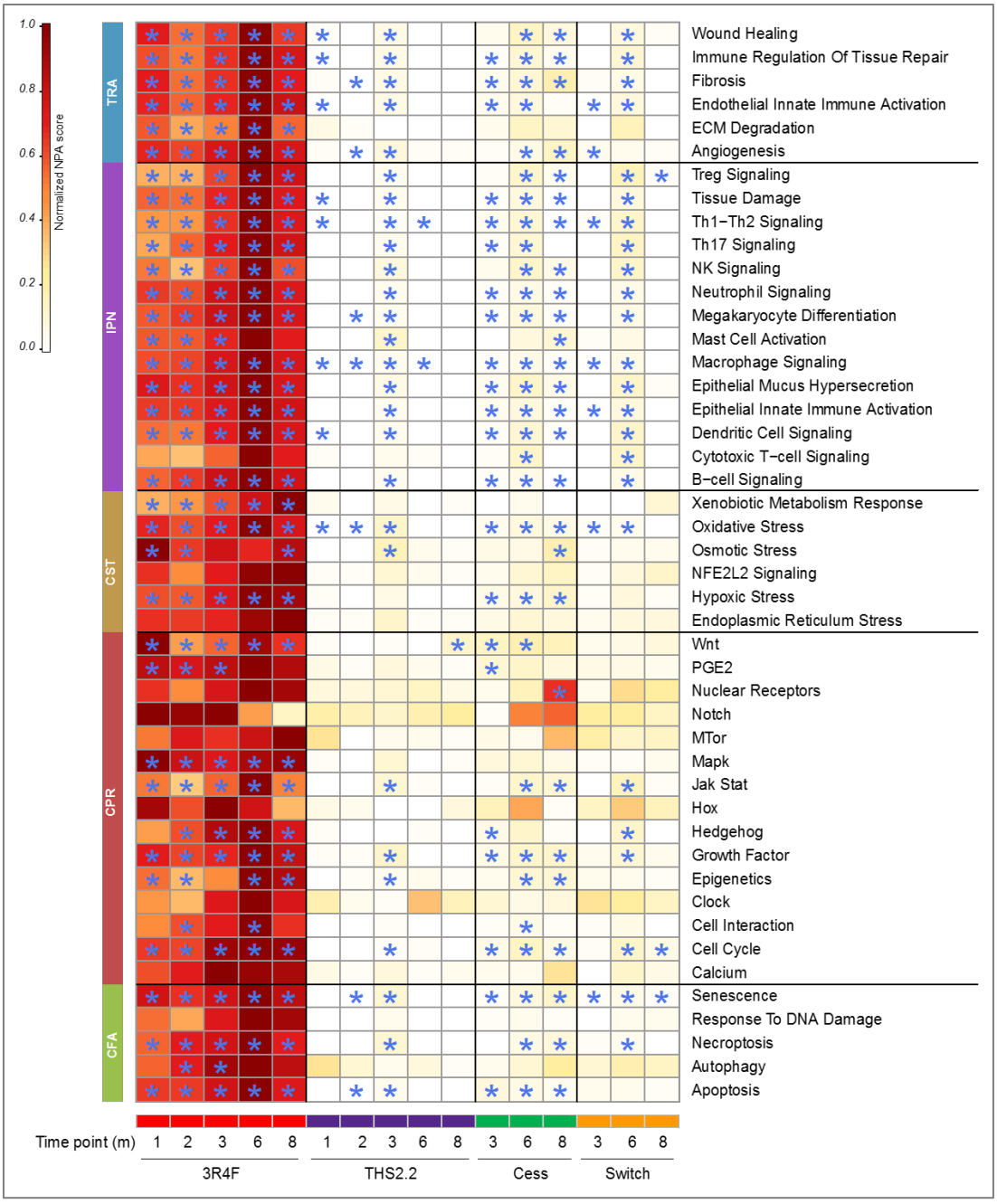


Figure 42. Network perturbations in *Apoe*$^{-/-}$ mouse lung tissues following exposure to 3R4F cigarette smoke and THS2.2 aerosol compared with air controls

Heatmap of network perturbation amplitude (NPA) scores summarizing subnetworks that were significantly perturbed in at least one treatment. A network is considered perturbed if, in addition to the significance of the NPA score with respect to the experimental variation, the two companion statistics (O and K) derived to inform on the specificity of the NPA score with respect to the biology described in the network, are significant. Significantly perturbed networks are indicated by * (i.e. O and K statistic *p*-values <0.05 and significant with respect to the experimental variation). Abbreviations: Cess, cessation; Switch, switching; CFA, Cell Fate; CPR,

Cell Proliferation; CST, Cell Stress; IPN, Inflammatory Process Network; TRA, Tissue Repair and Angiogenesis.

Nearly all of the processes encompassing the epithelial inflammatory response and the biology of innate and adaptive immunity in the lung were already significantly impacted by CS exposure for 1 month. They remained perturbed throughout the exposure period, with a peak in perturbation amplitudes at month 6. Such a peak was also seen with respect to the activity of inflammatory processes in the lungs of THS2.2 aerosol-exposed *Apoe*$^{-/-}$ mice, though this perturbation was only a fraction of that seen with 3R4F CS exposure. Moreover, the impact was generally low throughout the study. Cessation rapidly alleviated the CS exposure-related effects, and this was also the case for THS2.2 aerosol exposure (Figure 43).

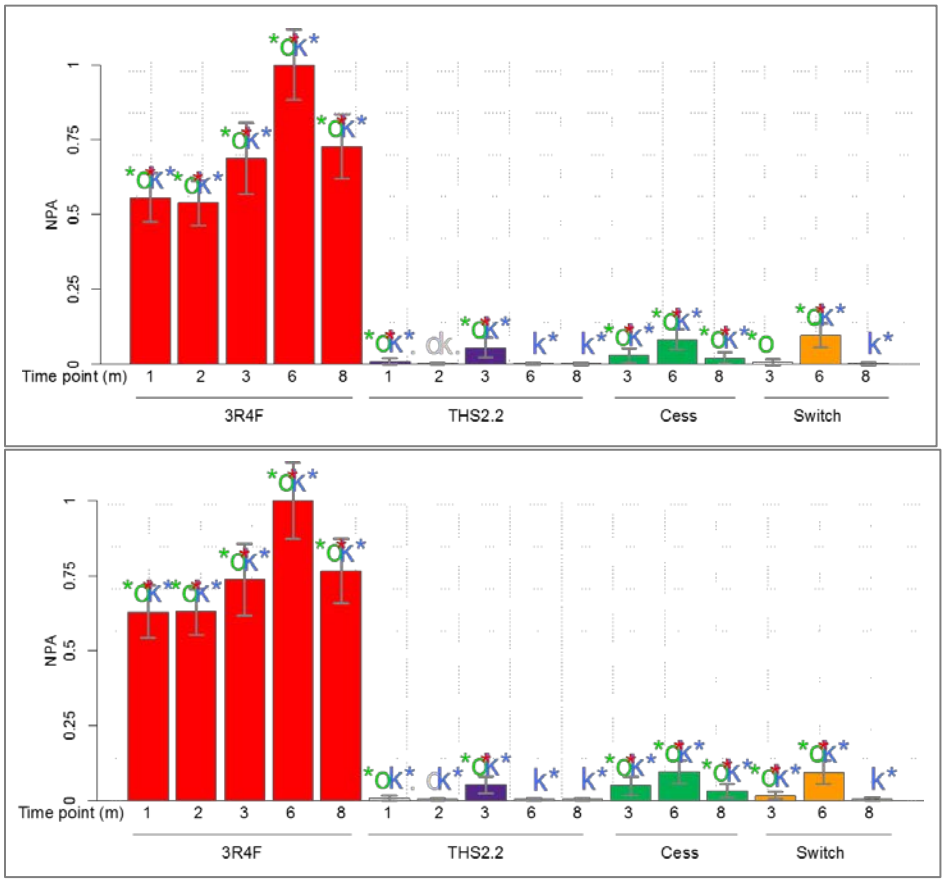


Figure 43. Relative network perturbation amplitude (NPA) scores of specific Inflammatory Process Network (IPN) subnetworks in *Apoe*$^{-/-}$ mouse lung tissues following exposure to 3R4F cigarette smoke and THS2.2 aerosol

The relative NPA scores for the (A) Tissue Damage and (B) Epithelial Innate Immune Activation subnetwork models are shown with their confidence interval accounting for experimental variation. Percentages give the relative NPA score for the subnetworks compared with the reference (treatment comparison showing the highest perturbation). In addition, companion statistics derived to inform on the specificity of the NPA score with respect to the biology described in the respective subnetwork models are shown as *O and K*, respectively, if their *p*-values are below the significance level. Symbol legend: *, O and K statistic *p*-values <0.05; .O and K., *p*-values between 0.05 and 0.1. Abbreviations: Cess, cessation; Switch, switching.

The effect of exposure on the lung proteome was also assessed by quantitative mass spectrometry-based proteomics. Exposure to 3R4F CS resulted in a clear time-dependent effect on the lung proteome, with the abundance of more than 700 proteins significantly altered after 8 months of exposure. There was a noticeable and significant increase in the number of differentially abundant proteins between months 3 and 6 in this exposure group. In contrast, exposure to THS2.2 aerosol had no significant effect on protein abundance during the entire 8-month exposure period. Both cessation and switching to THS2.2 aerosol resulted in a comparable and rapid attenuation of the 3R4F CS exposure effect; at the 3-month time point (1 month after switching/the start of cessation), differential abundance was still detectable for 10 and eight proteins in the cessation and switching groups, respectively. However, at 8 months, lung proteomes of animals from the cessation and switching arms were matching those of the sham group, with metallothionein-1 being the only remaining upregulated protein in the switching group. Functional association clustering revealed a range of exposure effects that are in line with previous findings for CS inhalation studies (Phillips et al, 2015). There was, for example, an increase in the numbers of proteins linked to inflammatory responses and tissue repair in the lungs of 3R4F CS-exposed mice. In contrast, expression of these proteins was not at all affected by exposure to THS2.2 aerosol (Figure 44).

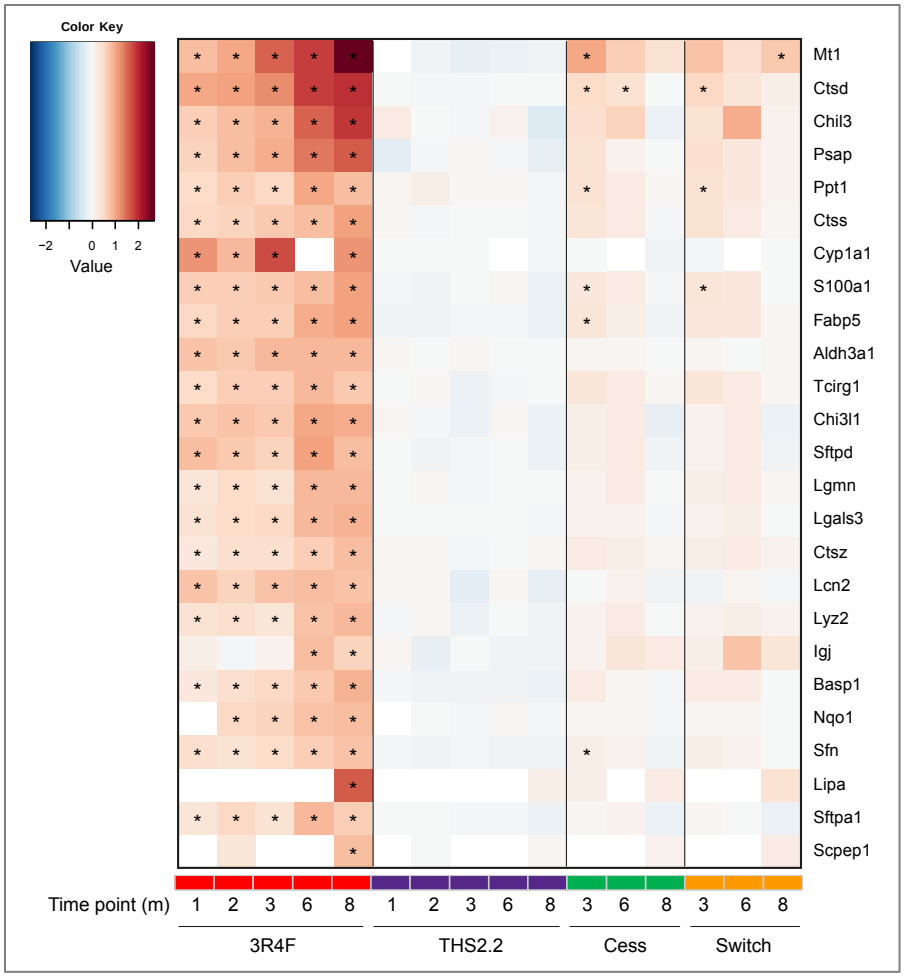


Figure 44. Altered expression levels of proteins in *Apoe*$^{-/-}$ mouse lung tissues following exposure to 3R4F cigarette smoke and THS2.2 aerosol

The heatmap depicts changes in protein expression of the top 25 ranked proteins (protein symbols listed on the right) relative to corresponding air-exposed controls in the lungs of *Apoe*$^{-/-}$ mice expressed as $\log_2$[fold change (value; fc)]. Upregulation and downregulation of gene expression levels are represented by orange and blue shades, respectively, according to the color key. Statistically significant fold changes are highlighted by * (adjusted $p<0.05$). Abbreviations: Cess, cessation; Switch, switching.

Analysis of 63 inflammatory mediators in BALF indicated a rapid increase in the levels of most analytes following 1 month of 3R4F cigarette smoke exposure, and, in general, those elevated levels persisted over the 8-month exposure period. Inflammatory mediator concentrations in BALF of THS2.2 aerosol-exposed mice were very similar to those in BALF samples obtained from sham animals. Both switching and cessation resulted in a decline of BALF protein levels towards those levels seen in sham or THS2.2 aerosol-exposed animals in most but not all cases. Among the mediators whose levels did not decline following switching and cessation were immunoglobulin A, eotaxin, IL-18, MIP-2, and TIMP-1, indicating that some portion of cigarette smoke-induced lung damage may have persisted for some time after exposure ceased (Figure 45).

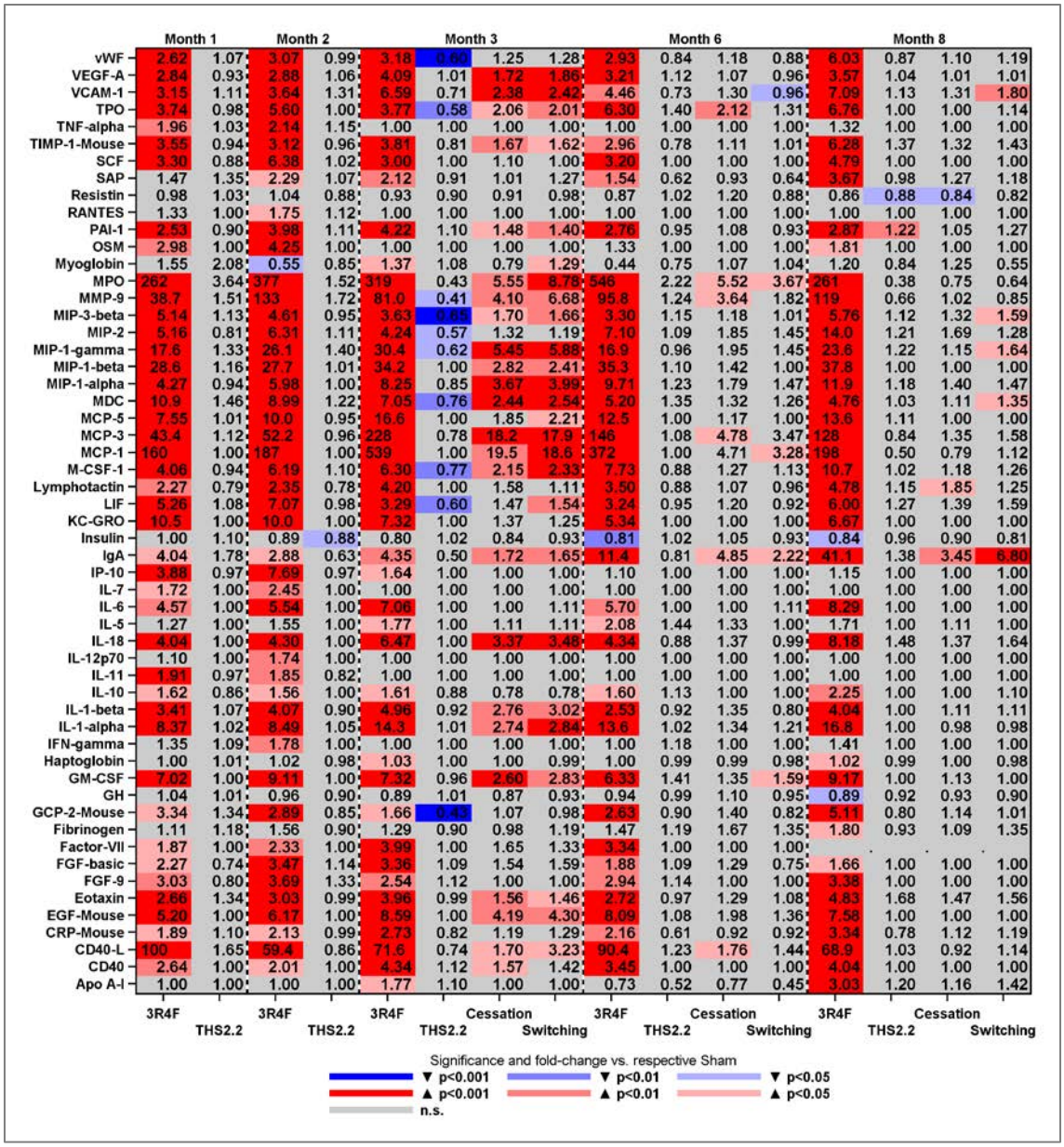


Figure 45. Alterations in levels of soluble inflammation mediators in bronchoalveolar lavage fluid of *Apoe*$^{-/-}$ mice exposed to 3R4F cigarette smoke or THS2.2 aerosol

The heat map depicts fold changes in mediator concentrations in bronchoalveolar lavage fluid of mice exposed to 3R4F cigarette smoke or THS2.2 aerosols for up to 8 months, or to 3R4F cigarette smoke for 2 months followed by a 6-month exposure to air (Cessation) or THS2.2 aerosol (Switching). Colors indicate a statistically significant increase (▲, shades of red) or decrease (▼, blue shades).

Together, these results demonstrate that exposure of *Apoe*$^{-/-}$ mice to THS2.2 aerosol for up to 8 months resulted in changes at the anatomical, physiological, and molecular levels that were largely indistinguishable from those seen in animals exposed to fresh air. Furthermore, following exposure to CS for 2 months, both cessation and switching to

THS2.2 aerosol exposure did not further aggravate CS exposure-induced alterations in lung function or the extent of atherosclerotic plaques and resulted in regression of inflammatory changes and reduction of molecular responses across a range of biological processes and mechanisms.

3.3.2.3 A/J Study

To assess the impact of lifetime exposure to THS2.2 aerosol relative to 3R4F CS on the development of emphysema and on lung tumor incidence and multiplicity, female A/J mice were exposed to fresh air (sham), 3R4F mainstream cigarette smoke corresponding to 13.4 µg nicotine/L, and aerosol from THS2.2 aerosol equivalent to nicotine concentrations of 6.7 (Low), 13.4 (Medium) and 26.8 µg/L (High) for 6 hours per day, 5 days per week, for up to 18 months following OECD Test Guideline 453 (OECD.). In addition, two groups of male A/J mice were exposed to fresh air (sham) and THS aerosol at 26 µg nicotine/L. Histopathological evaluation of respiratory tract organs and muscle tissues at interim dissections of female mice following 1, 5 and 10 months of exposure were accompanied by assessment of hematological and clinical chemistry parameters, lung function and pulmonary inflammation (months 1 and 5 only). Nasal epithelia and lungs were collected from exposed female animals for transcriptomics and proteomics analyses.

Since this study is currently still ongoing, this part of the dossier will be restricted to the available histopathological findings and the transcriptomics data from nasal respiratory epithelial and trachea samples collected during interim dissections at months 1, 5 and 10. Whether lifetime exposure to THS2.2 aerosol affects lung tumor incidences and multiplicities or causes pathologies in other than the respiratory organs will require analysis of samples obtained at terminal dissection.

Nasal respiratory and olfactory epithelium displayed morphological changes identified as reserve cell and goblet cell hyperplasia and squamous metaplasia following exposure to 3R4F CS and THS2.2 aerosol. However, the incidence and the severity of these adaptive lesions were generally lower in THS2.2 aerosol-exposed mice. Similarly, reserve cell hyperplasia and squamous metaplasia in both anterior and posterior laryngeal tissues were also prominent histopathological findings in 3R4F CS-exposed animals and occurred less frequently and were less extensive in mice exposed to THS2.2 aerosol, independent of the concentration. In addition, typical CS exposure-related epithelial changes including epithelial hyperplasia and squamous metaplasia were found at the carina of bifurcation at months 5 and 10, while tracheas from A/J mice exposed to THS2.2 aerosol did not exhibit any remarkable exposure-related effects.

The lungs of 3R4F CS-exposed animals exhibited inflammatory cell infiltrates that were absent in animals from the THS2.2 and sham study groups from month 1 onward. Pigmented and unpigmented macrophages were more frequently seen in A/J mice exposed to 3R4F CS from month 5, while those exposed to THS2.2 aerosol did not exhibit inflammatory cell infiltrates in the lungs. Furthermore, histopathological evaluation confirmed the presence of mild-to-moderate emphysematous lesions in mice exposed to 3R4F CS for 5 and 10 months. In contrast, lungs of THS2.2 aerosol-exposed mice showed no signs of the alveolar destruction that is typical of emphysema. Neoplastic lung lesions including nodular hyperplasia of the alveolar epithelium and

bronchioloalveolar adenoma were also detected from month 5 onward. Since their incidence was low at both time points, the sample number was small (n≤10), and these lesions were found across all study groups, it is premature to draw conclusions on the effects of THS2.2 aerosol exposure on lung tumor incidence and/or multiplicity.

To date, transcriptomics analysis of nasal respiratory and tracheal epithelia from female animals has been performed to gain insight into the mechanisms that may be involved in mediating exposure effects in this mouse strain. Nasal SRPs indicated an increase in the number of DEGs over time when A/J mice were exposed to 3R4F CS (relative to sham). In comparison, THS2.2 aerosol exposure caused upregulation of only one gene, *HMOX1*, in nasal epithelium at month 10, and this was independent of dose. Evaluating the data using the more sensitive systems toxicology approach indicated the highest biological impact for exposure to 3R4F CS for 10 months (RBIF = 100%; REF), whereas the effects of THS2.2 aerosol exposure on the nose were only a fraction of that and appeared to subside with time.

Nearly all networks were already affected at month 1 by exposure to 3R4F CS, and these perturbations persisted over time with very few exceptions. Of note, exposure to a matching (by nicotine) THS2.2 aerosol concentration did not cause comparable network perturbations, while THS2.2 aerosol at the highest concentration had a more widespread impact, albeit of smaller amplitude than 3R4F CS. By contrast, 1-month exposure to a low dose of THS2.2 aerosol predominantly impacted networks incorporating the biology of inflammation and tissue repair, while the effect on other networks was restricted to specific processes including senescence, apoptosis and oxidative stress. Of note, prolonged exposure to THS2.2 aerosol, independent of concentration, resulted in far fewer and less extensive network perturbations than were initially seen at the earlier time point. While most networks affected by THS2.2 aerosol exposure for 5 month suggested involvement of inflammatory processes, tissue repair and cell stress responses appeared to be more significantly affected at month 10 (Figure 46).

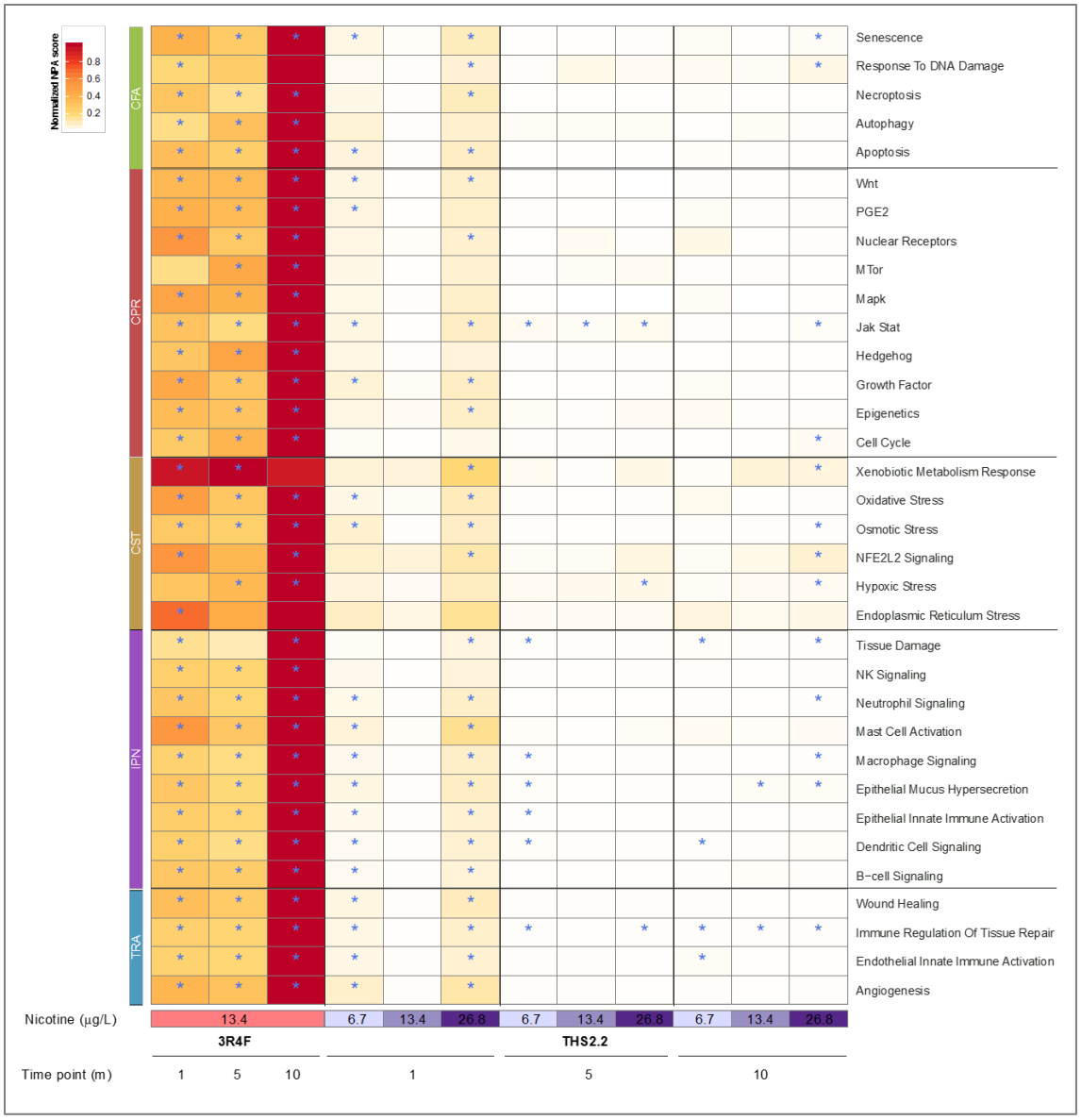


Figure 46. Network perturbations in A/J mouse nasal tissues following exposure to 3R4F cigarette smoke and THS2.2 aerosol compared with air controls

Heatmap of network perturbation amplitude (NPA) scores summarizing subnetworks that were significantly perturbed in at least one treatment. A network is considered perturbed if, in addition to the significance of the NPA score with respect to the experimental variation, the two companion statistics (O and K) derived to inform on the specificity of the NPA score with respect to the biology described in the network, are significant. Significantly perturbed networks are indicated by * (i.e. O and K statistic *p*-values <0.05 and significant with respect to the experimental variation). Abbreviations: CFA, Cell Fate; CPR, Cell Proliferation; CST, Cell Stress; IPN, Inflammatory Process Network; TRA, Tissue Repair and Angiogenesis.

Similar to observations in nasal epithelial samples, SRPs of the trachea exhibited an increasing number of DEGs following 3R4F CS exposure over time, while exposure to low and medium concentrations of THS2.2 aerosol did not cause a deregulation of gene expression in this tissue. However, in animals exposed to THS2.2 aerosol at the high nicotine concentration for 10 months, tracheal SRPs showed significant transcriptional changes. Systems toxicology analysis of transcriptomics data found the highest impact in tracheal samples from animals exposed to 3R4F CS (RBIF = 100%; REF), which was only slightly increased compared with the 3R4F CS impact seen at month 5. THS2.2 aerosol exposure exerted a dose-dependent effect, with small differences in amplitude from time point to time point and overall smaller amplitudes than those seen following exposure to 3R4F CS.

Examining the underlying biology of 3R4F CS-exposure effects highlighted network perturbations implicating a range of mechanisms. While most processes captured in the Cell Fate network were increasingly affected by CS over time, those reflecting various mechanisms governing cell proliferation appeared to be less significantly perturbed as exposure duration increased. At matching nicotine concentrations, exposure to THS2.2 aerosol caused perturbations in many of the networks that were affected by 3R4F CS exposure, although these perturbations were of smaller amplitude with the exception of cell proliferation involving calcium signaling at month 1. Over time, perturbations in the Senescence, PGE2, Nuclear Receptor and Calcium subnetworks diminished and no longer contributed to the overall impact of THS2.2 aerosol exposure. In contrast, networks encompassing mechanisms of tissue repair and innate and adaptive immune responses remained significantly impacted. Higher nicotine concentrations in THS2.2 aerosol amplified some, but not all, of these responses – an effect that was most pronounced after 5 months of exposure (Figure 47).

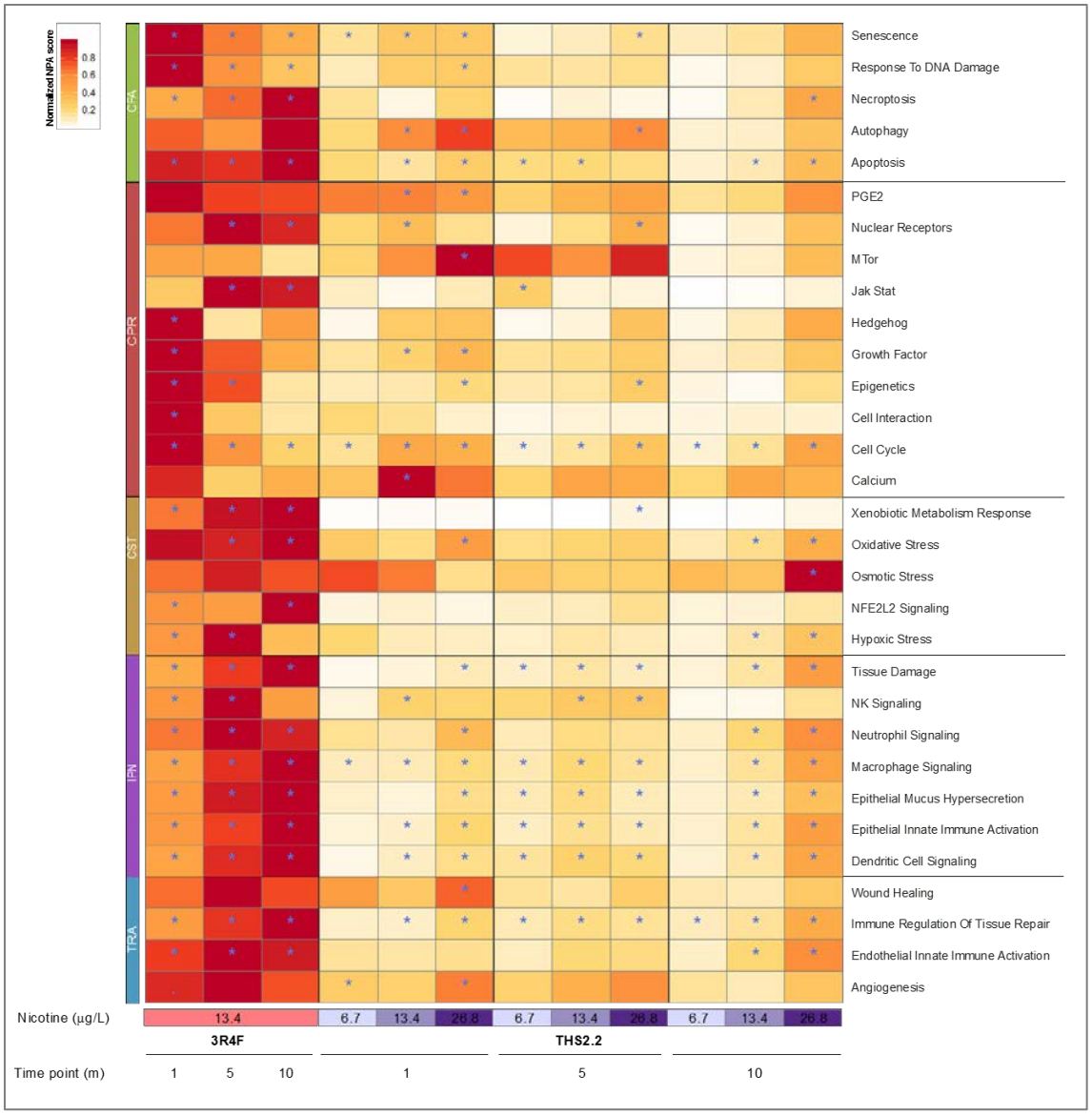


Figure 47. Network perturbation amplification (NPA) scores in A/J mouse tracheal tissues following exposure to 3R4F cigarette smoke and THS2.2 aerosol compared with air controls

Heatmap of network perturbation amplitude (NPA) scores summarizing subnetworks that were significantly perturbed in at least one treatment. A network is considered perturbed if, in addition to the significance of the NPA score with respect to the experimental variation, the two companion statistics (O and K) derived to inform on the specificity of the NPA score with respect to the biology described in the network, are significant. Significantly perturbed networks are indicated by * (i.e. O and K statistic *p*-values <0.05 and significant with respect to the experimental variation). Abbreviations: CFA, Cell Fate; CPR, Cell Proliferation; CST, Cell Stress; IPN, Inflammatory Process Network; TRA, Tissue Repair and Angiogenesis.

Together these preliminary data show moderate-to-severe adaptive and degenerative changes in the upper respiratory tract organs of 3R4F CS-exposed A/J mice, while such adaptive changes were far less frequent and less severe in THS2.2 aerosol-exposed animals. In addition, molecular changes observed in nasal respiratory and tracheal epithelium following 3R4F CS exposure were extensive, affecting a range of mechanisms. In comparison, the biological impact of THS2.2 aerosol exposure was much less pronounced and sustained.

4. CONCLUSIONS

In vitro studies using endothelial and monocytic cells demonstrated that exposure to THS2.2 aerosol had little effect on monocyte adhesion and transendothelial migration. Similarly, studies using NHBECs confirmed that THS2.2 aerosol fractions have little or no cytotoxic and genotoxic potential, eliciting predominantly physiological stress responses, but little inflammation. Results from organotypic studies using a variety of reconstructed human epithelia that closely mimic the upper aerodigestive tract corroborated these findings of low biological impact, showing that exposure to 3R4F CS results in time- and dose-dependent cytotoxicity, tissue damage, and epithelial inflammatory responses, while effects following THS2.2 aerosol exposure were far less extensive and limited in duration. Furthermore, the results of the *in vivo* inhalation studies presented here demonstrate that exposure to THS2.2 aerosol at matching or even higher nicotine concentrations elicited epithelial morphologies in the respiratory organs of rats and mice that were generally less frequent and less severe than following exposure to CS from 3R4F. Mechanistic studies in nasal respiratory epithelial, bronchial epithelial, and lung parenchyma samples from the exposed animals indicated the involvement of epithelial inflammatory and innate and adaptive immune responses in tissue repair following THS2.2 aerosol exposure. Of note, these responses were considerably weaker than those evoked by exposure to 3R4F CS, confirming an overall lower biological impact in experimental *in vivo* systems. In addition, switching to THS2.2 aerosol exposure after a 2-month 3R4F CS exposure did not cause further aggravation of CS exposure-related inflammation as shown by the reduction in IPN perturbations in a mouse model of CVD and emphysema. To the contrary, switching appeared to rapidly alleviate inflammatory responses, with sustained low activity over extended periods of time. These trends were also seen for the oxidative stress responses investigated in the same studies (see companion document on oxidative stress in this dossier).

Overall, the data obtained in these non-clinical studies demonstrated that exposure to THS2.2 aerosol does not cause systemic toxicity and very low or no toxicity in the respiratory tract of laboratory animals. Therefore, and in combination with the *in vitro* systems toxicology data collected, it is most likely that human adults using THS2.2 will not be exposed to additional hazards to those presented by smoking conventional cigarettes.

5. REFERENCES

Adair-Kirk TL, Atkinson JJ, Griffin GL, Watson MA, Kelley DG, DeMello D, Senior RM, Betsuyaku T (2008) Distal airways in mice exposed to cigarette smoke: Nrf2-regulated genes are increased in Clara cells. American Journal of Respiratory Cell and Molecular Biology 39: 400-411

Adams MR, Jessup W, Celermajer DS (1997) Cigarette smoking is associated with increased human monocyte adhesion to endothelial cells: reversibility with oral L-arginine but not vitamin C. Journal of the American College of Cardiology 29: 491-497

Adamson J, Haswell LE, Phillips G, Gaça MD (2011) In Vitro Models of Chronic Obstructive Pulmonary Disease (COPD): INTECH Open Access Publisher.

Arunachalam G, Sundar IK, Hwang J-w, Yao H, Rahman I (2010) Emphysema is associated with increased inflammation in lungs of atherosclerosis-prone mice by cigarette smoke: implications in comorbidities of COPD. Journal of Inflammation 7: 34-34

Azad N, Rojanasakul Y, Vallyathan V (2008) Inflammation and lung cancer: roles of reactive oxygen/nitrogen species. Journal of Toxicology and Environmental Health, Part B 11: 1-15

Barnes PJ (2004) Mediators of chronic obstructive pulmonary disease. Pharmacological reviews 56: 515-548

Barnes PJ (2008) Immunology of asthma and chronic obstructive pulmonary disease. Nature Reviews Immunology 8: 183-192

Barnes PJ, Shapiro SD, Pauwels RA (2003) Chronic obstructive pulmonary disease: molecular and cellular mechanisms. European Respiratory Journal 22: 672-688

Barnig C, Levy BD (2015) Innate immunity is a key factor for the resolution of inflammation in asthma. European Respiratory Review 24: 141-153

Berridge MJ. (2012) Cell Stress, Inflammatory Responses and Cell Death. Cell Signalling Biology. Portland Press.

Blake GJ, Ridker PM (2001) Novel clinical markers of vascular wall inflammation. Circulation Research 89: 763-771

Bloomer R (2007) Decreased blood antioxidant capacity and increased lipid peroxidation in young cigarette smokers compared to nonsmokers: Impact of dietary intake. Nutrition Journal 6: 39

Boué S, De León H, Schlage WK, Peck MJ, Weiler H, Berges A, Vuillaume G, Martin F, Friedrichs B, Lebrun S (2013) Cigarette smoke induces molecular responses in respiratory tissues of ApoE−/− mice that are progressively deactivated upon cessation. Toxicology 314: 112-124

Boué S, Tarasov K, Jänis M, Lebrun S, Hurme R, Schlage W, Lietz M, Vuillaume G, Ekroos K, Steffen Y (2012) Modulation of atherogenic lipidome by cigarette smoke in apolipoprotein E-deficient mice. Atherosclerosis 225: 328-334

Brusselle GG, Bracke KR, Maes T, D'Hulst A I, Moerloose KB, Joos GF, Pauwels RA (2006) Murine models of COPD. Pulmonary pharmacology & therapeutics 19: 155-165

Catanzaro DF, Zhou Y, Chen R, Yu F, Catanzaro SE, De Lorenzo MS, Subbaramaiah K, Zhou XK, Pratico D, Dannenberg AJ (2007) Potentially reduced exposure cigarettes accelerate atherosclerosis: evidence for the role of nicotine. Cardiovascular toxicology 7: 192-201

Celermajer DS (1997) Endothelial Dysfunction: Does It Matter? Is It Reversible? Journal of the American College of Cardiology 30: 325-333

Chen GY, Nunez G (2010) Sterile inflammation: sensing and reacting to damage. Nature Reviews Immunology 10: 826-837

Chen Y, Wang H, Luo G, Dai X (2014) SIRT4 inhibits cigarette smoke extracts-induced mononuclear cell adhesion to human pulmonary microvascular endothelial cells via regulating NF-κB activity. Toxicology letters 226: 320-327

Chen Z-H, Kim HP, Sciurba FC, Lee S-J, Feghali-Bostwick C, Stolz DB, Dhir R, Landreneau RJ, Schuchert MJ, Yousem SA (2008) Egr-1 regulates autophagy in cigarette smoke-induced chronic obstructive pulmonary disease. PLoS ONE 3: e3316

Chung KF, Adcock IM (2008) Multifaceted mechanisms in COPD: inflammation, immunity, and tissue repair and destruction. European Respiratory Journal 31: 1334-1356

Churg A, Cosio M, Wright JL (2008) Mechanisms of cigarette smoke-induced COPD: insights from animal models. American Journal of Physiology-Lung Cellular and Molecular Physiology 294: L612-L631

Churg A, Sin DD, Wright JL (2011) Everything prevents emphysema: are animal models of cigarette smoke-induced chronic obstructive pulmonary disease any use? American Journal of Respiratory Cell and Molecular Biology 45: 1111-1115

Churg A, Tai H, Coulthard T, Wang R, Wright JL (2006) Cigarette smoke drives small airway remodeling by induction of growth factors in the airway wall. American journal of respiratory and critical care medicine 174: 1327-1334

Comandini A, Rogliani P, Nunziata A, Cazzola M, Curradi G, Saltini C (2009) Biomarkers of lung damage associated with tobacco smoke in induced sputum. Respiratory Medicine 103: 1592-1613

Committee GE (2013) Global strategy for the diagnosis, management, and prevention of chronic obstructive pulmonary disease (Updated 2013). http://www goldcopd org

Condeelis J, Pollard JW (2006) Macrophages: obligate partners for tumor cell migration, invasion, and metastasis. Cell 124: 263-266

Curtis JL, Freeman CM, Hogg JC (2007) The immunopathogenesis of chronic obstructive pulmonary disease: insights from recent research. Proceedings of the American Thoracic Society 4: 512-521

Daugherty A, Puré E, Delfel-Butteiger D, Chen S, Leferovich J, Roselaar SE, Rader DJ (1997) The effects of total lymphocyte deficiency on the extent of atherosclerosis in apolipoprotein E-/-mice. Journal of Clinical Investigation 100: 1575

de Boer WI, Sont JK, van Schadewijk A, Stolk J, van Krieken JH, Hiemstra PS (2000) Monocyte chemoattractant protein 1, interleukin 8, and chronic airways inflammation in COPD. Journal of Pathology 190: 619-626

De León H, Boué S, Schlage WK, Boukharov N, Westra JW, Gebel S, VanHooser A, Talikka M, Fields RB, Veljkovic E, Peck MJ, Mathis C, Hoang V, Poussin C, Deehan R, Stolle K, Hoeng J, Peitsch MC (2014) A vascular biology network model focused on inflammatory processes to investigate atherogenesis and plaque instability. Journal of Translational Medicine 12: 185-185

Deanfield JE, Halcox JP, Rabelink TJ (2007) Endothelial Function and Dysfunction: Testing and Clinical Relevance. Circulation 115: 1285-1295

Demirovic D, Rattan SIS (2013) Establishing cellular stress response profiles as biomarkers of homeodynamics, health and hormesis. Experimental Gerontology 48: 94-98

Deng X, Luyendyk JP, Ganey PE, Roth RA (2009) Inflammatory Stress and Idiosyncratic Hepatotoxicity: Hints from Animal Models. Pharmacological reviews 61: 262-282

Doll R, Peto R (1981) The causes of cancer: quantitative estimates of avoidable risks of cancer in the United States today. Journal of the National Cancer Institute 66: 1192-1308

Doll R, Peto R, Boreham J, Sutherland I (2004) Mortality in relation to smoking: 50 years' observations on male British doctors. Bmj 328: 1519

Dong ZM, Brown AA, Wagner DD (2000) Prominent role of P-selectin in the development of advanced atherosclerosis in ApoE-deficient mice. Circulation 101: 2290-2295

Dovgan PS, Edwards JD, Zhan X, Wilde M, Agrawal DK (1994) Cigarette Smoking Increases Monocyte Adherence to Cultured Endothelial Cell Monolayer. Biochemical and Biophysical Research Communications 203: 929-934

Duplaa C, Couffinhal T, LABAT L, Fawaz J, Moreau C, BTETZ I, Bonnet J (1993) Monocyte adherence to endothelial cells in patients with atherosclerosis: relationships with risk factors. European Journal of Clinical Investigation 23: 474-479

Dvorak A, Tilley AE, Shaykhiev R, Wang R, Crystal RG (2011) Do airway epithelium air–liquid cultures represent the in vivo airway epithelium transcriptome? American Journal of Respiratory Cell and Molecular Biology 44: 465-473

Facchinetti F, Amadei F, Geppetti P, Tarantini F, Di Serio C, Dragotto A, Gigli PM, Catinella S, Civelli M, Patacchini R (2007) α,β-Unsaturated Aldehydes in Cigarette Smoke Release Inflammatory Mediators from Human Macrophages. American Journal of Respiratory Cell and Molecular Biology 37: 617-623

Fearon IM, Gaça MD, Nordskog BK (2013) In vitro models for assessing the potential cardiovascular disease risk associated with cigarette smoking. Toxicology in Vitro 27: 513-522

Fearon IM, Phillips G, Carr T, Taylor M, Breheny D, Faux SP (2011) The Role of Oxidative Stress in Smoking-Related Diseases. Mini-Reviews in Organic Chemistry 8: 360-371

Federico A, Morgillo F, Tuccillo C, Ciardiello F, Loguercio C (2007) Chronic inflammation and oxidative stress in human carcinogenesis. International Journal of Cancer 121: 2381-2386

Friedrichs B, Miert Ev, Vanscheeuwijck P (2006) Lung inflammation in rats following subchronic exposure to cigarette mainstream smoke. Experimental Lung Research 32: 151-179

Gairola CG, Drawdy ML, Block AE, Daugherty A (2001) Sidestream cigarette smoke accelerates atherogenesis in apolipoprotein E−/− mice. Atherosclerosis 156: 49-55

Gairola CG, Howatt DA, Daugherty A (2010) Dietary coenzyme Q10 does not protect against cigarette smoke-augmented atherosclerosis in apoE-deficient mice. Free Radical Biology and Medicine 48: 1535-1539

Gawaz M, Langer H, May AE (2005) Platelets in inflammation and atherogenesis. Journal of Clinical Investigation 115: 3378-3384

Gebel S, Lichtner RB, Frushour B, Schlage WK, Hoang V, Talikka M, Hengstermann A, Mathis C, Veljkovic E, Peck M, Peitsch MC, Deehan R, Hoeng J, Westra JW, Gebel S, Lichtner RB, Frushour B, Schlage WK, Hoang V, Talikka M, Hengstermann A, Mathis C, Veljkovic E, Peck M, Peitsch MC, Deehan R, Hoeng J, Westra JW (2013) Construction of a Computable Network Model for DNA Damage, Autophagy, Cell Death, and Senescence. Bioinformatics and Biology Insights 7: 97-117

Getz GS, Reardon CA (2012) Animal Models of Atherosclerosis. Arteriosclerosis, Thrombosis, and Vascular Biology 32: 1104-1115

Ghio AJ, Dailey LA, Soukup JM, Stonehuerner J, Richards JH, Devlin RB (2013) Growth of human bronchial epithelial cells at an air-liquid interface alters the response to particle exposure. Particle and Fibre Toxicology 10: 1-8

Giunzioni I, Bonomo A, Bishop E, Castiglioni S, Corsini A, Bellosta S (2014) Cigarette smoke condensate affects monocyte interaction with endothelium. Atherosclerosis 234: 383-390

Glover-Cutter KM, Lin S, Blackwell TK (2013) Integration of the Unfolded Protein and Oxidative Stress Responses through SKN-1/Nrf. PLoS Genet 9: e1003701

Gonzalez-Suarez I, Martin F, Marescotti D, Guedj E, Acali S, Johne S, Dulize R, Baumer K, Peric D, Goedertier D, Frentzel S, Ivanov NV, Mathis C, Hoeng J, Peitsch MC (2016) In Vitro Systems Toxicology Assessment of a Candidate Modified Risk Tobacco Product Shows Reduced Toxicity Compared to That of a Conventional Cigarette. Chemical Research in Toxicology 29: 3-18

Gray TE, Guzman K, Davis CW, Abdullah LH, Nettesheim P (1996) Mucociliary differentiation of serially passaged normal human tracheobronchial epithelial cells. American Journal of Respiratory Cell and Molecular Biology 14: 104-112

Groneberg DA, Chung KF (2004) Models of chronic obstructive pulmonary disease. Respiratory research 5: 18

Harris JE, Thun MJ, Mondul AM, Calle EE (2004) Cigarette tar yields in relation to mortality from lung cancer in the cancer prevention study II prospective cohort, 1982-8. Bmj 328: 72

Health UDo, Services H (2010) How tobacco smoke causes disease: the biology and behavioral basis for smoking-attributable disease: a report of the Surgeon General. Atlanta, GA: US Department of Health and Human Services, Centers for Disease Control and Prevention, National Center for Chronic Disease Prevention and Health Promotion, Office on Smoking and Health 2

Heguy A, O'Connor T, Luettich K, Worgall S, Cieciuch A, Harvey B-G, Hackett N, Crystal R (2006) Gene expression profiling of human alveolar macrophages of phenotypically normal smokers and nonsmokers reveals a previously unrecognized subset of genes modulated by cigarette smoking. J Mol Med 84: 318-328

Hengstermann A, Müller T (2008) Endoplasmic reticulum stress induced by aqueous extracts of cigarette smoke in 3T3 cells activates the unfolded-protein-response-dependent PERK pathway of cell survival. Free Radical Biology and Medicine 44: 1097-1107

Hodge S, Hodge G, Ahern J, Jersmann H, Holmes M, Reynolds PN (2007) Smoking alters alveolar macrophage recognition and phagocytic ability: implications in chronic obstructive pulmonary disease. American Journal of Respiratory Cell and Molecular Biology 37: 748-755

Hoeng J, Talikka M, Martin F, Sewer A, Yang X, Iskandar A, Schlage WK, Peitsch MC (2014) Case study: the role of mechanistic network models in systems toxicology. Drug discovery today 19: 183-192

Hogg JC, Chu F, Utokaparch S, Woods R, Elliott WM, Buzatu L, Cherniack RM, Rogers RM, Sciurba FC, Coxson HO, Pare PD (2004) The nature of small-airway obstruction in chronic obstructive pulmonary disease. N Engl J Med 350: 2645-2653

Hwang J-w, Chung S, Sundar IK, Yao H, Arunachalam G, McBurney MW, Rahman I (2010) Cigarette smoke-induced autophagy is regulated by SIRT1–PARP-1-dependent mechanism: implication in pathogenesis of COPD. Archives of Biochemistry and Biophysics 500: 203-209

Ioannidis I, Ye F, McNally B, Willette M, Flaño E (2013) Toll-like receptor expression and induction of type I and type III interferons in primary airway epithelial cells. Journal of Virology 87: 3261-3270

Iskandar A, Martin F, Talikka M, Schlage WK, Kostadinova R, Mathis C, Hoeng J, Peitsch MC (2013) Systems Approaches Evaluating the Perturbation of Xenobiotic Metabolism in Response to Cigarette Smoke Exposure in Nasal and Bronchial Tissues. BioMed Research International 2013: 512086

Iskandar A, Mathis C, Martin F, Leroy P, Sewer A, Majeed S, Kuehn D, Trivedi K, Grandolfo D, Cabanski M (2016) 3-D nasal cultures: Systems toxicological assessment of a candidate modified-risk tobacco product. Altex: [Epub ahead of print]

Iskandar AR, Xiang Y, Frentzel S, Talikka M, Leroy P, Kuehn D, Guedj E, Martin F, Mathis C, Ivanov N (2015) Impact assessment of cigarette smoke exposure on organotypic bronchial epithelial tissue cultures: a comparison of mono-culture and co-culture model containing fibroblasts. Toxicological Sciences 147: 207-221

Jetten AM (1989) Multistep process of squamous differentiation in tracheobronchial epithelial cells in vitro: analogy with epidermal differentiation. Environmental Health Perspectives 80: 149

Jongkind JF, Verkerk A, Hoogerbrugge N (1995) Monocytes from patients with combined hypercholesterolemia-hypertriglyceridemia and isolated hypercholesterolemia show an increased adhesion to endothelial cells in vitro: II. Influence of intrinsic and extrinsic factors on monocyte binding. Metabolism 44: 374-378

Kalra VK, Ying Y, Deemer K, Coates TD, Natarajan R, Nadler JL (1994) Mechanism of cigarette smoke condensate induced adhesion of human monocytes to cultured endothelial cells. Journal of Cellular Physiology 160: 154-162

King TE, Jr., Savici D, Campbell PA (1988) Phagocytosis and killing of Listeria monocytogenes by alveolar macrophages: smokers versus nonsmokers. J Infect Dis 158: 1309-1316

Kohli P, Levy BD (2009) Resolvins and protectins: mediating solutions to inflammation. British Journal of Pharmacology 158: 960-971

Koning H, Sayers I, Stewart CE, de Jong D, ten Hacken NH, Postma DS, van Oosterhout AJ, Nawijn MC, Koppelman GH (2012) Characterization of protocadherin-1 expression in primary bronchial epithelial cells: association with epithelial cell differentiation. The FASEB Journal 26: 439-448

Kuehn D, Majeed S, Guedj E, Dulize R, Baumer K, Iskandar A, Boue S, Martin F, Kostadinova R, Mathis C, Ivanov NV, Frentzel S, Hoeng J, Peitsch MC (2015) Impact Assessment of Repeated Exposure of Organotypic 3D Bronchial and Nasal Tissue Culture Models to Whole Cigarette Smoke. Journal of Visualized Experiments : JoVE: 52325

Kunitomo M, Yamaguchi Y, Kagota S, Yoshikawa N, Nakamura K, Shinozuka K (2009) Biochemical evidence of atherosclerosis progression mediated by increased oxidative stress in apolipoprotein E-deficient spontaneously hyperlipidemic mice exposed to chronic cigarette smoke. Journal of Pharmacological Sciences 110: 354-361

Lee JS, Park SJ, Cho YS, Huh JW, Oh Y-M, Lee S-D (2015) Role of AMP-Activated Protein Kinase (AMPK) in Smoking-Induced Lung Inflammation and Emphysema. Tuberculosis and respiratory diseases 78: 8-17

Leong X-F, Ng C-Y, Jaarin K (2015) Animal Models in Cardiovascular Research: Hypertension and Atherosclerosis. BioMed Research International 2015: 528757

Levy BD, Serhan CN (2014) Resolution of Acute Inflammation In The Lung. Annual Review of Physiology 76: 467-492

Li F-f, Shen J, Shen H-j, Zhang X, Cao R, Zhang Y, Qui Q, Lin X-x, Xie Y-c, Zhang L-h (2012) Shp2 plays an important role in acute cigarette smoke-mediated lung inflammation. The Journal of Immunology 189: 3159-3167

Libby P (2012) Inflammation in Atherosclerosis. Arteriosclerosis, Thrombosis, and Vascular Biology 32: 2045-2051

Libby P, Ridker PM, Maseri A (2002a) Inflammation and atherosclerosis. Circulation 105: 1135-1143

Libby P, Ridker PM, Maseri A (2002b) Inflammation and atherosclerosis. Circulation 105: 1135-1143

Lietz M, Berges A, Lebrun S, Meurrens K, Steffen Y, Stolle K, Schueller J, Boue S, Vuillaume G, Vanscheeuwijck P (2013) Cigarette-smoke-induced atherogenic lipid profiles in plasma and vascular tissue of apolipoprotein E-deficient mice are attenuated by smoking cessation. Atherosclerosis 229: 86-93

Lo Sasso G, Schlage WK, Boué S, Veljkovic E, Peitsch MC, Hoeng J (2016a) The Apoe−/− mouse model: a suitable model to study cardiovascular and respiratory diseases in the context of cigarette smoke exposure and harm reduction. Journal of Translational Medicine 14: 1-16

Lo Sasso G, Titz B, Nury C, Boué S, Phillips B, Belcastro V, Schneider T, Dijon S, Baumer K, Peric D, Dulize R, Elamin A, Guedj E, Buettner A, Leroy P, Kleinhans S, Vuillaume G, Veljkovic E, Ivanov NV, Martin F, Vanscheeuwijck P, Peitsch MC, Hoeng J (2016b) Effects of cigarette smoke, cessation and switching to a candidate modified risk tobacco product on the liver in Apoe−/− mice – a systems toxicology analysis. Inhalation toxicology 28: 226-240

Lopez-Souza N, Dolganov G, Dubin R, Sachs L, Sassina L, Sporer H, Yagi S, Schnurr D, Boushey H, Widdicombe J (2004) Resistance of differentiated human airway epithelium to infection by rhinovirus. American Journal of Physiology-Lung Cellular and Molecular Physiology 286: L373-L381

Malhotra D, Thimmulappa R, Vij N, Navas-Acien A, Sussan T, Merali S, Zhang L, Kelsen SG, Myers A, Wise R (2009) Heightened endoplasmic reticulum stress in the lungs of patients with chronic obstructive pulmonary disease: the role of Nrf2-regulated proteasomal activity. Am J Respir Crit Care Med 180: 1196-1207

March TH, Green FH, Hahn FF, Nikula KJ (2000) Animal models of emphysema and their relevance to studies of particle-induced disease. Inhalation toxicology 12 Suppl 4: 155-187

Martin F, Thomson T, Sewer A, Drubin D, Mathis C, Weisensee D, Pratt D, Hoeng J, Peitsch M (2012) Assessment of network perturbation amplitudes by applying high-throughput data to causal biological networks. BMC Syst Biol 6: 54

Martinez-Anton A, Sokolowska M, Kern S, Davis AS, Alsaaty S, Taubenberger JK, Sun J, Cai R, Danner RL, Eberlein M (2013) Changes in microRNA and mRNA expression with differentiation of human bronchial epithelial cells. American Journal of Respiratory Cell and Molecular Biology 49: 384-395

Mathis C, Gebel S, Poussin C, Belcastro V, Sewer A, Weisensee D, Hengstermann A, Ansari S, Wagner S, Peitsch MC (2015) A Systems Biology Approach Reveals the Dose- and Time-Dependent Effect of Primary Human Airway Epithelium Tissue Culture After Exposure to Cigarette Smoke In Vitro. Bioinformatics and Biology Insights 9: 19

Mathis C, Poussin C, Weisensee D, Gebel S, Hengstermann A, Sewer A, Belcastro V, Xiang Y, Ansari S, Wagner S, Hoeng J, Peitsch MC (2013) Human bronchial epithelial cells exposed in vitro to cigarette smoke at the air-liquid interface resemble bronchial epithelium from human smokers. American Journal of Physiology - Lung Cellular and Molecular Physiology 304: L489-L503

Mestas J, Hughes CC (2004) Of mice and not men: differences between mouse and human immunology. Journal of immunology (Baltimore, Md : 1950) 172: 2731-2738

Mio T, Romberger DJ, Thompson AB, Robbins RA, Heires A, Rennard SI (1997) Cigarette smoke induces interleukin-8 release from human bronchial epithelial cells. Am J Respir Crit Care Med 155: 1770-1776

Morbini P, Villa C, Campo I, Zorzetto M, Inghilleri S, Luisetti M (2006) The receptor for advanced glycation end products and its ligands: a new inflammatory pathway in lung disease? Mod Pathol 19: 1437-1445

Mucida D, Cheroutre H (2010) The many face-lifts of CD4 T helper cells. Adv Immunol 107: 139-152

Mudau M, Genis A, Lochner A, Strijdom H (2012) Endothelial dysfunction: the early predictor of atherosclerosis. Cardiovascular Journal of Africa 23: 222-231

Muller WA, Luscinskas FW (2008) Assays of Transendothelial Migration in vitro. Methods in Enzymology 443: 155-176

Münzel T, Sinning C, Post F, Warnholtz A, Schulz E (2008) Pathophysiology, diagnosis and prognostic implications of endothelial dysfunction. Annals of Medicine 40: 180-196

Murugan V, Peck MJ (2009) Signal transduction pathways linking the activation of alveolar macrophages with the recruitment of neutrophils to lungs in chronic obstructive pulmonary disease. Exp Lung Res 35: 439-485

Nakashima Y, Plump AS, Raines EW, Breslow JL, Ross R (1994) ApoE-deficient mice develop lesions of all phases of atherosclerosis throughout the arterial tree. Arteriosclerosis, Thrombosis, and Vascular Biology 14: 133-140

OECD Test No. 413: Subchronic Inhalation Toxicity: 90-day Study: OECD Publishing.

OECD. Test No. 453: Combined Chronic Toxicity/Carcinogenicity Studies: OECD Publishing.

Paquette J, Tremblay P, Bernier V, Auger F, Laviolette M, Germain L, Boutet M, Boulet L, Goulet F (2003) Production of tissue-engineered three-dimensional human bronchial models. In Vitro Cellular & Developmental Biology-Animal 39: 213-220

Parsanejad R, Fields WR, Morgan WT, Bombick BR, Doolittle DJ (2008) The time course of expression of genes involved in specific pathways in normal human bronchial epithelial cells following exposure to cigarette smoke. Experimental Lung Research 34: 513-530

Paul A, Ko KW, Li L, Yechoor V, McCrory MA, Szalai AJ, Chan L (2004) C-reactive protein accelerates the progression of atherosclerosis in apolipoprotein E–deficient mice. Circulation 109: 647-655

Phillips B, Veljkovic E, Boué S, Schlage WK, Vuillaume G, Martin F, Titz B, Leroy P, Buettner A, Elamin A, Oviedo A, Cabanski M, De León H, Guedj E, Schneider T, Talikka M, Ivanov NV, Vanscheeuwijck P, Peitsch MC, Hoeng J (2016) An 8-Month Systems Toxicology Inhalation/Cessation Study in Apoe−/− Mice to Investigate Cardiovascular and Respiratory Exposure Effects of a Candidate Modified Risk Tobacco Product, THS 2.2, Compared With Conventional Cigarettes. Toxicological Sciences 149: 411-432

Phillips B, Veljkovic E, Peck MJ, Buettner A, Elamin A, Guedj E, Vuillaume G, Ivanov NV, Martin F, Boué S (2015) A 7-month cigarette smoke inhalation study in C57BL/6 mice demonstrates reduced lung inflammation and emphysema following smoking cessation or aerosol exposure from a prototypic modified risk tobacco product. Food and Chemical Toxicology 80: 328-345

Plump AS, Smith JD, Hayek T, Aalto-Setälä K, Walsh A, Verstuyft JG, Rubin EM, Breslow JL (1992) Severe hypercholesterolemia and atherosclerosis in apolipoprotein E-deficient mice created by homologous recombination in ES cells. Cell 71: 343-353

Pollard JW (2004) Tumour-educated macrophages promote tumour progression and metastasis. Nature Reviews Cancer 4: 71-78

Poussin C, Gallitz I, Schlage WK, Steffen Y, Stolle K, Lebrun S, Hoeng J, Peitsch MC, Lietz M (2014) Mechanism of an indirect effect of aqueous cigarette smoke extract on the adhesion of monocytic cells to endothelial cells in an in vitro assay revealed by transcriptomics analysis. Toxicology in Vitro 28: 896-908

Poussin C, Laurent A, Peitsch MC, Hoeng J, De Leon H (2015) Systems biology reveals cigarette smoke-induced concentration-dependent direct and indirect mechanisms that promote monocyte-endothelial cell adhesion. Toxicological Sciences: kfv137

Poussin C, Laurent A, Peitsch MC, Hoeng J, De Leon H (2016) Systems toxicology-based assessment of the candidate modified risk tobacco product THS2.2 for the adhesion of monocytic cells to human coronary arterial endothelial cells. Toxicology 339: 73-86

Prytherch Z, Job C, Marshall H, Oreffo V, Foster M, BéruBé K (2011) Tissue-Specific Stem Cell Differentiation in an in vitro Airway Model. Macromolecular bioscience 11: 1467-1477

Puljic R, Pahl A (2003) Smoke induced changes in epithelial cell gene expression: development of an in vitro model for COPD. Altex 21: 3-7

Rajendran P, Rengarajan T, Thangavel J, Nishigaki Y, Sakthisekaran D, Sethi G, Nishigaki I (2013) The vascular endothelium and human diseases. International journal of biological sciences 9: 1057

Reynolds PR, Kasteler SD, Schmitt RE, Hoidal JR (2011) Receptor for advanced glycation end-products signals through Ras during tobacco smoke-induced pulmonary inflammation. Am J Respir Cell Mol Biol 45: 411-418

Richter A, O'Donnell RA, Powell RM, Sanders MW, Holgate ST, Djukanovic R, Davies DE (2002) Autocrine ligands for the epidermal growth factor receptor mediate interleukin-8 release from bronchial epithelial cells in response to cigarette smoke. American Journal of Respiratory Cell and Molecular Biology 27: 85-90

Rius C, Company C, Piqueras L, Cerdá-Nicolás JM, González C, Servera E, Ludwig A, Morcillo EJ, Sanz M-J (2013) Critical role of fractalkine (CX3CL1) in cigarette smoke-induced mononuclear cell adhesion to the arterial endothelium. Thorax 68: 177-186

Rogers DF (2007) Physiology of airway mucus secretion and pathophysiology of hypersecretion. Respir Care 52: 1134-1146; discussion 1146-1139

Ross R (1999a) Atherosclerosis - an inflammatory disease. N Engl J Med 340: 115-126

Ross R (1999b) Pathogenesis of Atherosclerosis-Atherosclerosis is an inflammatory disease. American Heart Journal 138: S419

Russell RE, Thorley A, Culpitt SV, Dodd S, Donnelly LE, Demattos C, Fitzgerald M, Barnes PJ (2002) Alveolar macrophage-mediated elastolysis: roles of matrix metalloproteinases, cysteine, and serine proteases. Am J Physiol Lung Cell Mol Physiol 283: L867-873

Sadik CD, Kim ND, Luster AD (2011) Neutrophils cascading their way to inflammation. Trends in immunology 32: 452-460

Schlage W, Westra J, Gebel S, Catlett N, Mathis C, Frushour B, Hengstermann A, Van Hooser A, Poussin C, Wong B, Lietz M, Park J, Drubin D, Veljkovic E, Peitsch M, Hoeng J, Deehan R (2011) A computable cellular stress network model for non-diseased pulmonary and cardiovascular tissue. BMC Syst Biol 5: 168

Schroeter MR, Sawalich M, Humboldt T, Leifheit M, Meurrens K, Berges A, Xu H, Lebrun S, Wallerath T, Konstantinides S (2008) Cigarette smoke exposure promotes arterial thrombosis and vessel remodeling after vascular injury in apolipoprotein E-deficient mice. Journal of vascular research 45: 480-492

Scott D, Palmer R (2003) The influence of tobacco smoking on adhesion molecule profiles. Tobacco Induced Diseases 1: 1-20

Serhan CN, Brain SD, Buckley CD, Gilroy DW, Haslett C, O'Neill LAJ, Perretti M, Rossi AG, Wallace JL (2007) Resolution of inflammation: state of the art, definitions and terms. FASEB journal : official publication of the Federation of American Societies for Experimental Biology 21: 325-332

Services UDoHaH (2010) How tobacco smoke causes disease: the biology and behavioral basis for smoking-attributable disease: a report of the Surgeon General. Atlanta, GA: US Department of Health and Human Services, Centers for Disease Control and Prevention, National Center for Chronic Disease Prevention and Health Promotion, Office on Smoking and Health 2

Shen CX, Z. CH, Ge JB (2004) The role of inflammatory stress in acute coronary syndrome. Chinese Medical Journal 117: 133-139

Shen Y, Rattan V, Sultana C, Kalra VK (1996) Cigarette smoke condensate-induced adhesion molecule expression and transendothelial migration of monocytes. American Journal of Physiology-Heart and Circulatory Physiology 270: H1624-H1633

Sima AV, Stancu CS, Simionescu M (2009) Vascular endothelium in atherosclerosis. Cell and tissue research 335: 191-203

Sopori M (2002) Effects of cigarette smoke on the immune system. Nat Rev Immunol 2: 372-377

Stampfli MR, Anderson GP (2009) How cigarette smoke skews immune responses to promote infection, lung disease and cancer. Nat Rev Immunol 9: 377-384

Starrett W, Blake DJ (2011) Sulforaphane inhibits de novo synthesis of IL-8 and MCP-1 in human epithelial cells generated by cigarette smoke extract. Journal of immunotoxicology 8: 150-158

Stevenson CS, Docx C, Webster R, Battram C, Hynx D, Giddings J, Cooper PR, Chakravarty P, Rahman I, Marwick JA, Kirkham PA, Charman C, Richardson DL, Nirmala NR, Whittaker P, Butler K (2007) Comprehensive gene expression profiling of rat lung reveals distinct acute and chronic responses to cigarette smoke inhalation. American Journal of Physiology - Lung Cellular and Molecular Physiology 293: L1183-L1193

Talikka M, Kostadinova R, Xiang Y, Mathis C, Sewer A, Majeed S, Kuehn D, Frentzel S, Merg C, Geertz M (2014) The Response of Human Nasal and Bronchial Organotypic Tissue Cultures to Repeated Whole Cigarette Smoke Exposure. International journal of toxicology: 1091581814551647

Tani S, Dimayuga PC, Anazawa T, Chyu K-Y, Li H, Shah PK, Cercek B (2004) Aberrant antibody responses to oxidized LDL and increased intimal thickening in apoE−/− mice exposed to cigarette smoke. Atherosclerosis 175: 7-14

Taraseviciene-Stewart L, Scerbavicius R, Choe KH, Moore M, Sullivan A, Nicolls MR, Fontenot AP, Tuder RM, Voelkel NF (2005) An animal model of autoimmune emphysema. Am J Respir Crit Care Med 171: 734-742

Tetley TD (2005) Inflammatory cells and chronic obstructive pulmonary disease. Curr Drug Targets Inflamm Allergy 4: 607-618

Thorley AJ, Tetley TD (2007a) Pulmonary epithelium, cigarette smoke, and chronic obstructive pulmonary disease. Int J Chron Obstruct Pulmon Dis 2: 409-428

Thorley AJ, Tetley TD (2007b) Pulmonary epithelium, cigarette smoke, and chronic obstructive pulmonary disease. International Journal of Chronic Obstructive Pulmonary Disease 2: 409-428

Tuder RM, Yoshida T, Fijalkowka I, Biswal S, Petrache I (2006) Role of lung maintenance program in the heterogeneity of lung destruction in emphysema. Proc Am Thorac Soc 3: 673-679

van der Toorn M, Frentzel S, De Leon H, Goedertier D, Peitsch MC, Hoeng J (2015a) Aerosol from a candidate modified risk tobacco product has reduced effects on chemotaxis and transendothelial migration compared to combustion of conventional cigarettes. Food and Chemical Toxicology 86: 81-87

van der Toorn M, Frentzel S, Goedertier D, Peitsch M, Hoeng J, De Leon H (2015b) A prototypic modified risk tobacco product exhibits reduced effects on chemotaxis and transendothelial migration of monocytes compared with a reference cigarette. Food and Chemical Toxicology 80: 277-286

Vasilios P (2008) Adaptative mechanisms during chronic hypoxia in COPD. ΠΝΕΥΜΩ 21: 134

Victoni T, Gleonnec F, Lanzetti M, Tenor H, Valença S, Porto LC, Lagente V, Boichot E (2014) Roflumilast N-Oxide Prevents Cytokine Secretion Induced by Cigarette Smoke Combined with LPS through JAK/STAT and ERK1/2 Inhibition in Airway Epithelial Cells. PLoS ONE 9: e85243

Von Holt K, Lebrun S, Stinn W, Conroy L, Wallerath T, Schleef R (2009) Progression of atherosclerosis in the Apo E−/− model: 12-Month exposure to cigarette mainstream smoke combined with high-cholesterol/fat diet. Atherosclerosis 205: 135-143

Wakai K, Inoue M, Mizoue T, Tanaka K, Tsuji I, Nagata C, Tsugane S, Development RGft, Japan EoCPSi (2006) Tobacco smoking and lung cancer risk: an evaluation based on a systematic review of epidemiological evidence among the Japanese population. Japanese journal of clinical oncology 36: 309-324

Westra JW, Schlage WK, Frushour BP, Gebel S, Catlett NL, Han W, Eddy SF, Hengstermann A, Matthews AL, Mathis C, Lichtner RB, Poussin C, Talikka M, Veljkovic E, Van Hooser AA, Wong B, Maria MJ, Peitsch MC, Deehan R, Hoeng J (2011) Construction of a Computable Cell Proliferation Network Focused on Non-Diseased Lung Cells. BMC Syst Biol 5: 105

Westra JW, Schlage WK, Hengstermann A, Gebel S, Mathis C, Thomson T, Wong B, Hoang V, Veljkovic E, Peck M, Lichtner RB, Weisensee D, Talikka M, Deehan R, Hoeng J, Peitsch MC (2013) A Modular Cell-Type Focused Inflammatory Process Network Model for Non-Diseased Pulmonary Tissue. Bioinformatics and Biology Insights 7: 167-192

Woodruff PG, Koth LL, Yang YH, Rodriguez MW, Favoreto S, Dolganov GM, Paquet AC, Erle DJ (2005) A distinctive alveolar macrophage activation state induced by cigarette smoking. Am J Respir Crit Care Med 172: 1383-1392

Yamaguchi Y, Haginaka J, Morimoto S, Fujioka Y, Kunitomo M (2005) Facilitated nitration and oxidation of LDL in cigarette smokers. European Journal of Clinical Investigation 35: 186-193

Yang S-R, Chida AS, Bauter MR, Shafiq N, Seweryniak K, Maggirwar SB, Kilty I, Rahman I (2006) Cigarette smoke induces proinflammatory cytokine release by activation of NF-κB and posttranslational modifications of histone deacetylase in macrophages. American Journal of Physiology - Lung Cellular and Molecular Physiology 291: L46-L57

Yoshida T, Tuder RM (2007) Pathobiology of cigarette smoke-induced chronic obstructive pulmonary disease. Physiol Rev 87: 1047-1082

Zanetti F, Sewer A, Mathis C, Iskandar AR, Kostadinova R, Schlage WK, Leroy P, Majeed S, Guedj E, Trivedi K, Martin F, Elamin A, Merg C, Ivanov NV, Frentzel S, Peitsch MC, Hoeng J (2016) Systems toxicology assessment of the biological impact of a candidate Modified Risk Tobacco Product on human organotypic oral epithelial cultures. Chemical Research in Toxicology: [Epub ahead of print]

Zhang SH, Reddick RL, Piedrahita JA, Maeda N (1992) Spontaneous hypercholesterolemia and arterial lesions in mice lacking apolipoprotein E. Science 258: 468-471

Zhang X, Wang L, Zhang H, Guo D, Zhao J, Qiao Z, Qiao J (2002) The effects of cigarette smoke extract on the endothelial production of soluble intercellular adhesion molecule-1 are mediated through macrophages, possibly by inducing TNF-alpha release. Methods Find Exp Clin Pharmacol 24: 261-265